PERFORMANCE ANALYSIS OF A MUI-BASIN COAL GASIFIER BASED ON FEED OXYGEN, WATER CONCENTRATION AND HEAT REGULATION

OYUGI GEORGE OYUGI

MASTER OF SCIENCE

(Mechanical Engineering)

JOMO KENYATTA UNIVERSITY OF AGRICULTURE AND TECHNOLOGY

2022

Performance Analysis of a Mui Basin Coal Gasifier Based on Feed Oxygen, Water Concentration and Heat Regulation

Oyugi George Oyugi

A Thesis Submitted in Partial Fulfillment of the Requirements for the Degree of Master of Science in Mechanical Engineering of the Jomo Kenyatta University of Agriculture and Technology

2022

DECLARATION

This thesis is my original work and has not been presented for a degree in any other university.

Signature..... Date.....

Oyugi George Oyugi

This thesis has been submitted for examination with our approval as the University Supervisors:

Signature……Date.....

Eng. Dr. Hiram M. Ndiritu, PhD

JKUAT, Kenya

Signature.....Date.....

Dr. Benson B. Gathitu, PhD

JKUAT, Kenya

DEDICATION

This work is dedicated to my wife Kernael George and my children for the sacrifices they made and the support they gave me during the research period.

ACKNOWLEDGEMENTS

My sincere and greatest gratitude goes, first, to God Almighty for His favor, protection and guidance throughout my research period. Secondly, I appreciate my supervisors; Eng. Dr. Hiram M. Ndiritu and Dr. Benson B. Gathitu for their supervision, assistance, and valued guidance throughout the study period. I thank Technical University of Mombasa (TUM) and National Research Fund (NRF) for supporting me financially during my study. I also thank Mr. Muigai and Mr. Waiyaki who worked tirelessly with me at the JKUAT Thermodynamics Laboratories during my experiments. I acknowledge all members of JKUAT and TUM staff that I worked with at different stages of the research. Finally, I appreciate all my fellow postgraduate students of Mechanical Engineering, and all my well-wishers. May God richly bless you all.

TABLE OF CONTENTS

LIST OF TABLES

LIST OF FIGURES

LIST OF APPENDICES

LIST OF ABBREVIATIONS

CCE	Carbon Conversion Efficiency
CCS	Carbon Capture and Storage
CGE	Cold Gas Efficiency
CFD	Computational Fluid Dynamics
ER	Equivalence Ratio
GC	Gas Chromatograph
GDP	Gross Domestic Product
HHV	High Heating Value
HRS	Heat Regulation System
IGCC	Integrated Gasification Combined Cycle
IEA	International Energy Agency
LCPDP	Least Cost Power Development Plan
LHV	Low Heating Value
MLS	Method of Least Squares
OAR	Oxygen-Air Ratio
OEA	Oxygen-Enriched Air
NO_x	Oxides of Nitrogen
So_x	Oxides of Sulfur

SOR	Steam-Oxygen Ratio
TPES	Total Primary Energy Supply
2D	Two Dimensional
UCG	Underground Coal Gasification
USA	United States of America

LIST OF SYMBOLS

A	Total heat transfer area
A_i	Heat transfer areas for inner tube
A_o	Heat transfer areas for outer tube
C_p	Specific heat of cold fluid
C_{ph}	Specific heat of hot fluid
d_i	Inner diameter of inner pipe
d_o	Outer diameter of inner pipe
HHV_{feed}	High heating value for the coal feed
HHV_{gas}	High heating value for the syngas
H_i	Convective heat-transfer coefficient of fluid in inner tube
H_o	Convective heat-transfer coefficient of fluid in outer tube
k	Thermal conductivity of inner pipe material
LHV_{gas}	Low heating value for the syngas
$\dot{m}$	Mass flow rate
$m_{a,\,st}$	Stoichiometric mass of air needed to burn 1 kg of coal sample used
$\dot{m}_c$	Flow rate of cold fluid
m_{coal}	Mass of coal used in the experiment
$\dot{m}_{feed}$	Mass flow rate for coal feed

$\dot{m}_{gas}$	Mass flow rate for syngas
$\dot{m}_h$	Flow rate of hot fluid
$m_{o,\,a}$	Mass of oxygen in 1 kg of air
$\dot{m}_{s,\,max}$	Maximum mass flow rate of steam from boiler
$m_{o,\,st}$	Stoichiometric mass of oxygen needed to burn 1 kg of coal sample
N	Mole fraction of each gas species
Q	Heat transferred by the heat exchanger
$\dot{Q}_c$	Rate of heat transfer to cold fluid
$\dot{Q}_h$	Rate of heat transfer to hot fluid
R_{fI}	Fouling factor inside the inner pipe
R_{fo}	Fouling factor outside the inner pipe
$T_{c,\,in}$	Inlet cold fluid temperature
$T_{c,\,out}$	Outlet cold fluid temperature
$T_{h,\,in}$	Inlet hot fluid temperature
$T_{h,\,out}$	Outlet hot fluid temperature
ΔT_1	Temperature difference at the inlet of the heat exchanger
ΔT_2	Temperature difference at the outlet of the heat exchanger
ΔT_{LM}	Logarithmic mean temperature difference

U	Overall heat transfer coefficient
U_i	Overall heat transfer coefficient for exchanger inner tube
U_o	Overall heat transfer coefficient for exchanger outer tube
$V_{a,\,st}$	Stoichiometric volume of air needed to burn 1 kg of coal sample
λ	Air-fuel equivalence ratio

ABSTRACT

Kenya depends mainly on electricity from hydroelectric power, which is unreliable due to climatic change, and thermal generators whose power is expensive due to high diesel prices. Innovative ways of providing affordable and reliable energy services to Kenyan citizens is thus necessary, one of which is use of coal for energy generation. Gasification of coal from Mui Basin, Kitui County, can be one of the mitigating ways of providing clean, affordable and reliable energy to Kenyans. Traditionally coal power plants included grated coal firing plants where coal was crushed into gravel-like form and used in the boiler. Later, pulverized (powdered) coal power plants like Sub-critical, and Super-critical coal plants, were used. These plants, however, had low efficiencies (37%-45%) and generated undesirable emissions like SO_x, NO_x, CO_2 and particulates. Currently, Integrated coal Gasification Combined Cycle (IGCC), is being used with oxidizing agents like steam, oxygen, and air to convert coal into clean syngas for power generation, giving better plant efficiencies. Integrated coal Gasification Combined Cycle includes tapping the unwanted emissions and using them in relevant industries, thus protecting the environment. The existing Mui Basin coal gasifier was developed based on coal gasification using air as the oxidizing agent. The syngas generated had high nitrogen content that led to low cold gas efficiency as well as the lower heating values. This study entailed performance improvement of a bench-scale fixed-bed gasifier using Mui Basin coal, based on regulation of reactor heat and the amounts of oxygen and steam inputs. Initially oxygen/air ratio into the gasifier was varied and an optimum ratio determined. Later the steam/oxygen ratio was varied and optimum ratio obtained. A Multi-gas Analyzer TY-6331P was used to analyze the syngas composition, while type-K thermocouples were used to monitor reactor temperatures. From the study, it was noted that, for air gasification, the optimum equivalence ratio was 0.30, with a mean reactor temperature of 748.8ºC and gasification efficiency was 43.1%. For gasification with oxygen-enriched air with no heat regulation, the cold gas efficiency was 73.1%, carbon conversion efficiency was 90.1%, mean temperature was 849.9ºC and syngas lower heating value was 8.58 MJ/Nm^3. However, when reactor heat was regulated, the optimum oxygen/air ratio rose from 0.61 to 0.71, gasification efficiency rose to 78.7% and lower heating value rose by 8.7%. Inclusion of steam improved the syngas lower heating value to 9.33 MJ/Nm^3, gasification efficiency to 87.0% and syngas yield rose by 14.53%. The optimum steam/oxygen ratio was 0.40. The data from this study is intended to play key role in the design of energy systems that utilize syngas for power generation help in developing small-scale coal gasifiers for domestic applications like small electric generators and small stationary engines. The gasifier can also be scaled up to industrial level for power generation.

CHAPTER ONE

INTRODUCTION

1.1 Background

Access to energy has direct impact on quality of life and influences social equality, economic growth and environmental safety. In a liberalized market such as Kenya, cost of energy is a significant determinant of competitiveness of locally produced goods and services relative to imports (MoE, 2018). Coal, being the most abundant fossil fuel resource globally, is used by many countries for energy production due to its abundance, reliability and relative low cost (Najafi *et al*. 2015; Clerici, & Alimonti, 2015.).

According to the International Energy Agency (IEA) report (2020), it was observed that fossil for the year 2018, fuels like natural gas, oil and coal accounted for about 81.3% of the total global energy used in that year. Renewable sources of energy like geothermal, wind and solar accounted for the least energy, as shown in Figure 1.1. In the same year, coal provided 38% of the global electrical power (IEAES, 2020; Newell *et al*., 2020). While accounting for only 9.3% of energy globally in 2018, bio-fuels and wastes were the biggest source of energy in Kenya that year, as shown in Figure 1.2 (IEAEB, 2020).

Energy cost in Kenya is quite high hindering investments. The average cost of electricity in Kenya as at March 2020 was USD 0.16 for businesses. This was three times that of South Africa and more than one and half times that of China and USA (GPP, 2020). The South African and Chinese economies depend heavily on coal, with about 83% of electricity generation in South African and 64% in China derived from coal (Keneilwe & Ramaano, 2019; IEACh, 2020). Electricity in USA is however derived majorly from natural gas, accounting for 40% and coal accounting for 23% in 2020 (IEAUS, 2020). The coal discovered in Mui Basin, Kitui County, can thus be used for production of electricity that can help reduce the electricity cost in Kenya.

The major challenge with using coal as an energy source is the considerably high emissions of CO_2, *SOx*, *NOx*, and particulates, which contributes to climate change and air pollution (Muthangya *et al*. 2012). In the year 2017, CO_2 emission from coal accounted for 40% of the total global CO_2 emissions originating from fossil fuels. *SOx* and *NOx* lead to acid rain and general water contamination (IEAES, 2020; Jale, 2014). Thus, better technologies that are friendly to the environment are needed for utilization of coal (Pandey, 2015).

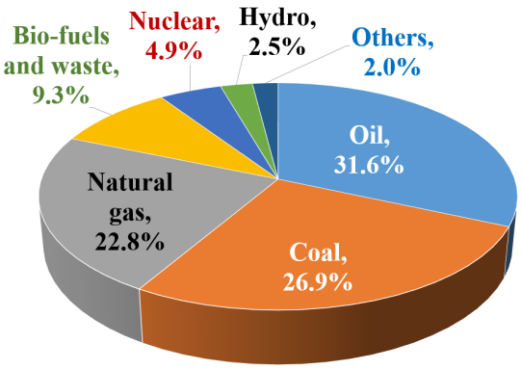

Figure 1.1: Global total primary energy supply by fuel for the year 2018 (IEAES, 2020)

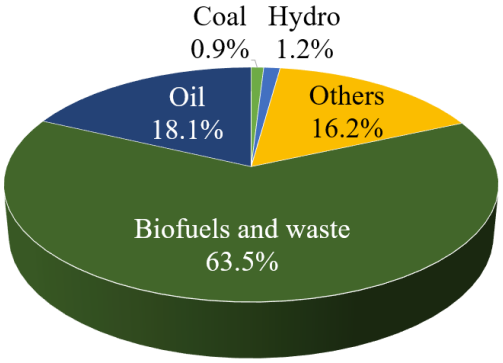

1.5 Justification

Today, the world is experiencing growing energy demands and increasing oil prices, leading to research on new and sustainable sources of energy. These energy sources would be used either in conjunction with the existing ones, or independently, for power generation. Kenyan economy currently depends on energy provided

principally by biomass and oil. Her electricity is largely generated from hydro, geothermal, and petroleum sources. These traditional energy sources, however, have become less reliable, hence the need for a transition to other more reliable energy sources.

Coal is an important energy source worldwide due to its cost and high energy density despite its influence on the environment. Gasification offers an attractive approach to utilize it sustainably in the transition period as reliable and cheap renewable sources are being sought. With discovery of coal in Mui Basin, Kenya has the potential to benefit from these advantages of coal as a means of mitigating problems associated with the energy requirements for her citizens.

Coal gasifier is an important component in the gasification process. The gasifier performance directly affects the cold gas efficiency and chemical energy of syngas. However, this performance mainly depends on the gasification parameters, such as oxygen/coal ratio, water/coal ratio, gasification pressure and temperature and the feedstock properties (Xie *et al.*, 2013). It is necessary to establish to what extent these factors affect the performance of the gasifiers. Hence optimizing a gasifier working on Mui Basin coal was the main focus of this research with the overall aim of effectively utilizing the local coal for enhanced and clean energy production in Kenya.

Figure 1.2: Total energy supply in Kenya for the year 2018 (IEAEB, 2020)

Gasification process is an environmentally friendly and efficient way of utilizing coal. It is the conversion of any solid fuel like coal, into synthesis gas (syngas) in the presence of a controlled supply of oxidizing or reducing medium like steam, air, carbon dioxide, oxygen or their mixtures in different ratios. The syngas produced consists of combustible gases like CH_2, CO, H_2, and non-combustible by-products like water, carbon dioxide and nitrogen (Zogala, 2014; Cempa-Balewicz *et al.*, 2013; Mikulandrić *et al.*, 2015). Syngas is considered less harmful to the environment due to production of less NO_X, SO_X and CO_2 emissions (Jin *et*

al., 2010). Syngas is applicable in chemical industry, power production or for domestic uses.

Many technologies have been used in reducing the unwanted emissions from coal. These include improvement of the energy efficiency of gasification equipment, and use of alternative technologies like Integrated Gasification Combined Cycle (IGCC), which reduce emission of NO_X and SO_X into the environment. Another method is the carbon capture and storage (CCS) technologies in which CO_2 gas released during gasification is captured and used in relevant chemical industry or injected under pressure into deep underground wells in a process called sequestration (Jayaraman & Gokalp, 2015).

1.2 The Coal from Mui Basin, Kenya

The traditional electric energy sources in Kenya, like hydropower, have become less reliable due to climate change (persistent droughts), evidenced by inadequate supply and frequent power outages. This has necessitated the need for new efficient energy sources or improvement in the efficiency of the existing ones. Among the alternative sources are geothermal, solar, and wind energies (Mokveld & Eije, 2018).

The coal deposit in Mui Basin is estimated to be about 400 million tons (Irungu, 2016; Owiro *et al*., 2015), with its composition ranging from lignite, which forms the bulk of the deposit, to bituminous (Muthui *et al*., 2014). Gasification is more applicable for low-rank coals like lignite, due to their high gasification reactivity (Mi *et al*., 2015). The application of the syngas produced depends on its chemical composition, its heating value, among other factors. For example, a syngas rich in methane is suitable for cooking purposes due to its high energy content, while that rich in *CO* gas is suitable for gas turbine power plants. These properties depend on factors like the type of gasifying agent, the coal properties, and the gasifier pressure and temperature. These factors should be evaluated in order to generate a high quality syngas for a desired application.

1.3 Problem Statement

The global energy matrix today is concentrated around the intensive use of fossil fuels, a situation that has led to climate change due to emission of greenhouse gas (CO_2) (Sthel *et al.*, 2013). In recent years, Kenya has struggled with the experience of an unreliable supply of electricity. For example, there were almost 90 000 power outage incidents in Nairobi alone between 2014 and 2015, a situation that was also captured in the World Bank report that analyzed the Kenyan power situation in 2016 (Taneja, 2017; World Bank, 2016). In addition, the Kenya electricity utility company recorded 9.3% reduction in energy sales in 2017, attributed to many factors including unreliable power sources like hydropower whose performance fluctuates with weather (Ahmad *et al*., 2017).

Kenyan electricity demand is projected to rise from 1700 MW in 2017 to over 6000 MW in 2037, as recorded in the Least Cost Power Development Plan (LCPDP) report (ERC, 2011). In order to meet this rise in demand, the total installed capacity should increase from the current 2200 MW to over 9900 MW in the same period. Although in recent years, geothermal has been the main source of electricity in Kenya, much of the electricity is still from hydro and thermal sources. For example, in 2018, geothermal accounted for 40% of net power generation, hydropower accounted for 30%, while petroleum-based thermal power plants accounted for 17.6% (IEAKE, 2019). The water levels in the reservoirs have dropped dramatically in recent past due to frequent droughts caused by global warming, making hydroelectric sources to be unreliable. On the other hand, electricity from diesel generators is environmentally-harmful due to emissions of pollutants like CO_2, SO_x and NO_x gases.

The use of coal in electrical power generation need to be carried out in an environmentally acceptable and economically competitive manner, and gasification is one of the processes used in producing clean electric power from coal. Coal gasification involves a reaction of coal and oxygen and/or steam under controlled conditions to produce syngas (mixture of carbon monoxide, hydrogen and methane).

Different coal ranks and qualities like lignite, bituminous, anthracite require different amounts of the gasifying agents in order to produce quality syngas (Markus *et al.*, 2010). Furthermore, depending on the application of the syngas, these oxidizing agents may be varied so as to produce the desirable composition of the syngas for the desired application (Dascomb, 2013). The prevailing reactor temperatures and pressures are also very important operating parameters in gasification, affecting both the heating value and the composition of the syngas, as well as the performance of the gasifier (James *et al.*, 2014).

1.4 Objectives

The main objective of this research was to analyze the performance of a bench-scale fixed-bed Mui Basin coal gasifier by regulation of the operating conditions.

The above main objective was achieved through the following specific objectives:

1. To design and fabricate an appropriate reactor heat regulation system for the Mui Basin coal gasifier.
2. To test the influence of feed oxygen and water supply on the performance of the gasifier.
3. To analyze the performance of the gasifier based on control of flow and temperature parameters.

1.6 Organisation of the Thesis

This thesis consists of five chapters, in which the present one is an introduction. This chapter contains a brief explanation about primary energy sources in the world compared to energy sources in Kenya. It also outlines the objectives of this study and why the study was necessary. Chapter 2 briefly discusses the gasification process and the various reactions in the gasifier that generate the syngas. An extensive review of research that has been done in the area of gasification, especially on gasifying agents and gasification pressure and temperature, is presented. The various methods used to control gasification heat are discussed and the chapter concludes with an enumeration of gaps identified. In Chapter 3, combustion

chemistry of the coal sample used is given. It also presents the design and construction of the equipment for the experiment, including design of the heat regulation system. Lastly, this chapter presents the experimental procedure used to obtain the research data as well as the gasifier performance test procedures. In chapter 4, the data from coal gasification using pure air, oxygen-enriched air, and steam are presented in graphical form and discussed. Effect of reactor heat regulation is clearly shown and discussed. The parameters discussed include gas composition, gas yield, syngas heating values, and gasification efficiency. The final chapter presents the deductions made from findings of the research, as well as the recommendations preferred for further research to improve efficiency of the gasifier.

CHAPTER TWO

LITERATURE REVIEW

2.1 Overview

Coal has been used for many years for energy production with many developed countries deriving the bulk of their electricity from it. However, the strict regulations on the levels of unwanted emissions permitted, has increased the need for research on better methods of utilizing coal as an energy source. One such method is integrated gasification combined cycle (IGCC). This method combines the gasification process with the units for separation and utilization of the environmentally harmful emissions like CO_2, *NOx* and *SOx*. Though gasification is an old technology, the variety of the technological arrangements like fixed-bed, fluidized-bed and entrained-flow reactors and its versatility (production of electricity, syngas, hydrogen and other products) makes it an important research area.

Coal gasification processes occur in the presence of oxygen, steam, air or their combinations in different ratios. These processes lead to generation of a product gas with different heating values and composition. The product gas has both combustible gases like *CO*, CH_4 and H_2, and non-combustible components like compounds of sulphur, compounds of nitrogen, CO_2, among others. If the non-combustible components are removed, the clean syngas can be used as fuel to generate electricity or steam. It can also act as a chemical building block for application in the petrochemical and refining industries, or for the production of H_2 gas (Breault, 2010).

Various techniques are employed for the removal of the non-combustibles. They include the counter-current acid gas absorption with regenerative solvent for removal of H_2S, CO2, *HCN*, *SOx* and NOx, and a water scrubbing method for removal of NH_3, *HCN*, *ZnS* and chlorides. Other methods include use of *ZnO* sulfidation to trap H_2S, chemisorption methods to remove mercury, and carbon dioxide capture and storage (CCS) for removing CO_2. These non-combustible components can also be used in various chemical industries like fertilizer industry, petrochemical and refining

industries among others (Chiche *et al.,* 2013). Thus, gasification adds value to coal by converting it to marketable fuels and products.

The efficiency of the gasification process and equipment, and the quality of the syngas depend on various factors. These include the quality of coal used, the composition, flow rate and temperature of the oxidizing medium, and the prevailing temperature and pressure in the gasifier reactor (Zogala and Tomasz, 2015). It is also important to consider how oxidizing agent is injected. For example, in a two-stage gasification process, where air and steam are used, air may be used in the first stage and steam in the subsequent stage. When oxygen is used then it may be injected in two stages (Cui *et al.,* 2014; Wang *et al*., 2014). These different configurations yield syngas of different qualities. These factors, therefore, need to be considered for the best gasification process output.

2.2 The Chemistry of Gasification

Series of physical and chemical processes occur when coal is injected into a high-temperature gasifier. The coal particles are heated, the moisture vaporized, the volatile matter devolatilized and the char burnt or gasified. Depending on the surrounding conditions and their intrinsic kinetics, the gases released from the coal particles will react with each other either exothermically or endothermically (Syed *et al*., 2012).

One of the main processes in gasification is combustion of coal, which is a heterogeneous exothermic reaction between carbon from coal and oxygen, to produce CO_2 and CO (Preciado *et al*., 2012). Eqns. 2.1 and 2.2 show complete and partial oxidation reactions of coal respectively.

$$C + O_2 \rightarrow CO_2 \quad (-393\ \text{MJ/kmol}) \tag{2.1}$$

$$C + 0.5\,O_2 \rightarrow C\,O \quad (-111\ \text{MJ/kmol}) \tag{2.2}$$

Char-H_2O and char-CO_2 gasification reactions are endothermic and rely on the heat from exothermic combustion reactions (Choi *et al.*, 2001). Eqn. 2.3 gives the water gas (steam) reaction while Eqn. 2.4 shows the Boudouard reaction.

$$C + H_2O \longleftrightarrow CO + H_2 \quad (+131 \text{ MJ/kmol}) \tag{2.3}$$

$$C + CO_2 \longleftrightarrow 2CO \quad (+172 \text{ MJ/kmol}) \tag{2.4}$$

There is a heterogeneous reaction of carbon with hydrogen, which is exothermic and produces methane. This is called methane-forming reaction and is shown in Eqn. 2.5 (Zogala, 2014; Choi *et al.*, 2001; Couto *et al.*, 2013).

$$C + 2H_2 \longleftrightarrow CH_4 \quad (-75 \text{ MJ/kmol}) \tag{2.5}$$

Apart from the heterogeneous reactions above, homogeneous reactions among the gases also occur in the reactor as shown in the Eqns. 2.6 - 2.10 (Couto *et al.*, 2013; Taba *et al.*, 2012; Bingxi *et al.*, 2013*)*

Eqn. 2.6 gives CO partial combustion reaction.

$$CO + 0.5\,O_2 \rightarrow CO_2 \quad (-283 \text{ MJ/kmol}) \tag{2.6}$$

Eqn. 2.7 below represents hydrogen partial combustion.

$$H_2 + 0.5O_2 \rightarrow H_2O \quad (-242 \text{ MJ/kmol}) \tag{2.7}$$

Water gas shift reaction is shown in Eqn. 2.8,

$$CO + H_2O \longleftrightarrow CO_2 + H_2 \quad (-41 \text{ MJ/kmol}) \tag{2.8}$$

Eqn. 2.9 gives steam-methane reforming reaction as,

$$CO + 3H_2 \longleftrightarrow CH_4 + H_2O \quad (-206 \text{ MJ/kmol}) \tag{2.9}$$

Eqn. 2.10 represents Methanation reaction.

$$CO_2 + 4H_2 \longleftrightarrow CH_4 + 2H_2O \quad (-165\ MJ/kmol) \qquad (2.10)$$

Other reactions occur that lead to formation of some non-combustible compounds. Some of these reactions are shown in Eqns. 2.11 – 2.16 (Preciado, 2012).

$$S_2 + O_2 \rightarrow SO_2 \qquad (-297\ MJ/kmol) \qquad (2.11)$$

$$SO_2 + 3H_2 \rightarrow H_2S + H_2O \qquad (-207\ MJ/kmol) \qquad (2.12)$$

$$C + 2S \longleftrightarrow CS_2 \qquad (+115\ MJ/kmol) \qquad (2.13)$$

$$CO + S \longleftrightarrow COS \qquad (+63\ MJ/kmol) \qquad (2.14)$$

$$N_2 + 3H_2 \longleftrightarrow 2NH_3 \qquad (-46\ MJ/kmol) \qquad (2.15)$$

$$N_2 + 2O_2 \longleftrightarrow NO_2 \qquad (+66\ MJ/kmol) \qquad (2.16)$$

Generally, when O_2 concentration is increased at high reaction temperature, then, for a constant coal-feeding rate, the reaction in Eqn. 2.4 occurs. This consumes the CO_2 generated in Eqn. 2.1 causing the concentration of CO_2 in the product gas to fall. However, high O_2 concentrations promotes combustion of coal in the reactor leading to increased production of CO_2. Therefore, an optimum value of O_2 should be maintained for efficient gasification reactions in the reactor.

2.3 Gasification Technologies

Gasification technologies are commonly categorized according to bed type based on the largest particles size the gasifier can accept. This method categorizes the technologies into three: moving-bed, fluidized-bed and entrained-flow gasification.

2.3.1 Fixed-bed Gasifiers

This is the oldest gasification technology and is still in use in some commercial practices. Its two main configurations are up draft and downdraft, depending on the flow-direction of gasifying medium in relation to the fuel. In up-draft, the coal is fed from the top of the gasifier while the oxidizer is fed from below creating a counter-

current flow in the gasifier. Concerning the down- draft configuration, the gasifying agent and the feedstock are both fed from the top creating a co-current flow in the gasifier. Fixed bed gasifier can accommodate feed- stock size of diameter 3–50 mm (Vamvuka, 2000). Some of the features of this technology include low oxidant requirements, high methane content in the product gas and production of hydrocarbon liquids like tars and oils. Others include high cold gas efficiency when the colorific value of tar and oils are considered. Its main disadvantages include inability to handle caking and very fine coals (Mishra *et al.*, 2018). This type of gasifier is shown in Figure 2.1 including a graph showing the typical temperatures of the gas and solids as they traverse through the gasifier for a dry ash gasification. From the graph it can be seen that the a maximum temperature in the reactor is about 1300ºC for the dry ash gasification, while the syngas exit temperature is about 600ºC. The main example of this gasifier in commercial application is the Lurgi gasifier.

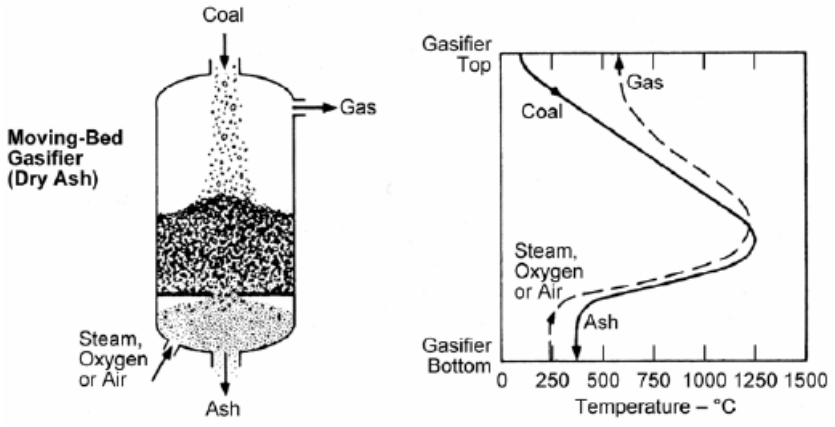

Figure 2.1: Typical fixed-bed gasifier (Breault, 2010).

2.3.2 Fluidized-bed Gasifier

In these gasifiers, feedstock is suspended in an oxygen rich gas. As the gasifying agent rises in the reactor, it reacts with the feedstock and maintains the coal particles in a fluidized state. These gasifiers operate with feedstock particle sizes of less than 3 mm and they exhibit uniform temperature distribution in the bed. Figure 2.2 shows a typical representation of a fluidized-bed gasifier with a graph showing the gas and coal particles temperature as they travel through the gasifier.

The graph shows that these gasifiers operate in the temperature range of below 1100º C, which is below the ash melting temperature, and as such they experience no clinker formation and defluidization of the bed (Vamvuka, 2000; Mishra *et al.,* 2018). The main characteristics of fluidized-bed gasifiers include extensive solids recycling, uniform temperature in the bed, and moderate oxidizer requirements (Vamvuka, 2000). Their main disadvantage is the losses occurring due to particle entrainment (Nayak et al., 2011).

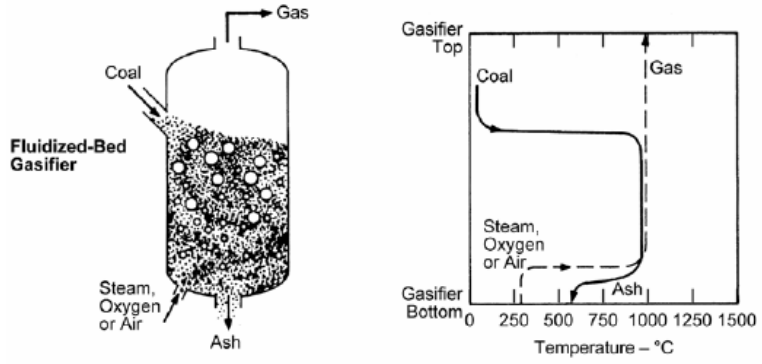

Figure 2.2: Typical fluidized-bed gasifier (Breault, 2010).

2.3.3 Entrained-flow Gasifier

Finely ground coal particles are suspended in a stream of steam and oxygen at high speed. The coal can be wet-fed, in which it is transported in water slurry, or dry- fed in which nitrogen is used as carrier gas. As can be seen in Figure 2.3, the coal and gasifying medium are both fed from the top, while the producer gas comes from near bottom of the gasifier. The graph shows that these gasifiers usually operate at high temperatures above 1400ºC, which is beyond the ash-melting temperature, and thus have high carbon conversion rate [Mishra *et al.,* 2018]. Entrained flow gasifiers have short gas residence time (usually seconds) hence they are considered as high capacity gasifiers. Examples of large-scale commercial entrained bed gasifiers are GE/Texaco, Conoco-Phillips, Shell and, Koppers-Totzek (Preciado *et al*., 2012; Mishra *et al.*, 2018). Some of the characteristics of entrained-flow gasifiers include high-temperature slagging operation, entrainment of some molten slag in the product gas and requires relatively large amounts of oxidants. Other properties are product

gas has large amount of sensible heat, and it is capable of gasifying all coals, regardless of ranks and types (Vamvuka, 2000).

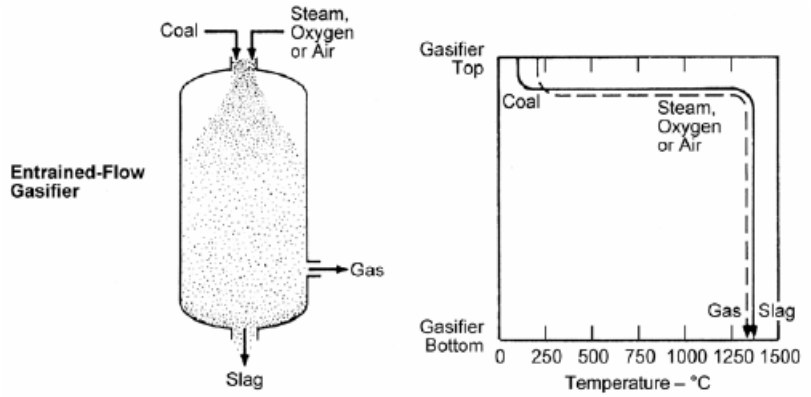

Figure 2.3: Typical entrained-bed gasifier (Breault, 2010).

2.4 Effect of Gasifying Medium on Gasification Products

Various gasifying media like O_2 , air, CO_2 , steam or their combinations, are used in gasification process; depending on the coal-type and the desired quality and application of the syngas (Markus et al., 2010). Low rank coals like lignite and sub-bituminous are more reactive thus requiring less oxidizer compared to bituminous and anthracite. In addition, considering the desired syngas application, these oxidizers may be varied to produce the desired composition of the syngas (Dascomb, 2013).

Lee et al., (2011) developed a model that analyzed chemical reaction processes in a dry-feeding entrained-bed coal gasifier, based on O_2 /coal and steam/coal ratios, and operating pressure. In their study, initially O_2/coal ratio was varied from 0.3 to 0.9 with a constant steam/coal ratio of 0.05. Later, steam/coal ratio was varied with an O_2 /coal ratio of 0.75, the pressure inside the reactor being kept at 4.2 MPa. It was found that carbon conversion rate increased with O_2 concentration leading to rise in syngas yield. Also increasing H_2O content slowly increased carbon conversion efficiency initially, but the rate improved with time. This was attributed to the decrease in the overall temperature in the reactor and cold gas efficiency with increasing steam concentrations. They however did not examine the influence of

these parameters on gasifier temperature, which is expected to vary with varying concentrations of O_2 and steam.

Park *et al*., (1998) studied the properties of entrained-flow coal gasifier where they varied O_2 /coal ratio and reactor temperature. They found that, for a short residence time reactor, O_2/coal ratio was critical to carbon conversion since the heat produced from exothermic reactions supported the endothermic gasification reactions. They concluded that for such gasifiers, O_2 /coal ratio of between 0.8 and 0.9 would give better carbon conversion and cold gas efficiencies. Their study however, used a slurry-fed gasifier, which has high water content compared to dry-fed.

Zogala, (2014) used stoichiometric equilibrium modeling technique to establish the factors affecting syngas composition from coal gasification. His model was implemented on Mathematica software to solve the model equations. The coal samples were of different ranks, and from four different Polish coalmines. The gasifying agents used included: mixtures of steam and air, steam and pure oxygen, and air and pure oxygen. He observed that a rise in the O_2 content in the oxidizer increased the Yields of H_2 , CO, H_2O and CO_2, and that the yield of CO_2 exceeded that of H_2O at higher concentrations of O_2. When H_2O concentrations were increased, yields of H_2 rose compared to when only O_2 and air were used. His research, however, assumed isothermal conditions, which is difficult to achieve in actual practice.

Baranowski *et al.,* (2017) investigated the effect of gasifying agents and CaO on gasification of low-rank coal and wastes. They used CO_2 and steam as gasifying agents in addition to varying the reactor temperature. They found that there were higher concentrations of CH_4 and H_2 gases in product gas when steam was used than in the case of CO_2. However, higher content of CO was recorded in the case of CO_2 than in the case of steam. Babu & Pratik, (2005) modeled a biomass gasifier to show the effects of O_2/air and steam/air ratio on gasification process. Their model equations were solved analytically. They found that the calorific value of syngas increased with rising O_2/air ratio but declined with the

rising steam/air ratio. It was also observed that the reaction temperatures rose for preheated air intake. Their model was how- ever based on wood fuel that is high in moisture and volatile matter compared to coal.

Preciado *et al.*, (2012) also modeled gasification of Colombian coal in a fluidized-bed gasifier. They used kinetics model to model the gasifier, and RGibbs model to estimate the gasification products, both of which were analyzed using Aspen Plus software. They found that gasifier thermal efficiency was most sensitive to O_2/carbon ratio and that an excessive increase in the O_2 flow rate caused a fall in thermal efficiency. They concluded that the O_2/carbon ratio should not exceed 0.8 for efficient operations. The simulation was however based on low temperature reactor (LTR). The findings were consistent with those realized by Xie *et al.*, (2013) who modeled coal gasification based on slurry-fed entrained-bed gasifier.

Li *et al.*, (2014) studied the effect of oxygen flow rate on gasification products. They modeled coal char gasification process based on the Gibbs free energy minimization method and analyzed through Aspen Plus software. In their study, coal and CO_2 feed rates were constant. It was observed that the amount of *C O* rose gradually up to O_2/coal ratio of 0.91 before starting to decrease, while H2 decreased gradually with increasing of O_2 flow. From the values of syngas LHV, they concluded that the optimum O_2/coal ratio was 0.91. They also inferred that preheating O_2 could improve both the syngas heating value and reaction temperature. Their study was however based on use of O_2 and CO_2 as the gasifying agents which yielded a syngas with fairly low heating value due to low hydrogen content.

2.5 Effect of Gasifying Agent on Reactor Temperature and Pressure

Nayak *et al.*, (2011), modeled coal gasification in a fluidized-bed gasifier using Aspen Plus software, and varied the H_2O/coal and O_2/coal ratios. They observed that the heat released by the exothermic reactions in the gasifier

maintained the reactor at the operating temperature. This heat also supported the endothermic gasification reactions occurring inside the gasifier. They further established that steam could only be used as a sole gasifying agent if an external source of heat that supported the endothermic reactions was provided. Biagini *et al.*, (2009) modeled a gasifier for hydrogen production optimization. They varied the O_2/coal ratio and the H_2O/coal ratio from 0.25-0.50, and 0.0-0.35 respectively. They found that higher O_2 /coal ratio, led to higher reactor temperatures. However, they did not identify the optimum values for the O_2/coal and H_2O/coal ratios that could give most favorable operating temperature for the efficient production of quality syngas.

Park et al., (1998) studied gasification process using an entrained-flow coal gasifier and varied O_2/coal ratio and reactor temperature. They discovered that distribution of temperature within the reactor depended upon the coal feed rate and oxygen, unless heat losses were considered. They observed that temperature in the reactor rose as in O_2/coal ratio increased. It was concluded that, considering the ash melting temperature and heat losses from the reactor, the desired O_2 /coal ratio were at least 0.6. They also observed that the O_2/coal ratio affects carbon conversion more significantly than the steam/coal ratio. The study, however, did not explore how the heat losses could be minimized to increase the efficiency of the process.

Yang *et al.*, (2006) investigated the influence of preheated air on performance of a fixed-bed biomass gasifier. They found that the solid-fuels temperatures rose much faster when higher air temperatures were used. This indicated occurrence of fast ignition in case of higher air temperatures. They observed that, for a feed air at 973 K, the peak temperature at the bed top was only 630 K, compared to about 900 K for the case of air at 623 K. This implied that higher feed air temperatures led to lower peak temperatures, due to reduced ignition temperature. Preheating the feed air to these high temperatures, however, increases the overall cost of the gasification process due to specialized facilities needed for such high temperatures.

Lee *et al.,* (2011) in their study modeled dry-feeding entrained-bed coal gasification process. They analyzed the chemical reactions and the operating conditions during the gasification of coal as they varied O_2/coal and steam/coal ratios. They observed that increase in steam/coal ratio lowered the temperature due to the relatively high heat capacity of steam. They also discovered that increasing the operating pressure improved both carbon conversion and cold gas efficiency due to improved reactivity of char. They concluded that the gasifier operating pressure is inversely proportional to the peak temperature. This model was however not validated due to lack of data on dry-fed gasifiers that could be used to bench mark the same.

2.6 Effect of Temperature and Pressure on Gasification Process.

The prevailing gasifier reactor temperatures and pressures are very important operating parameters in gasification process, affecting both the syngas heating value and composition, and the performance of the gasifier (Radwan, 2012). For instance, where the gasification processes target more methane generation, lower levels of operating temperatures should be maintained as opposed to cases where carbon monoxide or hydrogen are desired (Zogala, 2014; Zhang *et al.,* 2013).

Nearly all the coal gasification reactions are reversible and therefore, equilibrium point of any of these reactions can be shifted by manipulating the temperatures. This illustrates that temperature, as a parameter, has a great influence on the performance of coal gasifiers. The degree of equilibrium attained by the various gasification reactions in the gasifier determines the composition of the volatile matter generated from the gasifier (Zhang *et al*., 2013).

Mi *et al.,* (2015) investigated the catalytic effects of alkali and alkali earth metal species on char conversion during steam gasification. They studied char yields, surface area and pore volumes of different coals as a function of gasification temperature in the fluidized-bed reactor at lower heating rate. They observed that the three parameters above generally decreased with increasing reaction temperature from 700 to 900^{o}C 15% vol. of steam. Zhang *et al.,* (2013) conducted

an energy and exergy analysis based on results from the experiments of coal/biomass blend in a dual circulating fluidized bed gasifier. They found that increase in reactor temperature had a positive impact on syngas energy and exergy. These results were however based on fluidized bed gasifiers, with steam as the gasifying agent. There is thus need for further studies using dry-fed gasifier with inclusion of other gasifying agents like oxygen, air or their mixtures.

Adeyemi *et al.,* (2015) studied the effect of gasification parameters like equivalence ratio, pressure and temperature on gasification metrics. They also developed a numerical model based on the Lagrangian-Eulerian scheme that predicted the experimental results reasonably. They found that increased reactor temperature and pressure led to increased yield of CO, H_2 gases and higher heating value due to enhanced reactions between char and steam and CO_2. The higher temperatures also led to reduced levels of CO_2 and H_2O as these gases underwent endothermic reactions with char. The heat in this study was however supplied from built-in heating modules, which is not common to all gasifiers as some derive their heat majorly from the exothermic reaction in the reactor. These findings agreed with those made by Taba *et al*., (2012) and Baranowski *et al*., (2017) who in their studies observed that increase in reactor temperature and pressure improved carbon conversion, syngas yield and hence the calorific value of the syngas.

Shahbaz *et al.,* (2016) studied the effect of temperature and other parameters on palm kernel shell gasification using steam as the oxidizer. They observed that rise in gasification temperature enhanced carbon conversion rate in biomass up to about 725^{o} C and then starts reducing. The findings were consistent with those of Holt, (2001) who analyzed the needs and opportunities in coal gasification field. He noted that commercial gasifiers from Global E-Gas and Shell generally operated at higher temperatures accounting for the better carbon conversion rates realized in these gasifiers with petroleum coke. He observed that increasing the operating temperature would however, aggravate the

refractory wear, which is quite expensive and time consuming to replace. Therefore, operating temperature control is highly desired.

Wadhwani, & Mohanty, (2016) developed a 2D CFD model to investigate effects of operating pressure on coal chemical looping combustion. The governing equations were solved using FLUENT 6.3.26. The results obtained showed that increase in operating pressure led to reduction in gasifier reactor operating temperatures. The rate of decrease in reactor temperature however, escalated at higher pressures. Therefore, control of reactor pressure is necessary in order to achieve optimum operating temperature in the gasifier. Li *et al.*, (2013) also modeled biomass gasification in an auto-thermal gasifier using Aspen Plus software. They studied the effect of equivalence ratio, temperature and pressure, and their interactions on the gasification process. They found that reactor temperature increased with increasing gasification pressure. This was due to the increase in reacting molecules with increased pressure leading to more complete gasification process. They also observed that increasing pressure increased HHV of the syngas due to increase in CH_4 gas.

2.7 Regulation of Gasifier Reactor Temperature and Pressure

Gasification reactions take place at a given range of temperatures and pressures in the reactor and therefore, it is important that the heat in the gasifier is closely monitored and controlled. This not only ensure high quality syngas, but also enhanced lifespan of the equipment involved in the process.

Different manufacturers of coal gasifiers have employed different methods to control the reactor temperature and pressure for efficient gasification reactions. Examples of these methods include wall membranes, water jackets, controlled feeds of gasifying agents, wall insulation among other methods (Xie *et al.*, 2013; Choi *et al.*, 2001; Toporov *et al.*, 2015; Maurstad, 2005). Heat in the reactor has a direct impact on the quality and quantity of the syngas produced from the process. The reactor cooling method applied depends on the type, size and application of the gasifier as well as the kind of the gasifying agents used. For example, a commercial gasifier used in a big

power plant would use wall membranes compared to a gasifier meant for domestic applications, which would use water jackets (Maurstad, 2005). Also, where more hydrogen is needed, much steam would be preferred in the oxidizer which leads to low reactor temperatures compared to when carbon monoxide is needed in which much oxygen is preferred in the gasifying agent (Dascomb, 2013; Othman, 2007).

Wang *et al.*, (2014) studied temperature control in downdraft entrained-bed two- stage coal gasifier, and suggested a two stage injection of oxygen. Traditionally, a two-stage gasification process involved injecting all required oxygen in the first stage and only coal without oxygen in the second stage. This normally led to very high temperatures in the first stage and low temperatures in the second stage. In their research, however, they split oxygen feed between the two stages and discovered that this led to even distribution of temperature in the two stages and the peak temperatures reduced significantly. This process, however, still required an external source of heat to maintain the operating temperatures within the required limits.

An example of a commercially available process is the Shell coal gasification process that uses a dry feed system. The gasifier operates at pressures and temperatures of up to 40 bars and 1500ºC respectively. Its inner wall temperature is controlled by circulating water in a membrane wall to generate steam which is then used in the power cycle (Maurstad, 2005). The membranes are however expensive to install and maintain and thus May not be cost effective for small scale or domestic applications.

In slurry-fed entrained-bed gasifiers, the steam needed for gasification reactions is derived from the water in the slurry. The reaction temperatures in these gasifiers are between 1,200 - 1,600ºC. Choi *et al.,* (2001) studied, using an experimental model of slurry-fed entrained-bed gasifier, the ash fusion temperature with added CaO as a flux. They observed that the temperature control was achieved by the steam evaporated from the coal slurry in addition to the variation of the oxygen/coal ratio. This temperature was maintained at fairly high values to melt the mineral matter

in the coal into a slag. This would, however, not fully apply in a dry-fed gasifier where there is very little or no water supplied for gasification process.

Xie *et al*., (2013) in their studies also realized that O_2/coal ratio affects temperature directly (Figure 2.4). The availability of oxygen enhances the combustion reaction of *C* and *H* particles that releases heat that cause the rise in gasification temperature. They found that the O_2/coal ratio in the range of 0.67 to 0.85 was almost directly proportional to the gasification temperature. They further observed that for every 0.1 rise in O_2/coal ratio, there was a corresponding increase in gasification temperature by about 352 K. They concluded that gasification temperature could be effectively regulated by controlling O_2/coal ratio in the actual operation, which is consistent with the findings of Lee *et al.*, (2011).

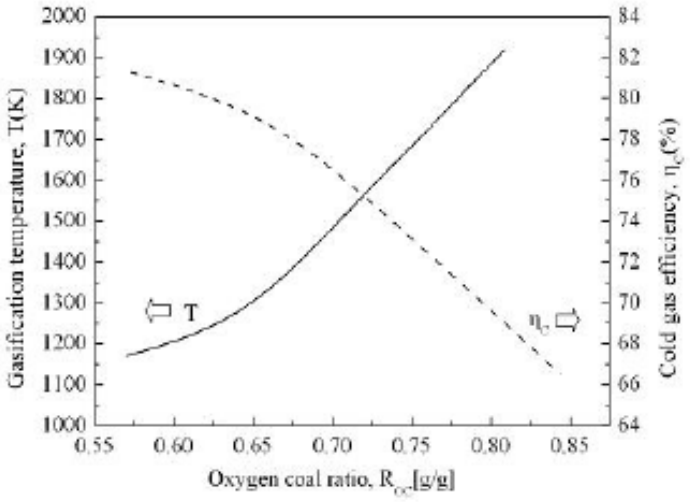

Figure 2.4: Effect of O_2/coal ratio on gasifier temperature and efficiency (Xie *et al.*, 2013)

Control of gasifier temperature through regulation of O_2/coal ratio however, may require process automation. This can be achieved by directly linking the temperature variations in the gasifier to the oxygen and coal feed lines, through sensors. This system may be more applicable for industrial gasifiers and may not be viable for a simple gasifier for domestic application.

2.8 Summary of Gaps

From the above reviewed studies, the following inferences are made:

- Most of the studies involved entrained and fluidized-bed gasifiers. Not much data is available on fixed-bed dry-fed gasifiers and their operating conditions.
- Much study has been done on large-scale coal gasification for commercial applications. Inadequate data is available on coal gasifiers for domestic application.
- Little information is available on simpler but effective ways of regulating reactor heat for small-scale gasifiers like use of water jackets.
- Most of the data available are based on the use of combination of oxygen- steam, air-steam, CO_2-steam or oxygen-air as the gasifying agents. Little data is available on the use of steam-oxygen-air as the oxidizing agent.

This research was, therefore, intended to address the above gaps. The next chapter consists of the details of the experimental method designed and constructed. It also entails how the gasification process performance would be evaluated.

CHAPTER THREE

METHODOLOGY

3.1 Background

Due to difference in mineral compositions of different coals, each coal from different ores react uniquely with the oxidizing agents yielding syngas of unique compositions. This research involved investigating the influence of feed oxygen, water concentration and heat regulation on the gasification process of Mui Basin coal. The methodology used entailed designing and conducting experiments to determine optimum amount of oxygen/air ratio and steam/oxygen ratio required for the gasification of Mui Basin coal. A bench-scale fixed-bed updraft gasifier existing at the JKUAT Thermodynamics Labs was used. Based on the experimental data obtained, a heat regulation system for maintaining the requisite gasifier thermal conditions for optimum gasification re- actions was developed. Thus a new bench-scale gasifier with the heat regulation system was fabricated, and tested for optimum operation.

3.2 Combustion Analysis of Mui Basin Coal

3.2.1 Coal Analysis

The proximate and ultimate analysis of the coal used was conducted using standard procedures. The proximate analysis involved determining the moisture content, the volatile matter, the ash content and the fixed carbon content of the Mui Basin coal used and was conducted according ASTM Standard D7582-10, (2010). First, the moisture content in the coal sample was determined according to ASTM Standard D3173-03, (2003). A sample of coal was taken, weighed and then placed in a special dry capsule of known weight. The capsule was then placed into an oven and heated for 45 minutes at temperature of between 105ºC - 110ºC, then removed from oven, covered tightly, and at temperature of between 105ºC - 110ºC, then removed from oven, covered tightly, and cooled in a desiccator.

The weight of the coal sample was measured as soon as it reached room temperature. The percentage moisture M %, in the coal was determined using Eqn. 3.1.

$$M\% = 100\left(\frac{C_{bh} - C_{ah}}{C_{bh}}\right) \tag{3.1}$$

Where, C_{bh} and C_{ah} are the weights of coal before and after heating respectively.

The volatile matter was determined according to ASTM standard D3175-11, (2011). One gram of pulverized coal was placed in a crucible of known weight and the crucible covered with a tight lid. It was then placed in a furnace chamber, heated for seven minutes at constant temperature of 950^{o} C, removed from the furnace, cooled to room temperature, and weighed. The percentage weight of the volatile matter $V\%$ in the coal sample was determined using Eqn. 3.2.

$$V\% = 100\left(\frac{C_{bh} - C_{ah}}{C_{bh}}\right) - M\% \tag{3.2}$$

The coal sample ash content was determined based on ASTM Standard D3174-12, (2012). One gram of pulverized coal sample was placed in a crucible of known weight which was then placed in a furnace and heated at 730ºC for three hours, and then removed. The covered crucible was then cooled in a desiccator to room temperature and the coal sample immediately weighed. The difference in the weight of the samples before and after heating indicated the ash contents of samples (Eqn. 3.3).

$$A\% = 100\left(\frac{C_{bh} - C_{ah}}{C_{bh}}\right) \tag{3.3}$$

Percentage of fixed carbon content FC %, was determined as the difference between 100% and the sum of the moisture, volatile matter and ash in the coal sample, as shown in Eqn. 3.4 (Omar *et al.*, 2017; Smolinski *et al.*, 2012)

$$FC\% = 100 - (M\% + V\% + A\%) \tag{3.4}$$

The ultimate analysis of the coal sample was conducted according to ASTM Standard D3176-15, (2015). The lower heating value of the coal sample was determined according to ASTM Standard D5865-10a, (2010) using NENKEN TYPE adiabatic bomb calorimeter Model 1013-B (accuracy 2.5%). The summary of the process is as follows: heat capacity of the bomb calorimeter was determined by burning a one gram of benzoic acid in oxygen. One gram of the coal sample was then burned in the calorimeter, after cleaning, under the same conditions. After several correctional steps as described in the standard, the heating value of coal was calculated from Eqn. 3.5.

$$Q_{net} = \frac{\left(Q_{gross} + Q_{v-p} - Q_h\right)(100 - M_{ar})}{\left(100 - M_{ad}\right) - Q_{M_{ar}}} \tag{3.5}$$

Where, Q_{net} is as-received net calorific value at constant pressure, Q_{gross} is as- determined gross calorific value at constant volume, Q_{v-p} is the constant volume to constant pressure heat correction, Q_h is heat of vaporization of water originating from hydrogen content in the coal sample, M_{ar} and M_{ad} are the as-received and as- determined moisture content in the coal respectively, and $Q_{M\,ar}$ is heat of vaporization of the as-received moisture value.

Table 3.1 shows the details of the equipment used during proximate and ultimate analyses of the coal sample. The equipment were adopted due to their wide range of respective parameter measurements. The results of the proximate and ultimate analyses are presented in section 4.2.

Table 3.1: Equipment used during proximate and ultimate analysis of coal sample

Equipment name	Model	Range	Accuracy
As One Crucible furnace	RMF-100	100 - 1200ºC	1.5%
Nenken Type adiabatic bomb	1013-B	Max. 50 MJ	2.5%

3.2.2 Combustion Stoichiometry Analysis

When coal is completely burnt in the presence of oxygen, CO_2, water vapour, and oxides of other chemical elements, like sulphur, present in the coal sample are formed. Combustion stoichiometry analysis leads to the determination of the exact amount of oxygen, and thus air, needed to completely burn the coal sample.

Gasification occurs under sub-stoichiometric supply of oxygen, thus the stoichiometric value of O_2 need to be determined. From the results of ultimate analysis (Table 4.1), the coal sample consisted of carbon, hydrogen, and sulphur which burn in oxygen to form respective oxides. The stoichiometric amount of oxygen needed to burn each element in the coal sample was found from combustion equations for the elements (Eqns. 3.6 -3.8). The sum of these individual oxygen needs gave the stoichiometric amount of oxygen for the fuel. Nitrogen is inert and is not expected to take part in the gasification reactions.

The complete combustion of carbon in oxygen is shown in Eqn. 3.6.

$$C + O_2 \rightarrow CO_2 \tag{3.6}$$

When molar masses are used: 12kg C + 32kg O_2 → 44kg CO_2

Eqn. 3.7 shows the complete combustion reaction of hydrogen in oxygen.

$$H_2 + 0.5O_2 \rightarrow H_2O \tag{3.7}$$

Substituting for molar masses: 2kg H_2 + 16kg O_2 → 18kg H_2O

Eqn. 3.8 shows the stoichiometric reaction between sulphur and oxygen,

$$S + O_2 \rightarrow SO_2 \tag{3.8}$$

Substituting for molar masses: 32kg S + 32kg O_2 → 64kg SO_2

The results above were summarized in Table 3.2. From the table it was observed that 2.3422 kg of oxygen was needed to completely burn 1 kg of the coal sample.

Let $m_{o,\,s}$ be the stoichiometric mass of O_2 needed to burn 1 kg of Mui Basin coal sample. Since the mass of O_2 in 1 kg of air is 0.233 kg, then the stoichiometric air/fuel ratio, AFR_{st}, is determined from Eqn. 3.9 below.

$$AFR_{st} = \frac{m_{o,s}}{0.233} \tag{3.9}$$

Let $\dot{m}_{coal}$ be the mass flow rate of coal used. The stoichiometric mass flow rate, $\dot{m}_{a,\,st}$ and volume flow rate, $\dot{V}_{a,\,st}$ of air, we determined using Eqns. 3.10 and 3.11 respectively.

$$\dot{m}_{a,st} = \dot{m}_{coal}.AFR_{st} \tag{3.10}$$

$$\dot{V}_{a,st} = \frac{\dot{m}_{a,st}}{\rho_a} \tag{3.11}$$

Table 3.2: Combustion analysis for 1 kg of the coal sample used

Constituents of coal	Mass fraction	Oxygen required (kg/kg of coal)	Mass of products (kg/kg of coal)
Carbon (C)	0.7264	1.9371	2.6635 (CO_2)
Hydrogen (H)	0.0589	0.4712	0.5301 (H_2O)
Sulphur (S)	0.0230	0.0230	0.0460 (SO_2)
Oxygen (O)	0.0891	-0.0891	-
Nitrogen (N)	0.0122	-	0.0122
Ash	0.0904	-	0.0904
Total	**1.0000**	**2.3422**	**3.3973**

Where ρ_a is density of air taken as 1.2 kg/m^3 (Rodgers & Mayhew, 2004).

Table 3.3 shows the summary of the stoichiometric flow properties as calculated from the equations above. From this table, AFR_{st} = 10.052 kg/h. In order to enhance gasification during the experiments, the *AFR* supplied was below this value since gasification reactions occur under limited oxygen supply. The flow rates used in this study were measured in volumetric form, hence the presentation of the mass and volume flow rates of air in the Table 3.3.

During this study, the input materials included air, air/oxygen mixture, steam, water and coal. Their applications are covered under Sections 3.7 and 3.11. Some of the equipment used include air blower, mixing chamber, boiler and gasifier. Other equipment for the flow and analysis of the syngas were gas analyzer, cooler and flow meters. The design and construction of these equipment are described in the subsequent sections in this chapter.

Table 3.3: Stoichiometric flow properties of air and coal used

Parameter	**Magnitude**
Stoichiometric air-fuel ratio, AFR_{St}	10.052 kg/h
Mass flow rate of coal feed	4 kg/h
Stoichiometric mass flow rate of air	40.21 kg/h
Stoichiometric volume flow rate of air	33.51 m^3/h

3.3 Experimental Design and Set-up

In designing the experiment for this research, the four basic steps recommended by Montgomery, (2001), were followed. First was identification of the problem to be investigated followed by selection of the input factors, their levels and range. The third step involved selecting the response variables, and lastly, selection of the experimental design.

The main input variables were the types of gasifying agents used. They included air, oxygen-enriched air, and steam/oxygen-enriched air mixture. Syngas compositions

and yields, and reactor temperatures were the response variables. These were identified from the screening experiments as explained in Section 3.7.

The experimental setup shown in Figure 3.1, consisted of a blower for pumping air into the mixing chamber where it mixed with pure oxygen (from cylinder), before being directed into the gasifier. The coal supply into the gasifier was constant at a pre- determined flow rate. Thermocouples, strategically placed along the height of the gasifier and connected to a data recorder, measured the gasifier temperatures.

The producer gas exited the gasifier at the top and was taken through a cooler. It was then sampled at predetermined 30-minutes time intervals, into Portable Multi-gas Analyzer TY-6331P (2% accuracy), where its composition was determined, especially CO, CO_2, H_2, CH_4, H_2O and N_2. The quality of syngas and performance of the gasification system were analyzed by determining heating values, cold gas and carbon conversion efficiencies. Due to the presence CO that is harmful, the study was conducted in open space to ensure safety of the personnel. The actual equipment set-up is shown in Figure 3.2.

3.4 The Existing JKUAT Gasifier

Two gasifiers were used during this research study. The first one was an existing gasifier at the JKUAT Thermodynamics Lab shown in Figure 3.3, and whose performance was to be investigated by variation of its operating conditions. It was a bench-scale fixed bed, updraft coal gasifier. The data obtained from experiments using this gasifier were used to optimize a modified gasifier that was fabricated based on the dimensions of the existing one shown in Table 3.4.

The gasifier consisted of three sections namely: the bottom chamber, the reactor section where gasification takes place and freeboard section where the gases expand and are partially cooled before exiting the gasifier. The construction of these parts is explained in section 3.8.

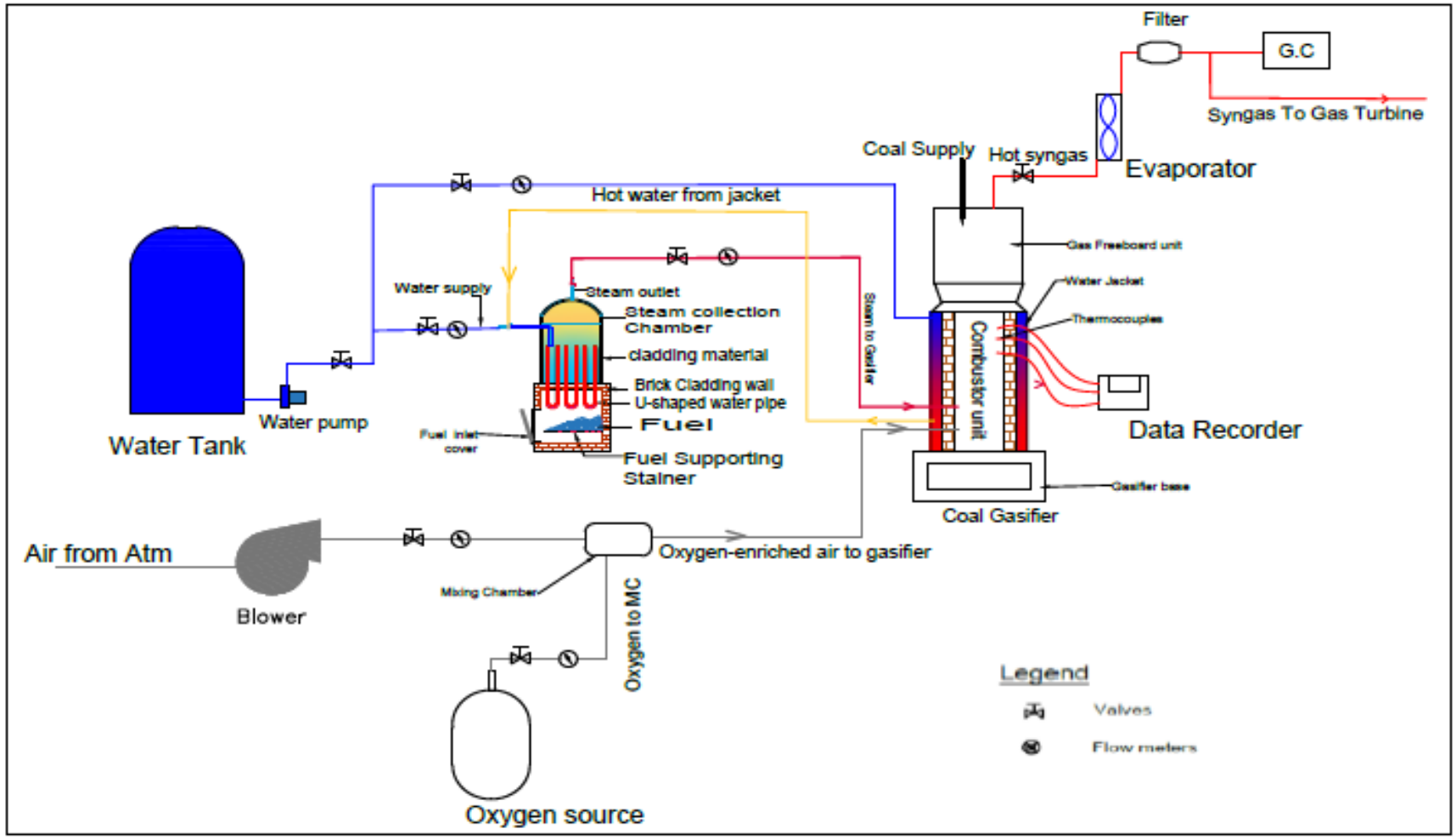

Figure 3.1: Schematic diagram of the system set-up

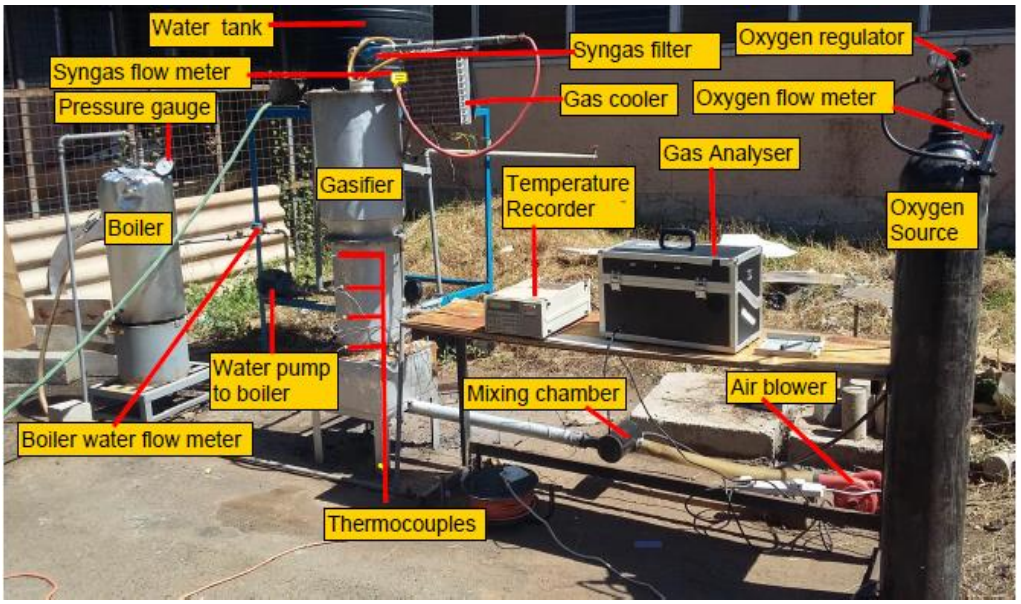

Figure 3.2: Actual equipment set-up

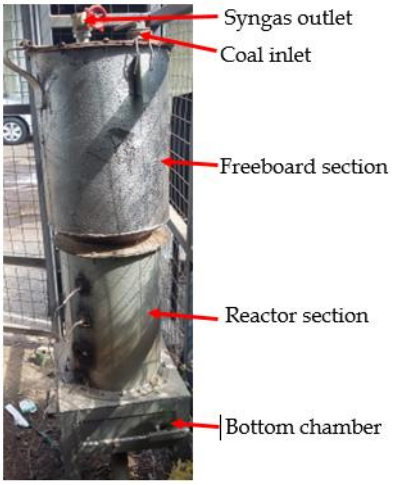

Figure 3.3: The existing gasifier

Table 3.4: Dimensions of the existing JKUAT gasifier

a) Reactor Section

Dimension	Magnitude
Height	500 mm
Inner diameter	244 mm
Refractory thickness	25 mm
Mild steel casing thickness	2 mm

b) Freeboard Section

Dimension	Magnitude
Height	500 mm
Diameter	360 mm
Wall thickness	2 mm
Bottom flange	400 mm dia. by 3 mm thick
Top flange	410 mm dia. by 3 mm thick

3.5 The Mixing Chamber

Mixing chamber is a device used for mixing two or more fluid streams to ensure a homogeneous particle distribution at the outlet. Based on the principle of conservation of mass, the sum of mass flow into and out of the chamber should be equal. In this research, pure oxygen and air streams were mixed in varied ratios and the mixture used for coal gasification. Variation of the mixture quality was achieved by varying the flow rates of the individual streams.

The mixing chamber used was a modification of an existing one, that had been designed for another application. This was necessitated by the differences in the volumes and mixture distribution required. The modification entailed increasing the dimensions to suit the volumes of the mixture needed for this

research and also to increase turbulence that would enhance proper mixing of the two streams.

3.5.1 Design Factors

The mixer design was based on the criteria proposed by Novosád *et al.*, (2017), namely; the required mixture volume and mixture homogeneity. The limiting volume of air needed was 33.51 m^3/h (Table 3.3). The mixture homogeneity was ensured through improved turbulence and residence time in the mixer.

For good quality syngas, the equivalence ratio should range between 0.2 to 0.35 depending on the coal type and the reactor conditions (Nzove *et al.*, 2019;Laciak *et al.*, 2016). Taking $\lambda = 0.35$, the ideal maximum air volume needed in this study was 11.73 m^3/h. To allow for losses, a volume of 15 m^3/h was adopted translating to 4.17×10^6 mm^3/s.

3.5.2 Mixing Chamber Construction

The mixer was made from a cylindrical MS pipe of diameter as shown in Figure 3.4, and thickness 2 mm. Based on mixer volume of 4.17×10^6 mm^3, the mixer length was determined using Eqn. 3.12.

$$L_{mc} = \frac{4V_{mc}}{\pi D_{mc}^2} \tag{3.12}$$

Where L_{mc}, V_{mc} and D_{mc} are mixer length, volume and diameter respectively.

Eqn. 3.12 above gives the mixer length to be 329.18 mm. Bakker & LaRoche, (2000) stated that the mixing length should not be less than 2.5D and thus the design is sufficient. However, in order to increase residence time and allow for proper gas mixing, a length of 400 mm was adopted. The design drawing and the picture of the new mixing chamber is shown in Figures 3.4 and 3.5 respectively.

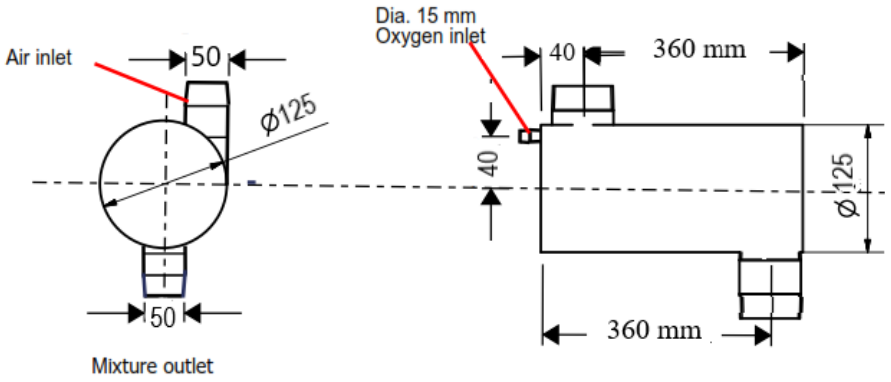

Figure 3.4: Design drawing of the mixing chamber used

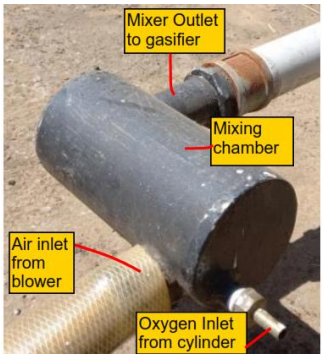

Figure 3.5: The mixing chamber used in this research

The off-set of the axis of air and oxygen inlets nipples (as shown in Figure 3.4) from the mixer central axis, was to create a swirl in the chamber that would enhance mixing of air and oxygen (Chen & Chen, 2011). The positioning of oxygen and air inlet pipes next to each other were to enhance turbulence in the chamber needed for proper mixing (Bakker & LaRoche, 2000). The outlet nipple was placed perpendicular to the chamber axis with no offset to allow free flow of the mixture into the gasifier. Detailed drawing of the mixing chamber is shown in Appendix C.

3.6 Steam Generator

A steam generator was designed to produce the steam used during gasification in this study. Various researchers have shown that steam/oxygen gasification generates syngas with improved quality due to enhanced production of H_2 and

CO gases (Zogala, 2014; Baranowski *et al*., 2017: Hervy *et al*., 2019). Thus, this research investigated the performance of the developed bench-scale coal gasifier when steam/oxygen mixture was used as oxidizer.

The boiler developed was a simple one-drum vertical water-tube type, which was easy to construct and was meant to generate nominal steam for the gasification process. The motion of water in the drum was by natural convection caused by thermo-siphon effect. Its main parts included the furnace and the steam drum.

3.6.1 Design Considerations

The design of the boiler was guided by the criteria recommended by Richmond, (1999). First was safety; the boiler was to be safe to operate. Second was steam conditions; it was to be able to generate steam at the desired rate and pressure. Third factor was cost; it was to be economical to construct and operate. The production cost was reduced by fabricating it using locally available materials.

Concerning steam flow rate, some researchers have studied coal gasification with maximum steam/coal ratios ranging from 0.75 to 1.26 (Zogala, 2014; Karimipour *et al.,* 2011; Lee *et al.,* 2002). They all recorded improved syngas quality with increasing steam/coal ratio. In this study, a steam/coal ratio of 1.25 was chosen, giving a steam flow rate of 5.0 kg/h. However, to allow for wide range of application and the losses due to leakages and evaporation, the boiler was designed for flow rate of 7.0 kg/h, a 40% increase (Basu *et al*., 2000)

Since the gasifier operated at 1.013 bars, the boiler design temperature and pressure were 200ºC and 1.5 bar respectively. The low temperature and pressure chosen reduced the cost of producing the boiler since it allowed use of less sophisticated materials, while still producing good quality steam for the study.

3.6.2 Design Parameters

Table 3.5 shows the design parameters and conditions of boiler and steam required for the gasification experiment in this research. Based on the mass conservation

principle, the maximum mass flow rate of water to the boiler was equal to the maximum mass flow rate of steam.

Based on the parameters listed in Table 3.5, various other parameters needed for boiler design were obtained from thermodynamic tables of properties of steam and water as shown in Table 3.6. The specific heat capacity of water was taken at 70°C, the nearest to the average temperature of water, which was 68.2° C. Since the saturation temperature of steam (111.4°C) was less than the design temperature of steam (200°C), (Tables 3.5 and 3.6), the steam was superheated (Rodgers and Mayhew, 2004)

The amount of heat required to heat 7 kg/h (0.00194 kg/s) of water at 25°C to steam at 200°C and 1.5 bar pressure is the sum of heat added at three stages; sensible heating, vaporization and superheating to 200° C.

Table 3.5: Boiler and steam design parameters

Parameter	**Magnitude**
Water temperature at inlet, T_1	25°C
Maximum design water flow rate into boiler	7.0 kg/h
Maximum design steam flow rate from boiler	7.0 kg/h
Design boiler operating pressure	1.5 bar
Design steam temperature at boiler outlet, T_3	200° C

Let $\dot{Q}_B$ be the total heat required by the boiler to generate superheated steam, $\dot{Q}_1$ be sensible heat required to raise water temperature from 25°C to 111.4°C, $\dot{Q}_2$ be heat required to vaporize saturated water to steam at 111.4°C and 1.5 bars, and $\dot{Q}_3$ be heat required to superheat steam from 111.4°C to 200°C. $\dot{Q}_1$, $\dot{Q}_2$ and $\dot{Q}_3$ were determined using Eqns. 3.13, 3.14 and 3.15 respectively.

Table 3.6: Properties of water and steam from tables (Rodgers & Mayhew, 2004; Cengel & Afshin, 2015)

Property	Magnitude
Saturation temperature of water at 1.5 bar, T_2	111.4°C
Specific volume of steam (at 1.5 bar, 200°C), v_s	1.445 m^3/kg
Specific heat capacity of water at 70°C, C_{pw}	111.4°C

$$\dot{Q}_1 = \dot{m}_{w,max}.C_{pw}.\Delta T \tag{3.13}$$

$$\dot{Q}_2 = \dot{m}_w.h_{fg} \tag{3.14}$$

$$\dot{Q}_3 = \dot{m}_s.C_{ps}.\Delta T \tag{3.15}$$

A boiler usually experiences heat losses of which the major ways include: through flue gas, surface heat losses, losses due to hydrogen in fuel and losses due to partial combustion of carbon to *CO* gas, (Harimi, 2008). These losses can reduce the boiler efficiency by up to 30%, (Lahijani & Supeni, 2018) Taking the boiler efficiency for this design to be 70.0%, then $\dot{Q}_B$ was determined from Eqn. 3.16, while mass flow rate of boiler fuel, in kg/h, was determined from Eqn. 3.17.

$$\dot{Q}_B = \frac{\dot{Q}_1 + \dot{Q}_2 + \dot{Q}_3}{0.70} \tag{3.16}$$

$$\dot{m}_{fb} = \frac{3600\dot{Q}_B}{HHV_{fb}} \tag{3.17}$$

Where HHV_{fb} is the higher heating value of fuel used in the boiler.

The maximum quantity of heat and fuel needed to generate required steam are summarized in the Table 3.7.

Table 3.7: Quantity of heat and fuel properties for steam generation

Quantity	Magnitude	Quantity	Magnitude
Boiler fuel	Charcoal	HHV_{fb}	26272 kJ/kg
$\dot{Q}_1$	0.7021 kW	$\dot{Q}_2$	4.3184 kW
$\dot{Q}_3$	0.3532 kW	$\dot{Q}_B$	7.6767 kW
$\dot{m}_{fb}$	1.05 kg/h		

3.6.3 Design of Steam Drum

This is the part of the boiler where water was heated and changed into steam. It consisted of water and steam chambers. The main design factors were enough volume to hold water and steam, large surface area for heat transfer to water, minimum heat loss from water and steam to environment, safety for the operators, and minimum floor space occupied by the boiler (Richmond, 1999; Kolmetz & Aprilia, 2011).

The boiler was to supply water flow rate of 7.0 kg/h, translating to water volume of 7.0×10^6 mm^3. To ensure adequate water and steam capacity, the water chamber volume was conveniently designed for double the water volume. It is also recommended that the water chamber should not exceed two-thirds of the drum volume (Nag, 2008). The design volumes chosen for the drum are thus summarized in Table 3.8. Ratio of steam chamber volume to total drum volume R_s is given by Eqn. 3.18:

$$R_s = \frac{V_s}{V_D} \tag{3.18}$$

Based on the required water and steam flow rates, the drum diameter was chosen as 250 mm. A short frustum, whose dimensions were conveniently chosen as indicated in Figure 3.6, was designed at the upper end of the drum for smooth steam flow.

Let $V_{s1\ and}$ V_{s2} be volumes of cylindrical and frustum sections of steam chamber. If V_s is the total volume of steam chamber, then from Eqn. 3.19, steam chamber height H_2 can be obtained.

$$V_s = V_{s1} + V_{s2} = \left[\frac{\pi D_2^2 H_2}{4}\right] + \left[\frac{1}{12}\pi H_1\left[D_2^2 + (D_2.D_1) + D_1^2\right]\right] \qquad (3.19)$$

The height H_3 of water chamber in the drum was determined from Eqn. 3.20.

$$V_w = \frac{\pi D_2^2 H_3}{4} \qquad (3.20)$$

The criteria used to design water tubes included: their arrangement was to allow plenty of space for flame path between them, they were to fit well in the furnace and their cost was to be economical (Nag, 2008). Based on these factors and the dimensions of the furnace, and the need to make the boiler simple, five U-shaped tubes were used. Figure 3.6 shows the schematic design of the boiler including the dimensions of the various components. The steam drum with tubes installed is shown in Figure 3.7.

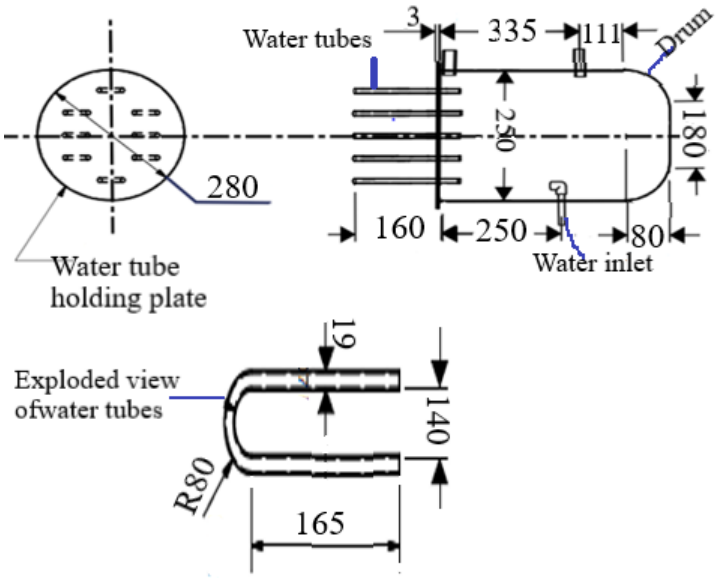

Figure 3.6: The schematic design of the boiler drum

Figure 3.7: The water tubes installed in steam drum

Some of the features of the water and steam chambers, as well as those of the water tubes are summarized in Table 3.8.

Table 3.8: The steam drum and tubes features

Feature	**Magnitude**
Volume of steam chamber (V_s)	8.0×10^6 mm^3
Volume of water chamber (V_w)	15.0×10^6 mm^3
Total volume of steam drum (V_D)	23.0×10^6 mm^3
Steam chamber volume to total drum volume ratio, (R_s)	0.3478
Height of cylindrical section of steam chamber, (H_1)	115.2 mm
Height of the water chamber, (H_2)	331.5 mm
Height of each tube hanging in the furnace (H_3)	157 mm
Number of water tubes, n	5

3.6.4 Design of Boiler Furnace

The furnace allowed combustion of fuel to release heat for steam generation. The design considerations for the furnace included enough space for complete fuel combustion, larger surface area for heat transfer, free flow of flue gas, compact

enough to minimize the cost of construction, and reduction in heat loss to the environment (Basu, 2000). Complete combustion of fuel under all operating conditions was essential to harness the maximum heat potential of the fuel under combustion. Figure 3.8 shows the schematic design of the boiler including the furnace section.

The boiler furnace was sized based on the heat release rate per unit furnace volume, qv expressed as shown in Eqn. 3.21. From this equation, the required furnace volume was determined and Eqn. 3.22 was used to determine the furnace height.

$$q_v = \frac{\dot{Q}_B}{V_F} \tag{3.21}$$

$$H_4 = \frac{V_F}{\pi D_5} \tag{3.22}$$

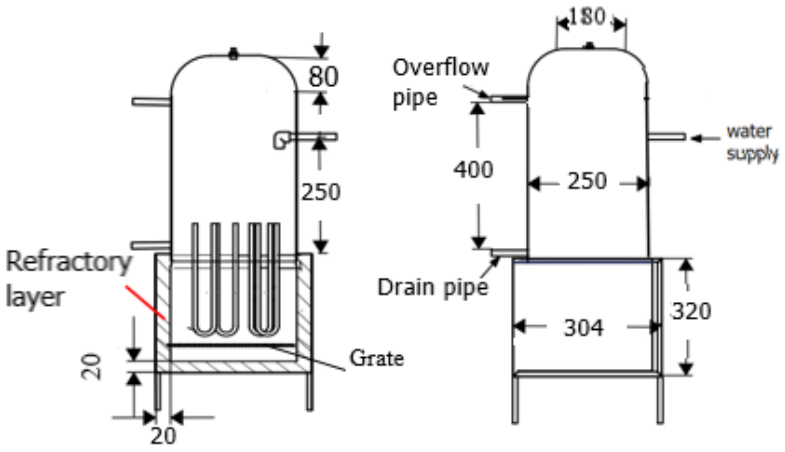

Figure 3.8: The schematic design of the boiler

Let A_t and A_p be the total heat transfer area of all the water tubes and the drum bottom plate respectively. A_t and A_p were determined from Eqns. 3.23 and 3.24, and their sum gave the total heat transfer area, A_{HT} in the furnace.

$$A_t = \pi D_t . H_3 . 2 . n \tag{3.23}$$

$$A_p = \frac{\pi D_4^2}{4} - \frac{\pi D_3^2 .2.n}{4} \tag{3.24}$$

Where D_t is the diameter of the water tube.

The typical range of qv for fuel like charcoal is 450 - 523 kW/m^3 **(**Basu, 2000). Likewise, the furnace combustion chamber diameter D_5 was limited by that of drum. The values chosen for qv and D_5 for this design together with the calculated value of furnace volume, height and the heat transfer areas are summarized in Table 3.9. It is notable from Table 3.9 that the tubes increased heat transfer area by 61.5%.

3.6.5 Construction of Steam Generator

The construction of the steam drum entailed cutting the materials needed according to the design shown in Figure 3.6. The materials used and method of construction is shown in Table 3.10. The water drain, inlet, and overflow pipes were each fitted with gate valves. A 3 mm thick flange, with holes for fastening bolts, was welded to the top part of the frustum. Another circular solid plate of similar thickness, with provisions for steam outlet, boiler pressure gauge and steam pressure relief valve connections was fastened to the top flange. Another plate with the U-shaped water tubes fixed was welded to the bottom of the drum.

Table 3.9: Summary of some boiler furnace parameters

Parameter	**Magnitude**
Heat release rate, q_v	4.50×10^{-7} **kW/mm3**
Furnace inner diameter, (D_5)	260 mm
Volume of combustion chamber, (V_F)	17.06×10^6 mm^3
Outer diameter of furnace (D_6)	304 mm
Height of furnace (H_4)	320 mm
Total tube surface area exposed to furnace heat (A_t)	93713.709 mm^2
The drum bottom plate heat transfer area (A_p)	58739.929 mm^2
Total heat transfer area in furnace (A_{HT})	152453.638 mm^2

The cylindrical furnace had a grate inside on which the fuel would be placed. The grate had 5 mm diameter holes to allow passage of air into the combustion chamber and ash to the bottom. A refractory lining inside the furnace was made from fire clay. While the top of the combustion chamber was left open to allow installation of the drum, the air inlet pipe was installed at the bottom of the chamber. A stand supported the furnace above the ground.

During operation, water supply from a tank to the boiler was done using DAYLIFF DDP 60 water pump with a maximum head of 7 m. The drum was filled with water to a depth of 330 mm, and the tubes, protruding inside the drum, would thus be filled with water. The tubes, also overhanging in the furnace, would be heated, thus heating the water in them and creating a convective current needed to generate the steam. The flue gases escaped through the openings between the drum base and the combustion chamber hence eliminating the need for a chimney. Table 3.10 summarizes the materials and the construction methods of the boiler.

Table 3.10: The dimensions of the boiler furnace

Parameter	Description
Material used for drum	3 mm thick MS sheet
Method of construction	Rolling and high pressure welding
Thickness of the refractory lining	20 mm
Furnace material	2 mm thick MS sheet
Method of construction	Rolling and welding
Dimensions of the stand	350 mm × 350 mm
Water tubes material	High-pressure MS pipes
Air inlet tube	50 mm dia. GI pipe

3.7 Screening Experiments

3.7.1 Need for Screening Experiments

Screening or characterization experiments are general preliminary experiments aimed at determining the main factors affecting the system from a pool of factors, (Montgomery, 2001). Initial test of individual variables is necessary in determining the variables with major effects in the experiments, which should be included in the main study (Bradley, 2007). They help in identifying the required range of values for specific input variables that are close to the optimal values of the system (Morshedi, & Akbarian, 2014).

In this study, screening experiments entailed proceeding from a known lower and higher levels of the effects of the input variables, up to a level where the relative importance of the variables could be assessed under the principle of factor of sparsity (Carlson and Carlson, 2005; TRP, 2007; Woods and Lewis, 2015, Schoen *et al*., 2019; Nair *et al*., 2008). Based on the level of influence of the variable, less important ones were eliminated and ones that are more influential adopted for main experiments. The experiments took three steps as proposed by Carlson *et al*., (2005). First step involved identifying the input variables to be studied, the second step was estimating a suitable range of the input variables, and lastly conducting the screening experiments to identify the input variables for the main experiments.

3.7.2 The Input Variables for the Screening Experiments

The input factors considered included the fuel particle size, the type of gasifying agent, and the quantity of the gasifying agent. Concerning fuel particle size, fixed-bed coal gasifiers can use fuel particles of diameter between 5 - 50 mm (Breault, 2010; Quaak et al., 1999). The range adopted was between 5 - 12 mm, because small fuel particles provide large surface area and enhance complete gasification reactions.

The types of oxidizing agents used in this study included: air, oxygen-enriched air, and mixture of oxygen-enriched air and steam. These were considered based on the

literature review and the quality of the syngas needed. Gasification with air involved use of atmospheric air. When oxygen-enriched air was used, the amount of oxygen in the mixture was increased gradually, with a pre-determined air feed kept constant, thus increasing the oxygen content in the gasifying medium. As for gasification with oxygen-enriched air/steam mixture, a constant amount of oxygen-enriched air and a varied amount of steam were supplied into the gasifier during gasification, thus varying the steam content in the mixture.

For pure air gasification, the variation was based on equivalence ratio air-fuel ratio, λ, determined from Eqn. 3.25.

$$\lambda = \frac{AFR_{act}}{AFR_{st}} \tag{3.25}$$

Where AFR_{act} is the actual air/coal ratio used and AFR_{st} is the stoichiometric air/coal ratio shown in Table 3.3 under Section 3.2.

In the case of oxygen-enriched air gasification, the quantity of oxygen-enriched air was measured in terms of oxygen/air ratio, (OAR), which was the ratio of oxygen content in air to the quantity of air supplied. This was achieved by mixing predetermined constant amount of air with varied amounts of pure oxygen using a mixing chamber. Lastly, for the gasification with oxygen-enriched air and steam, the quantity of oxygen-enriched air/steam mixture was measured in terms of steam/oxygen ratio, (SOR). This was a ratio of the amount of steam supplied to the amount of oxygen in the oxygen/air mixture supplied. The SOR was varied by varying the amount of steam supplied to the gasifier, while keeping constant the supply of a predetermined amount of oxygen/air mixture. Table 3.11 summarizes the range of quantities used for the gasifying agents during the screening experiments.

During these experiments, λ, OAR and SOR were varied in steps of 0.05. The lower ranges were based on the minimum need of the gasifying agent for gasification reaction to occur. The higher ranges helped identify the upper limits for the oxidizer

supply during the main experiments. The minimum OAR was based on the fact that normal air consists of 21% oxygen by volume while for SOR, the starting point was taken as zero steam supply.

Table 3.11: Gasifying agents and their range during screening experiments

Gasifying agent	Variable	Lower range	Upper range
Pure air	Equivalence ratio	0.05 - 0.20	0.50 - 0.65
Oxygen-enriched air	O_2/air ratio	0.21-0.36	0.91-1.06
Oxygen-enriched air/ mixture	Steam/O_2 ratio steam	0.0 -0.2	-

The main outputs for these screening experiments included the composition, and yield of syngas produced as well as the temperature in the reactor. These were monitored as the input variables were varied.

3.7.3 Conducting the Screening Experiments

The performance of the screening experiments involved preliminary activities in which the necessary materials and equipment were prepared before the experiments. It also entailed the actual experimental activities in which procedures were followed in the use of the inputs and the equipment in order to get preliminary outputs.

The procedure involved filling the water tank and assembling the gasification system components. The coal mass was then sieved using 3 different sieve sizes. This separated the fuel into three different particle-size categories: 5 - 6 mm, 6 - 9 mm and 10 -12 mm. The lower limit was constrained by the gasifier grate pore sizes which were of diameter 5 mm, while the upper limit was constrained by gasifier reactor height and diameter (Karimipour *et al.*, 2011) A shorter reactor height meant a shorter residence time hence shorter reaction time, requiring smaller fuel particles for efficient reactions.

Initially, the gasifier was heated under excess air to increase heating rate, until the temperature approached 550ºC, when λ was gradually reduced to 0.05 to reduce the bed heating rate. As the heating progressed beyond 600ºC, the amounts of fuel and air were increased gradually and the output gas composition monitored using ECOM J2KN PRO gas analyzer with an accuracy of ±2.0%. The temperature at which the *CO* level at the gasifier outlet reached 15% was recorded as the initial temperature to which the gasifier should be heated before any readings could be taken (Taba *et al.*, 2012). Equivalence ratio was then increased from 0.05 to 0.15 in steps of 0.05 and then to between 0.50 and 0.65 to test for the upper limit. The reactor was then allowed to cool gradually down to 700ºC.

Coal particle sizes were changed to 6 - 8 mm and later to 10 -12 mm categories, and the same procedure followed for each particle size. Based on the results, coal particle size of 5 - 6 mm was adopted and used in subsequent studies since it had the best yield of *CO*, indicating better reaction compared to the other sizes.

Concerning coal feed, three values 4 kg/h, 5 kg/h and 6 kg/h were chosen based on the feed rate of 5 kg/h used by Nzove *et al.*, (2019) whose gasifier was being improved. The flow rates were limited by the size of mixing chamber and gasifier used. Though 5 kg/h feed gave better gas yield, 4 kg/h was adopted for this study due to the limited size of mixing chamber designed based on the materials available.

After cooling the system down to 700ºC, the next set of experiments were conducted using $0.21 \leq OAR \leq 0.36$ and $0.91 \leq OAR \leq 1.06$, in steps of 0.05. The coal feed rate and particle size were kept constant at 4 kg/h and ≤ 6 mm respectively. The system was again cooled to 700ºC and the last set of screening experiments conducted by fixing *OAR* at 0.36 and gradually introducing steam from the boiler, with steam/oxygen ratio (SOR) increasing between $0.00 \leq SOR \leq 0.3$.

During air and O_2/air mixture experiments, the gas composition in terms of CO, NO_x and CO_2, the reactor temperature and the gas yield were monitored as the outputs. In the case of O_2/air/steam mixture, the reactor temperature and gas yield were the main outputs. The gas composition was not considered since the exhaust gas analyzer used for these preliminary experiments could not measure amount of H_2 in the producer gas. This was used since these were preliminary experiments that were to inform the main experiments described in Section 3.11.

3.7.4 The Identified Variables for the Main Experiments

From the screening experiments, it was noticed that a mixture of oxygen and air would give an improved quality of syngas evidenced by improved yield of CO compared to air gasification. When steam was introduced into the system, the system appeared unstable for a while before stabilizing. This was attributed to the higher heat capacity of water that led to sudden reduction in temperature. Therefore, small amount of steam was gradually supplied into the gasifier during heating.

From these experiments, three oxidizing agents were identified for further investigation during the main experiments. They included air varied in terms of air-fuel equivalence ratio (λ), oxygen-enriched air varied in terms of oxygen/air ratio (*OAR*), and steam/oxygen-enriched air varied as steam/oxygen ratio (*SOR*). These and other variables identified from screening experiments and their values or range of values are summarized in Table 3.12. Other parameters like mass flow rate of coal and coal particle size were kept constant throughout the main experiments. The output variables identified were producer gas and syngas yields, syngas composition, and the reactor temperature.

Table 3.12: The variables for the main experiments

Property/ Variable	Range
Coal flow rate	4 kg/h
Coal particle size	5 - 6 mm
Air feed rate	$0.1 \leq ER \leq 0.45$
Oxygen-enriched air feed rate	$0.21 \leq OAR \leq 1.0$
Minimum reactor gasification temperature	700ºC
Minimum steam feed rate to stabilize reactor	$SOR_{min} = 0.05$

3.8 Design of the Heat Regulation System

Development of heat regulation system (HRS) entailed design and fabrication of a system to regulate the reactor temperature for efficient gasifier operation. Gasification reactions are temperature dependent - very high temperatures promote combustion reactions, while very low temperatures inhibit reactions in the gasifier hence the need for reactor heat regulation.

3.8.1 Design Criteria

The design of the heat regulator was based on criteria proposed by Kakac *et al.*, (2002). The criteria included simplicity and ease of construction, heat exchange surface area, and flexibility to allow future modifications, cost effectiveness, compactness, and maintenance requirements.

Two methods were considered in this study: wall membranes, and water jackets. They were subjected to the criteria mentioned above and the scores are presented in Table 3.13. Based on the scores, water jacket was chosen and was constructed around the reactor section of the gasifier.

The HRS was assumed to take the form of a double pipe counter-flow heat exchanger (Figure 3.9). The fluids were hot reactor gases and the cooling water in the jacket, both of which entered and exited the exchanger from the opposite ends (Chaudhari & *Adroja,* 2014; Mazumder & Mandal, 2016).

Table 3.13: Heat exchanger design criteria scores

Heat Exchange Method	Criteria				
	HE surface area	Flexibility	Compactness	Ease of construction	Cost
Wall Membranes	✓	X	✓	X	X
Water Jackets	✓	X	✓	✓	✓

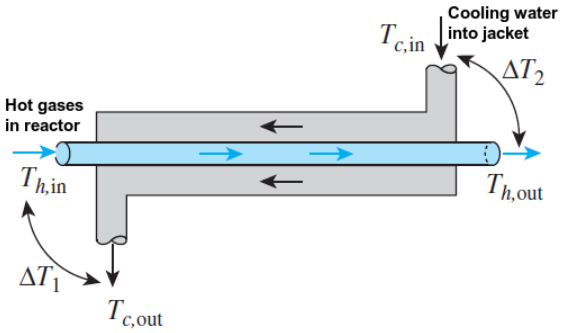

Figure 3.9: Counter-flow double pipe heat exchanger configuration (Cengel & Afshin, 2015)

The logarithmic mean temperature difference (LMTD) method, governed by Eqn. 3.26, was used for sizing the heat exchanger (Cengel & Afshin, 2015; Lazova et al., 2016; Hussein, 2015).

$$\dot{Q} = UA(\Delta T_{LM}) = \frac{\Delta T_{LM}}{R_T} \tag{3.26}$$

Where $\dot{Q}$ is the heat transfer rate, U is the overall heat transfer coefficient, A is the total heat transfer area, ΔT_{LM} is the logarithmic mean temperature difference, and R_T is the total thermal resistance for a fouled heat exchanger surface.

ΔT_{LM} and R_T were determined from the expressions in Eqn. 3.27 and 3.28 respectively (Cengel & Afshin, 2015; Mazumder & Mandal, 2016; Theodore et al., 2011).

$$\Delta T_{LM} = \frac{\Delta T_1 - \Delta T_2}{\ln\left(\frac{\Delta T_1}{\Delta T_2}\right)} \tag{3.27}$$

$$R_T = \frac{1}{UA} = \frac{1}{h_i A_i} + \frac{R_{fi}}{A_i} + \frac{1}{2\pi k_1 L}\ln\left(\frac{d_2}{d_1}\right) + \frac{1}{2\pi k_2 L}\ln\left(\frac{d_3}{d_2}\right) + \frac{R_{fo}}{A_o} + \frac{1}{h_o A_o} \tag{3.28}$$

Where, U_i and U_o are overall heat transfer coefficients for reactor inner and outer surfaces respectively, A_i and A_o are heat transfer areas for reactor inner and outer surfaces respectively, h_i and h_o are convective heat-transfer coefficients for reactor gases and jacket water respectively, R_{fi} and R_{fo} are fouling factors inside and outside the reactor respectively, k_1 is thermal conductivity of reactor refractory material (fireclay brick), k_2 is thermal conductivity of reactor casing material (mild steel plate), d_1 and d_3 are inner and outer diameters of reactor respectively, d_2 is the intermediate diameter of reactor mild steel casing, and L is the height of the reactor section of the gasifier.

The temperatures used in the design are shown in Table 3.14. It was notable that heat exchanger outlet temperature $T_{c,\,out} = 100^oC$ was desired since the hot water was to be re-used in the boiler. The maximum reactor temperature measured during the study was 1221.3^oC, but 1500^oC was chosen to ensure safety of the system. Gasification reactions occur at temperatures between 700^oC - 900^oC hence the choice of $T_{h,\,out}$ (Begum et al., 2013).

Table 3.14: Temperatures considered for the design of the heat exchanger

Temperature	Design magnitude
Inlet temperature of water into jacket, $T_{c,in}$	25º C
Desired outlet temperature of water from jacket, $T_{c,out}$	100ºC
Maximum reactor temperature before cooling, $T_{h,in}$	1500ºC
Desired reactor temperature after cooling, $T_{h,out}$	700ºC
Temperature difference at HE inlet, ΔT_1	1400ºC
Temperature difference at HE outlet, ΔT_2	675º C
Mean temperature of cooling water, $T_{m,w}$	62.5ºC

The cross-sectional design of the gasifier reactor is shown in Figure 3.10. Its dimensions are summarized in Table 3.15.

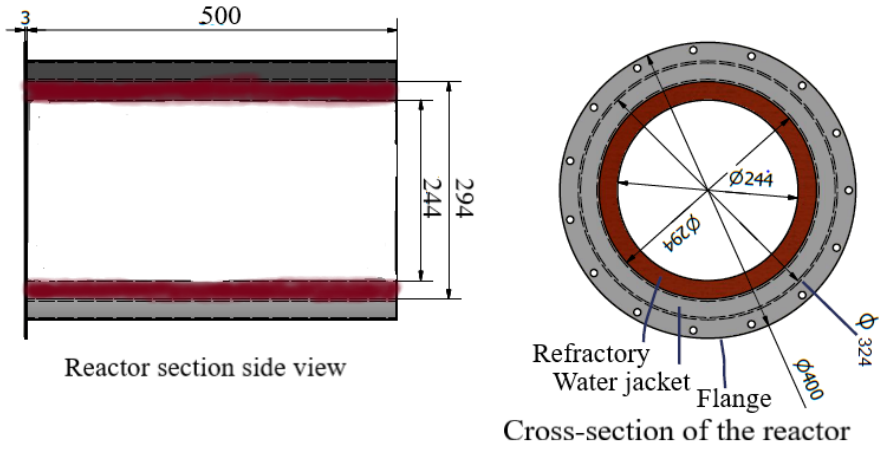

Figure 3.10: Schematic drawing of the reactor section with water jacket

Table 3.15: Dimensions of the reactor section of the gasifier

Dimension	Magnitude
Height of the reaction chamber, *L*	500 mm
Inner diameter of the reaction chamber, *d*1	244 mm
Intermediate inside diameter of the mild steel casing, *d*2	294 mm
Intermediate outside diameter of the mild steel casing, *d*3	296 mm
Outer diameter of the water jacket, *d*4	320 mm
Thickness of the metal sheet used, *tr*	2 mm

Some of the properties used in Eqn. 3.28 were obtained from various heat transfer analysis tables and resources, and are summarized in Table 3.16.

Table 3.16: Heat transfer properties of the reactor section (Cengel & Afshin, 2015; Theodore et al. 2011; Whitelaw, 2020; Engineering Edge, 2020; Kakac & Hongtang, 2002; TEMA, 2007; Shan, 2001)

Property	Magnitude	Property	Magnitude
h_i	56.78 W/m^2-K	h_O	3000 W/m^2-K
k_1	1.8 W/m-K	k_2	45.3 W/m-K
R_{fi}	0.001761 m^2-K/W	R_{fo}	0.000352 m^2-K/W
C_{pw} at T_{mw} and 1 atm.	4186 J/kg-K	ρ_w at T_{mw} and 1	982.2 kg/m^3

Assuming that no heat was lost to the environment, since the reactor was insulated by lagging, for a steady state heat transfer, heat lost from the hot gases equals the heat gained by the cooling water, which equals to the overall heat duty. This is shown in Eqn. 3.29, from which the mass flow rate of water into the heat exchanger was determined. The volume flow rate of water was determined using Eqn. 3.30.

$$\dot{Q} = \dot{m}_g C_{pg} (T_{h,\,in} - T_{h,\,out}), = -\dot{m}_W C_{pw} (T_{c,\,out} - T_{c,\,in}) \quad (3.29)$$

$$\dot{V}_W = \dot{m}_W / \rho_W \tag{3.30}$$

where subscripts g and w denote hot gases and cooling water respectively, and C_p is the specific heat capacity of the fluid.

These heat exchanger parameters are summarized in Table 3.17.

The maximum design volume flow rate of water through the jacket at maximum design reactor temperature (1500°C), was determined as 136.42 l/h or 2.27 l/min.

Table 3.17: Summary of some HRS heat transfer parameters

Parameter	Magnitude	Parameter	Magnitude
A_i	0.3833 m^2	Q	11684 W
A_o	0.4650 m^2	m_w	134 kg/h
R_T	0.08506 K/W	V_w	136 l/h

The volume of the jacket is given by the expression in Eqn. 3.31 from which d_4, which is the outside diameter of the jacket was determined.

$$V_j = \frac{\pi L}{4}\left(d_4^2 - d_3^2\right) \tag{3.31}$$

Considering the volume of the jacket to be 2.274 litres or 2.274×10^6 mm^3, and the values of l and d_3 are as shown in Table 3.15, then the value of d_4 was found to be 305.62. A value of 320 mm was adopted to take care of the losses that may occur, hence the value shown in the table.

To supply the water through the HRS, a three-speed DAYLIFF DQ25/6 water pump was used. It had a maximum flow rate and pressure of 5.5 l/min and 10 bars respectively. Given the HRS maximum design flow rate of 2.27 l/min, the bigger pump flow rate was chosen so as to take care of any losses and

accommodate future sys- tem expansions in terms of water needs. The variety of pump speeds enhanced the regulation of water flow through the system.

3.9 The Modified Gasifier

This gasifier was an improvement of the existing gasifier. Its dimensions were based on those of the existing one, but with the inclusion of a heat regulation system (HRS) around the reactor section. Figure 3.11 shows the schematic design of the gasifier while Figure 3.12 shows the fabricated modified gasifier

The bottom chamber of the gasifier was a steel box within which was installed a perforated grate which allowed air to flow upwards and ash to pass downwards. The Air-oxygen mixture inlet pipe was installed from below the box, 15 mm below the grate. The gasifier stood on angle lines welded to each corner of this chamber.

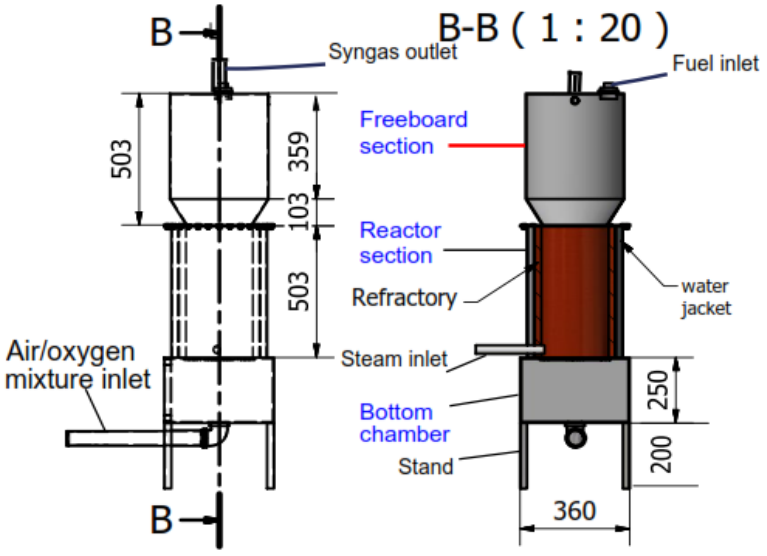

Figure 3.11: Various components of the optimized gasifier

The reactor chamber steel casing was lined with a refractory brick 20 mm thick while a water jacket, designed in Section 3.7, was installed around it. The chamber had four holes through which thermocouples were inserted for gasification temperature measurement. The reactor was welded to the bottom

chamber and near its base was a steam inlet pipe. At the top edge, a flange, 3 mm thick, was welded and fastening holes provided for the attachment of the freeboard section.

Figure 3.12: The modified gasifier

The freeboard section was a hollow chamber, situated above the reactor, for residual reactions of the gases and their free expansion before exiting the gasifier. Its lower end was shaped into a conical frustum and was welded on a flange that attached it to the reactor section. Another 3 mm thick flange was welded to its top end on which a 3 mm thick circular plate was fastened to seal the gasifier, with a gasket in between to ensure a fluid tight sealing. This top flange had provisions for gas exit pipe, pressure relief valve, and coal inlet.

3.10 Rig Instrumentation

This research needed different instruments for measurement of several parameters including flow rates, pressure, temperatures and gas compositions some of which are shown in Figure 3.13. Boiler feed water flow rate was measured by MID Brass Water Meter R315 of ±5.0% accuracy, while boiler pressure was measured using MEIXU MX-YB-02 (±3.0% accuracy) pressure gauge which was easy to read and was stable even at higher pressure fluctuations. The steam flow rate into the gasifier

was measured using LUGBML DN40 Vortex Flow Meter of ±1.0% accuracy, which had high accuracy, wide range and minimum pressure loss.

The mass of gasifier coal feed was measured using Precision EHW30H Industrial weighing scale of ±2.5percentage accuracy. The syngas output (volume flow rate) was measured using Krohne H250 M40 Variable Area flow meter with ±1.5% accuracy. The composition of the syngas produced was analyzed using in-line Portable Multi-gas Analyzer TY-6331P (Figure 3.14) of ±2.0% accuracy with the ability to analyze wide range of specific gases in a given mixture.

Type-K thermocouples of ±0.75% accuracy were used in measuring reactor temperature due to their durability and ability to measure wide temperature range of up to 1300°C. They were connected to Advantest TR2724 Multi-channel Digital Recorder (±1.0% accuracy), with an in-built computer from where temperature printouts were obtained. The temperatures of steam and HRS outlet water were measured using WSS Bi-metal Temperature Gauge of ±1.5% accuracy, while that of feed water to the cooling system and boiler was measured by an immersion-type digital Hanna HI98501 thermometer, of ±2.5% accuracy.

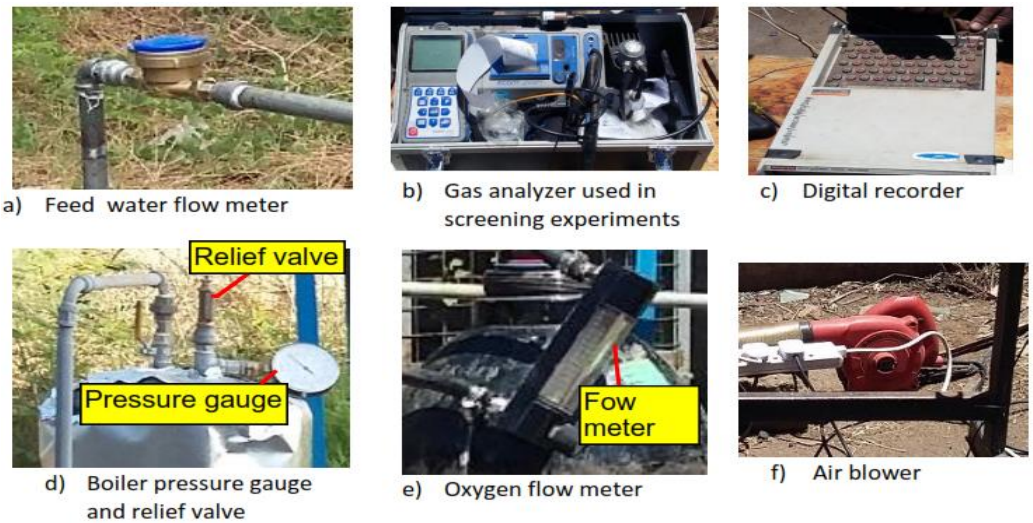

a) Feed water flow meter
b) Gas analyzer used in screening experiments
c) Digital recorder
d) Boiler pressure gauge and relief valve
e) Oxygen flow meter
f) Air blower

Figure 3.13: Some of the instruments used

Figure 3.14: Multi-gas Analyzer TY-6331P

The air supply to the mixing chamber was through Black + Decker BDB530 Variable- speed blower, which consumed less power, enabled variation on flow rates, and produced less noise when operating. The air flow rate was, however, measured using Aalborg in-Line M-type flow meter, with accuracy of ±3.0%. PTFE-Single glass flow meter type P16A6-BC0 was used to measure oxygen flow rate to the mixing chamber. This low cost and easy to read tube flow meter had an accuracy of ±2.0% and a repeatability of ±0.25%.

3.11 Experimental Procedure

This study was conducted using the earlier designed fixed-bed gasifiers, which operated at atmospheric pressure. To achieve the objectives of this study, four experiments were conducted. Experiment 1 involved gasification with pure air, while experiment 2 was on gasification with oxygen-enriched air without reactor heat regulation. Experiment 3 involved gasification with oxygen-enriched air with reactor heat control, while experiment 4 was on gasification with a combination of oxygen-enriched air and steam.

At the beginning of the experiment, some coal was added on the bed, air blower switched on, the fuel ignited and the gradual bed heating started. As the bed heating progressed, water heating in the boiler also commenced. Once the bed temperature reached 500 ^{o}C, 0.3 m^3/h steam feed into the gasifier started to stabilize bed conditions (Lee *et al*., 2011) The reactor bed was heated to 700^{o} C, as predetermined from the screening experiments, taking an average of 2 hours, consistent with the findings by Soria-Verdugo *et al*., (2019)

When the bed temperature approached 700^{o} C, coal and steam feeds were enhanced to 4 kg/h and 5% respectively, as identified from Section 3.7. These rates were constant for all experiments except during steam gasification. Thirty minutes after enhancing coal and steam feeds, the conditions in the gasifier were stable and initial readings of reactor temperature and producer gas sample were taken, a process that lasted for 15 minutes for each run.

In Experiment 1, effect of using air on gasification of Mui Basin coal was investigated. Air input was varied based on air-fuel equivalence ratio (λ), in steps of 0.05, from $0.1 \leq \lambda \leq 0.45$. The air flow rate was regulated using valves and flow meters. The data obtained are presented and analyzed in Section 4.3.

In Experiment 2, oxygen-enriched air (*OEA*) was used as gasifying agent and was varied based on oxygen/air ratio (*OAR*). This was the ratio of volume of oxygen in the oxidizer to the total volume of oxidizer used. Air at $\lambda = 0.25$, as derived from Experiment 1, was used as initial oxidizer since it yielded high amounts of H_2 and *CO* with low concentrations of N_2 (Figure 4.1 in Section 4.2). With $\lambda = 0.25$ kept constant, the concentration of O_2 in the oxidizer was increased gradually, from an external source to achieve the $0.21 \leq \text{OAR} \leq 1.1$ range used varied in steps of 0.1. The results obtained are presented and analyzed in Section 4.4.

The gasifier used in Experiments 1 and 2 is shown in Figure 3.3, and is available at the JKUAT Thermodynamics laboratories. An optimum OAR and its related temperature at which the best quality syngas was realized was noted. Based on this temperature, a heat regulation system (HRS) for the gasifier was developed (Section 3.8) to optimize the process. A new modified gasifier was then fabricated with the HRS included as explained in Section 3.9 (Figure 3.12). The modified gasifier was then used for the subsequent experiments 3 and 4.

During Experiments 1 and 2, it was noted that at higher values of λ and OAR, the reactor temperatures went beyond the optimum gasification temperatures of

between 700 - 900 °C. In Experiment 3, the reactor temperature was regulated to within this range using the HRS. The procedure for Experiment 3 was similar to that of Experiment 2 save for the inclusion of temperature control. This temperature control involved appropriately adjusting water flow rate in HRS according to the prevailing temperatures. The results for Experiment 3 are analyzed in Section 4.4.

Experiment 4 involved investigating the effect of mixture of steam and oxygen- enriched air on coal gasification process with the oxidizer content varied based on Steam/oxygen ratio (*SOR*). This was the ratio of volume of steam to that of oxygen present in the oxidizer. From Experiment 3, syngas quality was highest at 0.71 *OAR* based on syngas lower heating value (LHV) (see Section 4.4). However, 0.61 *OAR* was used in Experiment 4, since more oxygen would come from steam. With oxygen supply kept constant at 0.61 *OAR*, the steam concentration was increased gradually to vary SOR between 0.05 and 0.60, in steps of 0.1. The steam used was from the boiler developed earlier. An optimum SOR at which the syngas LHV was highest was then noted. Results from Experiment 4 are presented in Section 4.5.

During this study, reactor temperatures were monitored using four type-K thermo- couples that were immersed in the bed at various positions through the holes provided along the height of the reactor. Another thermocouple located at the freeboard section measured the temperature of syngas as it expanded. The thermocouples were connected to a data logger, with an in-built computer, to which the temperatures were recorded and analyzed.

The producer gas from the gasifier was passed through a heat exchanger where it was cooled to an average temperature of between 60º C and 80º C. Thereafter, a sample was taken to a Portable Multi-gas Analyzer TY-6331P (2% accuracy) from which its composition was analyzed. The producer gas yield was measured using gas flow meter. The syngas yield was determined as the volume of syngas generated per unit mass of fuel consumed in gasifier on dry basis (Equation 3.32) and was expressed in m^3/kg of coal (Karimipour et al., 2011).

$$Y_{syn} = \frac{Y_{prod}\left(X_{CO} + X_{H_2} + X_{CH_4}\right)}{\dot{m}_{coal}} \quad (3.32)$$

Where Y_{syn} and Y_{prod} are syngas and producer gas yields respectively, and X_i, are mole fractions of gas the species in the producer gas as determined by the gas analyzer. $\dot{m}_{coal}$ is the mass flow rate of coal.

3.12 Gasifier Performance Parameters

The syngas quality was measured in terms of its lower heating value (LHV). The syngas LHV depended on the percentage concentrations of CO, H_2 and CH_4 in the producer gas and was determined from the relation in Eqn. 3.33 (Tasma and Tanase, 2012)

$$LHV_{gas} = X_{CO}LHV_{CO} + X_{H_2}LHV_{H_2} + X_{CH_4}LHV_{CH_4} \quad (3.33)$$

Where, X_i is the mole fraction of each gas species.

The LHVs for the gas species are shown in Table 3.18 (Tasma and Tanase, 2012).

Performance of the gasifier was analyzed based on the cold gas efficiency (CGE) (Dascomb, 2013) and carbon conversion efficiency (CCE). CGE is the percentage of the chemical energy of coal that is recovered in the cooled syngas (Botero *et al.*, 2013; Syed *et al.*, 2012). CCE represents the amount of carbon in the biomass material, which is converted into gases (Ahmad *et al.*, 2015; Ramarao *et al.*, 2016).

Table 3.18: LHV of the gas species in syngas

Gas	LHV(MJ/Nm^3)
Carbon monoxide	13.1
Hydrogen	11.2
Methane	37.1

CGE and CCE were determined from the relations in Eqns. 3.34 and 3.35 respectively.

$$CGE = 100\left[\frac{\dot{V}_{gas}}{\dot{m}_{coal}} . \frac{LHV_{gas}}{LHV_{coal}}\right] \tag{3.34}$$

$$CCE = 100\left[\frac{\dot{V}_{gas}}{X_{c,coal}\,\dot{m}_{coal}}\left(\frac{12X_{CO}}{28} + \frac{12X_{CO_2}}{44} + \frac{12X_{CH_4}}{16}\right)\right] \tag{3.35}$$

Where LHV_{coal} is the lower heating value of coal feed, $\dot{V}_{gas}$ is the syngas volume flow rate and $\dot{m}_{coal}$ is the mass flow rate of coal feed, and $X_{c,\,coal}$ is the carbon percentage in the coal sample used as fuel.

3.13 Measurement Uncertainty Analysis

Measurement uncertainty characterizes the dispersion of the values of measurement that could generally be attributed to the measurand (Rendall *et al.*, 2016). Any measurement made always has an error associated with it, no matter the precision of the measuring tool. Uncertainty is probabilistic information and the probability density function attributed to a measurement result gives the range of results around which the measurement value has a specific probability to contain the true value (Nicola & Dirnberger, 2017).

Alan & Reza, (2012) classified measurement errors into two groups; systematic and random errors. Systematic errors describe measurement inaccuracies that are consistently in one direction, either positive or negative, are not easily detectable and cannot be analyzed statistically. They are caused by system disturbance during measurements, effect of environmental changes, wear in the instruments, among others. On the other hand, random errors are perturbations or statistical fluctuations of the measurement in either side of the true value caused by precision limitations of the instrument. They can be analyzed statistically and may be reduced by averaging repeated measurements. The causes of random errors may include electrical noise and human error when taking measurements by observation of an analogue gauge. In this study,

uncertainty has been analyzed under two categories: instrumentation uncertainty and statistical uncertainty, each of which is a combination of systemic and random errors.

During measurement operations in this study, it was important that errors were minimized and the remaining uncertainty existing in any instrument output reading was quantified. By using up-to-date measuring instruments and reducing disturbances on the instruments as possible, systematic errors were reduced. As for random errors, several readings for each interval were taken where possible and an average value recorded as the output reading. This reduced human effects especially on reading of analogue instruments like pressure gauges.

However, some parameters like carbon conversion efficiency and lower heating value were determined by combining two or more individual measurements of separate physical variables like flow rates and mole fractions in syngas. In such cases, special consideration was given to determining how the error levels in each separate measurement would be combined to give the best estimate of the uncertainty in the calculated output quantity.

3.13.1 Instrumentation Uncertainty Analysis

The accuracy of a measuring instrument is an indication of how close the actual reading of the instrument is to the correct value. However, it is more common to quote the inaccuracy or measurement uncertainty value rather than the accuracy value for an instrument (Alan and Reza, 2012). Inaccuracy or measurement uncertainty is the extent to which a reading might deviate from the true value. It is often given as a percentage of the full-scale reading of an instrument. Instrumental uncertainties are usually estimated by considering the measuring procedure and examination of the measuring instruments to estimate the reliability of the measurements.

Several instruments were employed to measure the various parameters during this research study each with a different level of uncertainty. The relative

uncertainties for each parameter measured during this research are shown in Table 3.19. These are related to the uncertainties provided by the manufacturers of the respective measuring instruments.

Most of the instruments had a relative error of 3% or less. The air and water flow meters had slightly higher relative errors attributed to variation in weather patterns through the day thus increasing the random error. Despite the fact that syngas analyzer is quite precise, its relative error of ± 2% was attributed to the non-linear detector response in the analyzer which is sensitive to viscosity variations in the gas (Dascomb, 2013). Since viscosity of gases increase with increasing temperature, the syngas was cooled before sampling. But the varying temperature of the sampled gas after cooling, still affected to, small extent, the sensitivity of the analyzer detector. The sampled gas temperature varied between 70° C and 106° C depending on the prevailing temperature in the reactor as seen in the next chapter.

The carbon conversion efficiency (CCE) was evaluated from flow rates of producer gas and coal feed, and the carbon contents of the producer gas and coal, Eqn. 3.35.

Table 3.19: Experimental instrumentation relative errors

Parameter	Relative uncertainties
Reactor temperature	± 0.75%
Water flow rate	± 5.0%
Coal mass	± 2.5%
Gas composition	± 2.0%
Steam flow rate	± 1.0%
Air flow rate	± 3.0%
Oxygen flow rate	± 2.0%
Syngas flow rate	± 1.6%
Steam temperature	± 1.5%
Feed water temperature	± 2.5%

Based on the instrumentation inaccuracies, the total uncertainty in the values of CCE, expressed as a percentage, was determined using Kline and McClintock, (1953) method shown in Eqn. 3.36.

$$\frac{\sigma}{CCE} = 100\left[\sqrt{\left(\frac{\sigma_{V_g}}{\dot{V}_g}\right)^2 + \left(\frac{\sigma_{m_f}}{\dot{m}_f}\right)^2 + \left(\frac{\sigma_{X_f}}{X_f}\right)^2 + \left(\frac{\sigma_{X_{CO}}}{X_{CO}}\right)^2 + \left(\frac{\sigma_{X_{CO_2}}}{X_{CO_2}}\right)^2 + \left(\frac{\sigma_{X_{CH_4}}}{X_{CH_4}}\right)^2}\right] \quad (3.36)$$

Where σ_i is the uncertainty in the measuring instruments for the respective quantities (Table 3.19), X_i is the mole fraction of the element in the total sample and $\dot{V}_{gas}$ is the volumetric flow rate of the producer gas, while $\dot{m}_c$ is the mass flow rate of coal.

From Eqn. 3.35, the uncertainty on carbon conversion efficiency for steam/oxygen mixture gasification was found to be 4.81%. The uncertainties for lower heating value, syngas yield and cold gas efficiency were calculated in similar manner and the results summarized in Table 3.20.

Table 3.20: Uncertainties for derived properties of syngas

Property	Uncertainty
Syngas yield, Y_{syn}	4.5%
Lower heating value, LHV	4.33%
Cold gas efficiency, CGE	5.46%
Carbon conversion efficiency, CCE	4.81 %

As can be seen from Table 3.20, all the derived properties had uncertainties below 5% except cold gas efficiency, which suggests that the data obtained were good representation of the system performance. As opposed to the other quantities that had their error calculated from primary measured values, CGE uncertainty calculation included the uncertainty from LHV of the syngas, which was another

derived property. This may have caused the uncertainty in CGE to be slightly higher. Dascomb, (2013) obtained up to 12% uncertainty in gasification efficiencies.

3.13.2 Statistical Uncertainty Analysis

For this section, gas yield obtained from gasification with oxygen-enriched air/steam mixture was taken as sample to help evaluate statistical uncertainty. Standard deviation was the method chosen to characterize the spread of the data set. Though standard deviation was slightly greater than the average deviation, it was adopted due to its association with the normal distribution that is frequently encountered in statistical analyses. Table 3.21 shows the producer gas yield obtained from gas flow meter during the coal gasification with steam/oxygen mixture as the oxidizer.

The mean value of the sample results above were determined using Eqn. 3.37.

$$\bar{Y} = \frac{1}{N}\sum Y_i \tag{3.37}$$

The percentage standard deviation of these sample results was evaluated to determine the statistical uncertainty by applying Bessel Eqn. 3.38 (Alan & Reza, 2012).

$$S = \sqrt{\frac{1}{N-1}\sum_{i=1}^{N}\left(Y_i - \bar{Y}\right)^2} \tag{3.38}$$

Table 3.21: Gas yield from gasification with steam/oxygen mixture

Property	Steam/Oxygen Ratio						
	0.05	0.15	0.25	0.35	0.45	0.55	0.65
Producer gas yield (m^3 /h)	9.05	9.33	9.88	10.38	11.07	11.31	11.47

Where, S - standard deviation, N - number of repeated measurements, Y_i - instantaneous average syngas yield and $\bar{Y}$ - mean syngas yield from Eqn. 3.37.

The standard deviation $\boldsymbol{u}$ of sample mean was determined using Eqn. 3.39.

$$u = \frac{S}{\sqrt{N}} \tag{3.39}$$

These statistical data for the sample results above are summarized in Table 3.22.

Table 3.22: Statistical quantities for the data sample

Statistic	Value
Mean, $\bar{Y}$	10.36 m^3/h
Standard deviation, S	0.9701
Standard deviation on mean, u	0.1386

It was notable that, based on the values of the statistical quantities above, the data obtained had minimum deviations from the true values and thus is a fair representation of the true performance of the gasification system under study.

CHAPTER FOUR

RESULTS AND DISCUSSION

4.1 Introduction

In this chapter, influence of various gasifying agents and temperature regulation on gasification process and products is analyzed. The experimental results from gasification with the different gasifying agents are presented and discussed. The optimum values of oxidizers and gasification temperature are also determined. Further, the quality of the syngas generated is analyzed based on the lower heating values (LHV) and the oxidizer that generates the best quality syngas is identified. The cold gas and carbon conversion efficiencies (CGE and CCE) of the process are also analyzed. These results are compared with the existing data from other researchers.

4.2 Proximate and Ultimate Analysis of Mui Basin Coal

In this section, the composition of the Mui-Basin coal is presented and analyzed. The density and lower heating value of the coal is also presented.

Table 4.1: Proximate and ultimate analysis of coal

(a) Proximate Analysis

Coal property	Average value
Fixed carbon	54.42%
Moisture content	4.27%
Volatile matter	34.27%
Ash content	9.04%
Bulk density	1434.7 kg/m^3
LHV	29.678 MJ/kg

(b) Ultimate Analysis

Constituents	% by mass
Carbon	72.64
Hydrogen	5.89
Oxygen	8.91
Nitrogen	1.22
Sulphur	2.30

Table 4.1 shows proximate and ultimate analyses of the coal sample. It was notable from Table 4.1 (a) that the coal sample had high quantity of volatile matter making it fairly reactive (Mi *et al*., 2015). Table 4.1 (b) showed that its carbon content was also fairly high. Based on the results of proximate and ultimate analysis, it was observed that the Mui-Basin coal sample used in this study could be classified as bituminous (ASTM, 1999).

4.3 Effect of Using Normal Air as Gasifying Agent

In this section, the effect of air as a gasifying agent, measured in terms of air-fuel equivalence ratio (λ) is presented. The syngas composition and quality, and the gasification efficiencies are discussed and compared to the findings of other researchers.

Figure 4.1 shows the effect of equivalence ratio (λ) on syngas composition. The concentrations of *CO* increased marginally by 10.8%, attributed to the limited supply of oxygen at low values of λ that promoted gasification reaction (as observed in Eqn.2.2). However, subsequent rise in λ caused decrease in *CO* content by about 45% attributed to enhanced combustion reactions at higher values of λ. These findings were in agreement with those of Jayathilake & Rudra, (2017) and Hervy *et al.*, (2019)

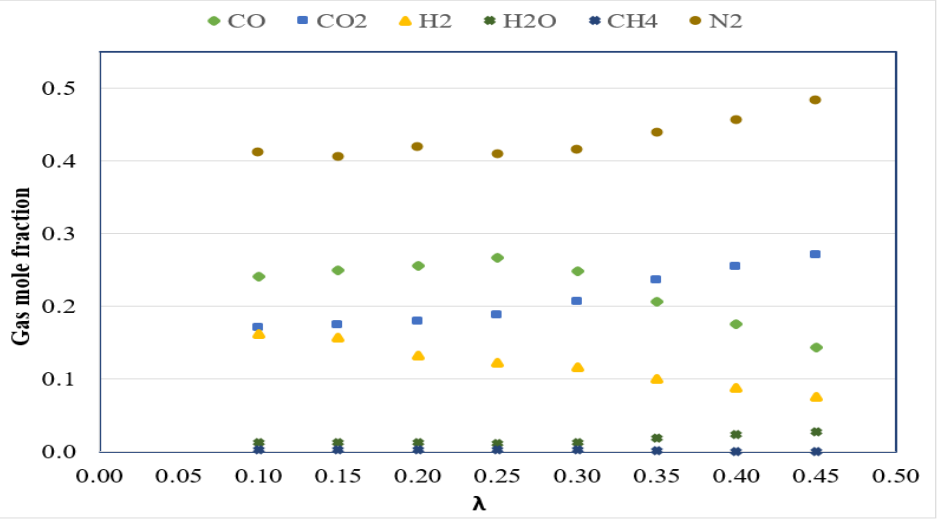

Figure 4.1: Effect of equivalence ratio on syngas composition

The concentration of H_2, decreased by 53.1%, which was attributed to the increased oxidation of H_2 to H_2O with increasing air, feed. The CH_4 content in syngas was however negligible due to low H_2 content in the oxidizer. The concentrations of CO_2, H_2O and N_2 increased by 57.9%, 125.0% and 17.5% respectively. The increase in CO_2 and H_2O was attributed to increased oxidation of carbon, H_2, and CO as λ increased. Increased N_2 content was due to the abundance of N_2 in air. Nitrogen in air does not take part in the gasification reactions, except at very high reactor temperatures. These trends were consistent with those observed by Nzove *et al.* (2019), Bingxi et al., (2013) and Tasma *et al.*, (2012)

The gas output per unit mass of coal is shown in Figure 4.2. Two gases are presented; producer gas and syngas. Producer gas is a gas mixture consisting of N_2, CO_2, CO, H_2, CH_4 and water vapour, while syngas, consists of the combustible (fuel) gases in the producer gas which include CO, H_2 and CH_4 gases.

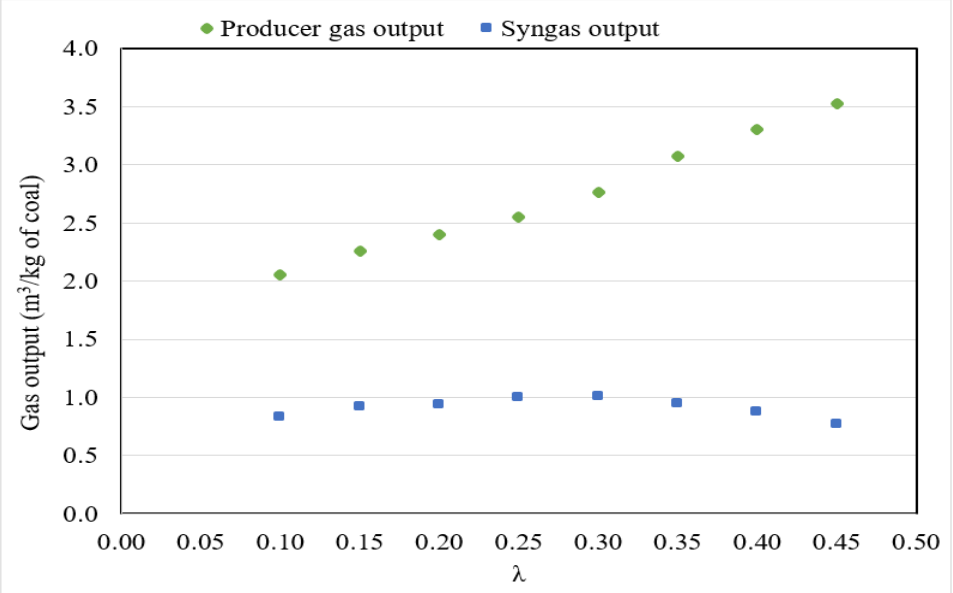

Figure 4.2: Effect of equivalence ratio on syngas yield

From Figure 4.2, producer gas output increased by 71.4%. This was attributed to the rise in N_2 content with rising air supply, as well as increased production of CO_2.

Syngas output, however, initially increased by 21.7% up to λ = 0.3, but reduced by 23.8% with subsequent increase in λ. This was attributed to the initial increase in *CO* content as explained earlier. The subsequent decrease in syngas content as equivalence ratio increased was attributed to the enhanced combustion reactions due to more oxygen content in the oxidizer, yielding more non-combustible gases like CO_2 and H_2O and less *CO* and H_2 gases. A significant difference between the quantities of producer gas and syngas was observed. This was attributed to high levels of N_2 and CO_2 in producer gas (Figure 4.1). The syngas output compares closely with those obtained by Laciak *et al*., (2016) and Hervy *et al*., (2019).

The syngas quality was expressed based on the lower heating value (LHV), and the variation of syngas LHV with λ is shown in Figure 4.3. A rise in air-fuel equivalence ratio by about up to 2.5 times has a minimal influence on syngas LHV. However, subsequent rise in equivalence ratio caused a reduction of LHV by about 45%. The decrease in syngas LHV with increasing λ was attributed to the dilution of the producer gas with N_2 from air. Seo *et al*., (2011) observed that the syngas LHV reduced with increasing N_2 /coal ratio, while Nzove *et al*., (2019) and Hervy *et al*., (2019) observed that the syngas heating value decreased with increasing air flow rate.

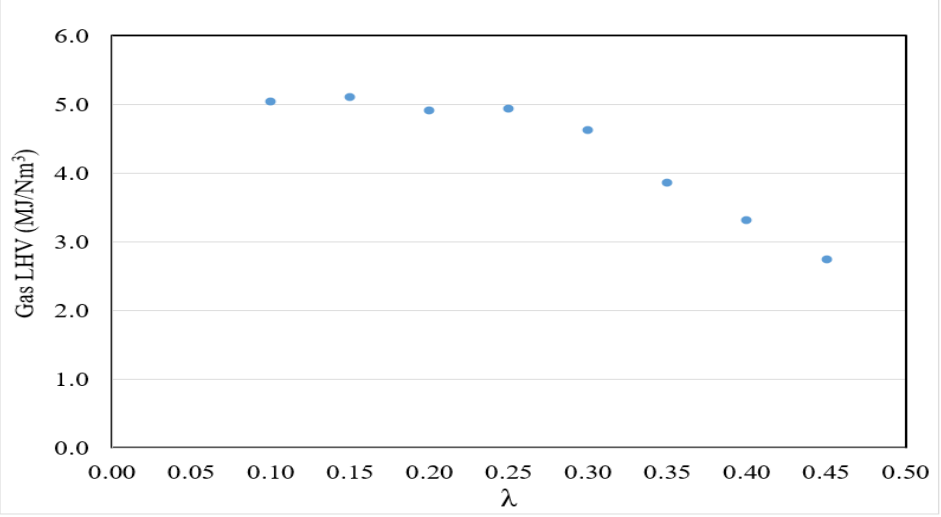

Figure 4.3: Effect of equivalence ratio on syngas LHV

The performance of the gasification process was analyzed in terms of cold gas efficiency (CGE) and carbon conversion efficiency (CCE) and their variations with λ are shown in Figure 4.4. CGE increased by 23.1% at λ=0.3. However, subsequent increase in λ led to 24.4% reduction in CGE. The increase in CGE was attributed to gasification reactions at low λ levels, while the decrease was attributed to enhanced combustion reactions that reduced the production of fuel gases. CCE increased by 54.1%, which was attributed to the increasing temperature favoring carbon conversion. The low values of CGE was due to dilution of the producer gas with non-combustible gases like N_2, CO_2 and water as seen in Figure 4.1. The observations made agreed with those of Chen et al., (2013). Singh *et al.*, (2018) found that CGE increased up to $\lambda = 0.31$ before reducing with increasing λ values.

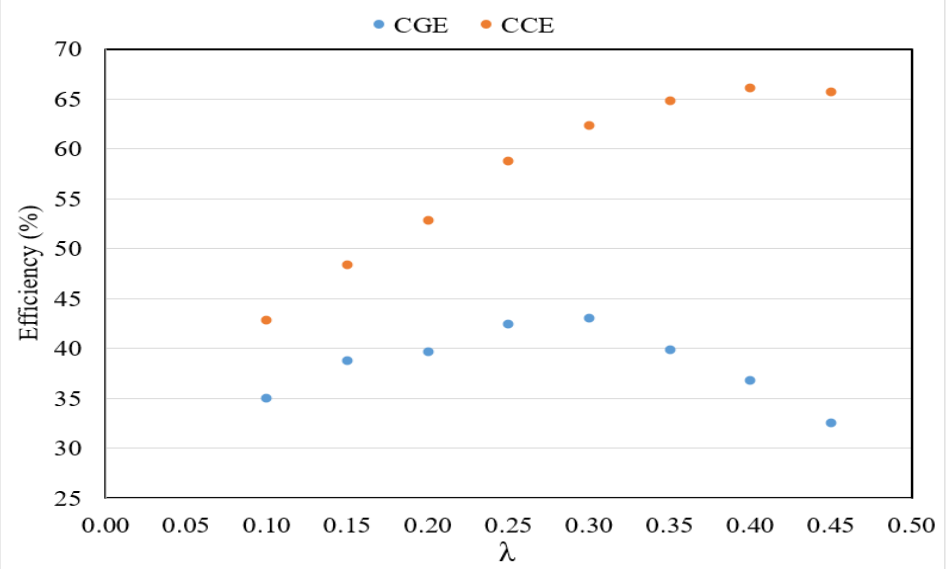

Figure 4.4: Effect of equivalence ratio on syngas CGE and CCE

Temperature in the reactor affects gasification reactions thus influencing syngas com- position and the process efficiency. Shown in Figure 4.5 is the variation of reactor temperature with equivalence ratio. The reactor temperature increased by 55.3%, which was attributed to the exothermic reactions inside the gasifier. Initially heat from the exothermic gasification reactions increased the gasifier temperature minimally. As λ increased, oxygen supply increased, combustion reactions became

dominant leading to increased rate of reactor temperature rise. These findings were consistent with those of Nzove *et al*., (2019).

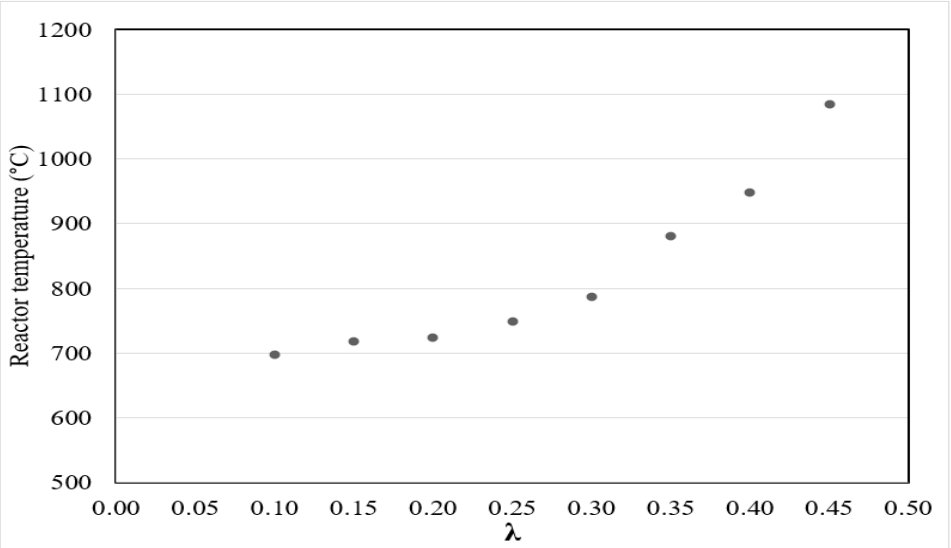

Figure 4.5: Effect of equivalence ratio on reactor temperature

4.4 Effect of Oxygen/Air Ratio and Gasifier Heat Regulation

In this section, the results on the effect of reactor heat regulation and variation of oxygen content in the oxidizer, varied based on oxygen/air ratio (OAR), are presented and analyzed. The data presented is for gasification without and with reactor heat control. The parameters analyzed include syngas composition, output and LHV, and gasification temperatures and efficiencies. These results are compared with the existing data from other researchers.

4.4.1 Variation of Reactor Temperature with OAR

Figure 4.6 shows the variation of reactor temperatures with OAR. When heat was not controlled, the reactor temperature increased by 73.8%. The rate of temperature rise was initially low due to exothermic gasification reactions at low oxygen concentrations. However, the rate was accelerated at higher *OAR*, attributed to enhanced exothermic combustion reactions favored by increased amounts of oxygen input. The best quality syngas output was at temperatures

between 700ºC and 900ºC. When heat was regulated, therefore, the temperatures oscillated between 750ºC and 900ºC (Figure 4.6). These conclusions agreed with the findings of Begum *et al.*, (2013) and Zdeb *et al.*, (2019) who observed that temperatures of between 650ºC and 850ºC favored gasification reactions.

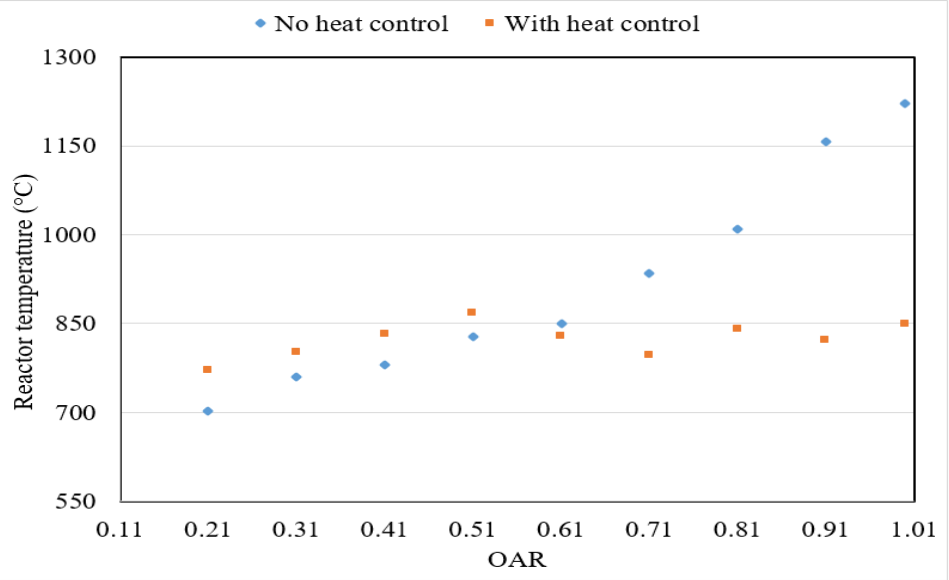

Figure 4.6: Effect of OAR on reactor temperature

4.4.2 Effect of OAR and Heat Control on Gas Composition

Figure 4.7 show variations of syngas composition with OAR for the case without and with reactor heat regulation. The concentrations of all gas species increased with increasing *OAR*, except N_2 that reduced to near zero. When heat was regulated, *CO*, H_2 and CH_4 contents increased overally by 57.5%, 35.1% and 171.4% respectively, compared to 53.8%, 17.4% and 116.7% respectively when there was no heat control. The findings agreed with those of Zogala, (2014).

In both cases, the increase in concentrations of *CO* at low *OAR* was attributed to enhanced gasification reactions favored by low supply of O_2 (as observed in Eqn. 2.2). The slight reduction in the content of *CO* at higher *OAR* was due to improved combustion reactions favored by high O_2 supply. Initially, increasing reactor temperature with *OAR* promoted the Boudouard reaction (Eqn. 2.4) which

consumed the CO_2 produced from reaction in Eqn. 2.1. This led to slow rise in CO_2 content at *OAR* below 0.51. However, further increase in *OAR* promoted combustion reactions in Eqns. 2.1 and 2.6 increasing *CO2* content in producer gas. These observations agreed with those made by Choi *et al.*, (2001).

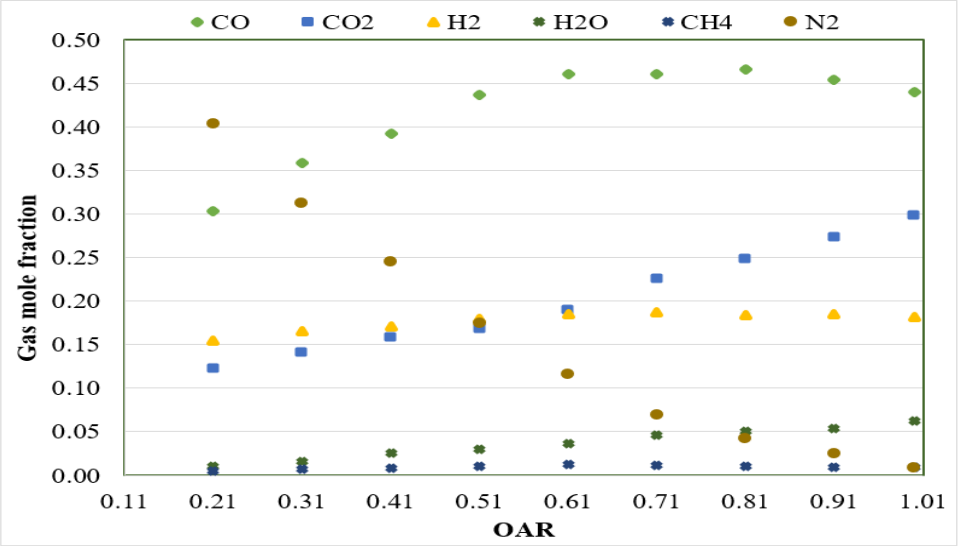

a) No heat control

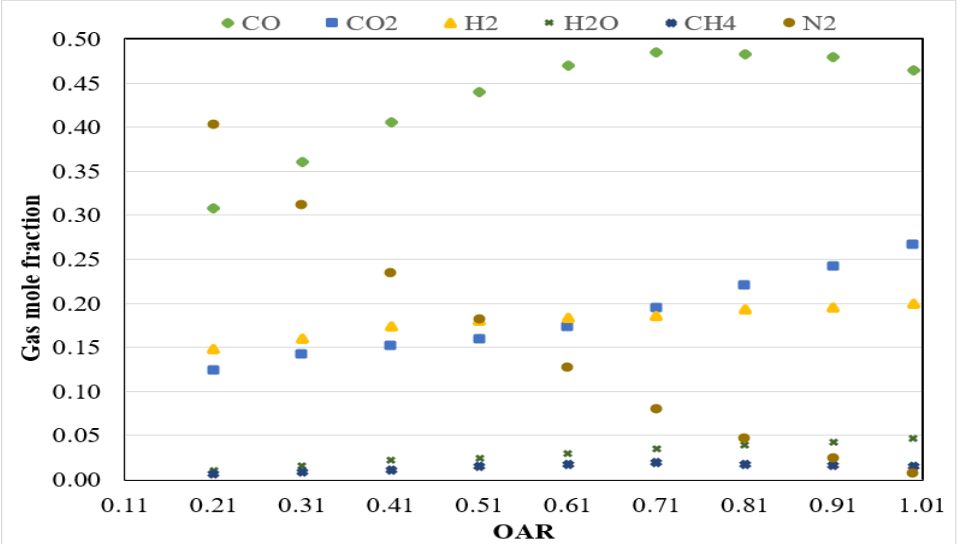

b) With heat control

Figure 4.7: Effect of OAR and heat regulation on syngas composition

The increase in methane content was attributed to homogenous steam-methane re- forming reaction (as observed in Eqn. 2.9) in which CO and H_2 produced, reacting with each other, produced methane and water. The increase in H_2 content was attributed to the water-gas reaction in Eqn. 2.3 and water-gas shift reaction in Eqn.2.8. Both reactions were improved by increased reactor temperatures as OAR rose leading to consumption of steam to generate H_2. This led to low H_2O content in the product gas even at higher OAR. These findings agreed with those of Stanczyk *et al.*, (2011). Wongsiriamnuay & Tippayawong, (2012) also found that increased reactor temperature promoted water gas reactions yielding more H_2 in the syngas.

The contents of CO_2, and H_2O in product gas increased by 115.3% and 370.0% respectively when heat was not controlled and by 142.3% and 520.0% respectively when heat was controlled. N_2 content reduced by 97.7% and 98.3% for the two cases respectively which was attributed to the reducing air content in oxidizer. The increased supply of O_2 enhanced combustion of coal, CO, and H_2 leading to rise in H_2O and CO_2 contents in the syngas (Eqns. 2.1, 2.6, and 2.7) (Zogala, 2014).

4.4.3 Effect of OAR and Heat Control on Gas Yield

Figure 4.8, showed that gas yields increased with increasing values of OAR. In the case of no heat control, producer gas yield increased by 20.4% for the whole range of OAR used. On the other hand, there was an increase of 16.9% in gas yield when heat was regulated. The average yields, however, showed no significant difference, maintaining at about 2.44 m^3/kg of coal in both cases. The increase in yields were attributed to increased supply of O_2 which enhanced both gasification and combustion reactions in the reactor generating more producer gas. The slight decrease in average yield when heat was regulated was attributed to reduced combustion reactions leading to reduced volumes of CO_2 and steam in product gas. Taba *et al.*, (2012) found that gas yield increases with

increasing temperature, while Stanczyk *et al.*, (2011) observed that gas yield improved with increasing O_2/air ratio.

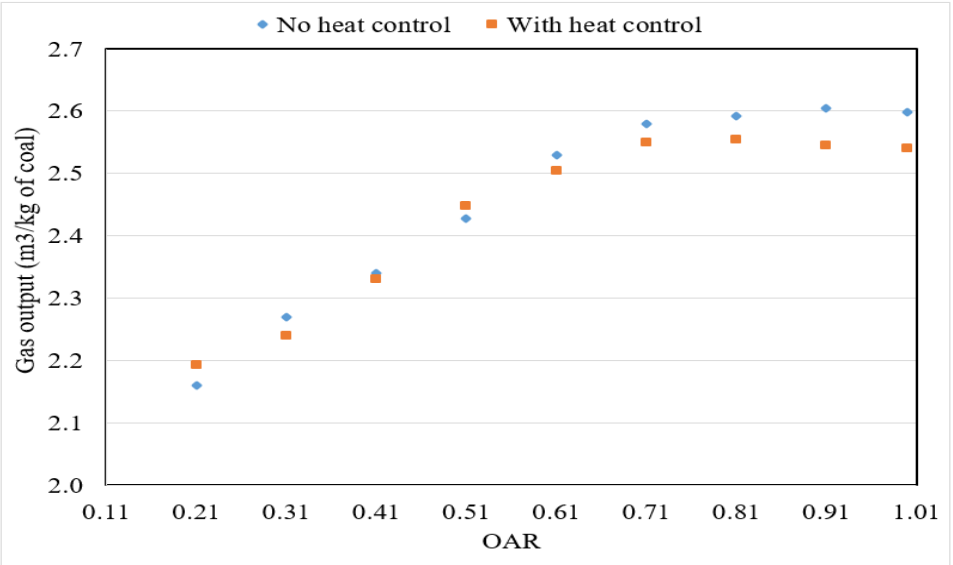

Figure 4.8: Variation of producer gas output with OAR and heat control

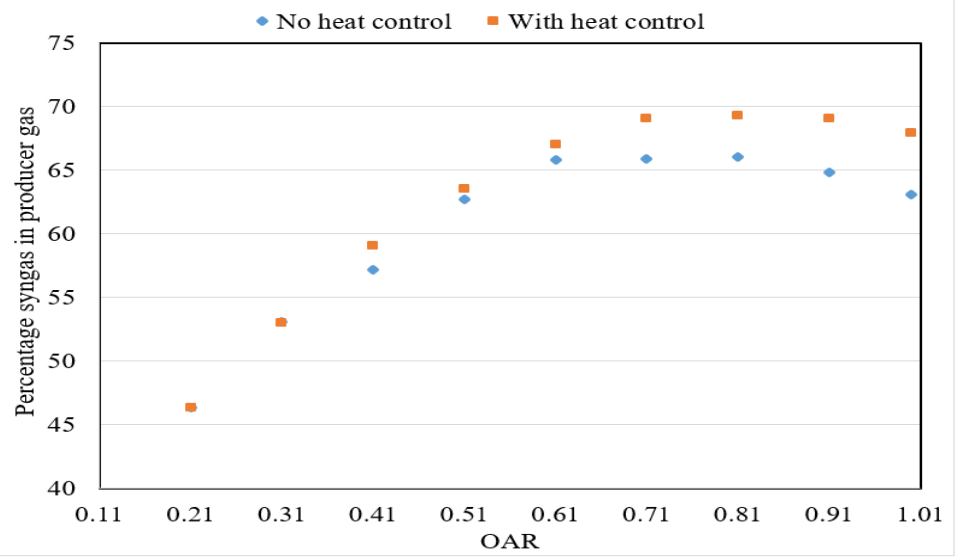

Figure 4.9: Effect of OAR and heat control on percentage syngas in producer gas

The variation of quantity of syngas in producer gas with *OAR* and heat regulation is shown in Figure 4.9. The percentage syngas in producer gas at

optimum *OAR* increased by 5.0% when heat was controlled compared to the case of no heat control. This shows that the quantity of fuel gases in a unit volume of producer gas increased marginally when reactor heat was regulated. This was attributed to increased gasification reactions that generated more fuel gases compared to combustion reactions that are favored by high temperatures.

4.4.4 Effect of OAR and Heat Control on Syngas LHV

There was steady improvement in the quality of syngas as *OAR* increased, as seen in Figure 4.10, before showing a decline at higher levels of *OAR*. When reactor heat was not controlled, the syngas LHV increased by 45.2% up to 0.61 *OAR*, before reducing slightly. When reactor heat was controlled, syngas LHV increased by 53.9% up to 0.71 *OAR*, an 8.7% improvement. The increase, in both cases, was attributed to the increased yield in *CO*, H_2 and CH_4 gases. The slight decline in LHV at high *OAR* was due to enhanced combustion reactions, which were attributed to increased availability of oxygen content and elevated reactor temperatures (Figure 4.6).

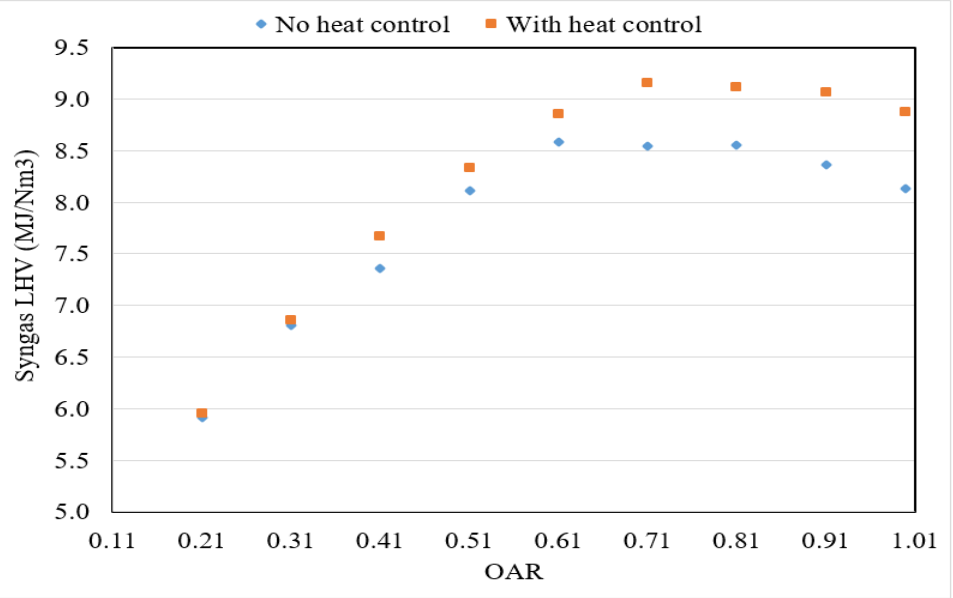

Figure 4.10: Effect of OAR and heat control on syngas LHV

Controlling reactor heat between 700ºC and 900ºC (gasification range) improved production of CH_4, H_2 and CO and led to higher syngas LHV. It also led to optimum point shifting to 0.71 OAR from 0.61 when heat was not controlled. These findings agreed with those of Zogala (2014).

4.4.5 Effect of OAR and Heat Control on Gasification Efficiencies

The gasifier performance improved as illustrated from the cold gas efficiency (CGE) shown in Figure 4.11. CGE rose by 72.3%, which was attributed to the enhanced syngas LHV and increased yield of CO and H_2. Likewise, it was noted that with heat regulation, the maximum CGE improved by 7.1% compared to when heat was not controlled. The trend is in agreement with the findings of Karimipour *et al.*, (2011).

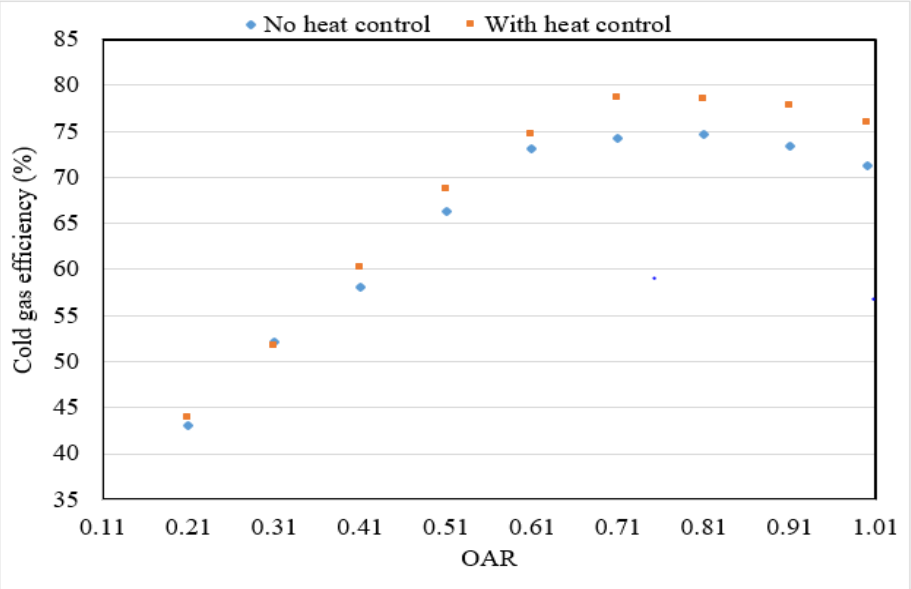

Figure 4.11: Effect of OAR and heat control on syngas CGE

Figure 4.12 shows the variation of CCE with *OAR*. It was observed that there was minimal difference between the two curves. This showed that heat regulation did not significantly affect the carbon conversion since temperature was maintained to within gasification temperature range. The high values of CCE in both curves was

attributed to the increased O_2 supply that enhanced carbon conversion reactions. These findings were consistent with those of Li *et al.*, (2014)

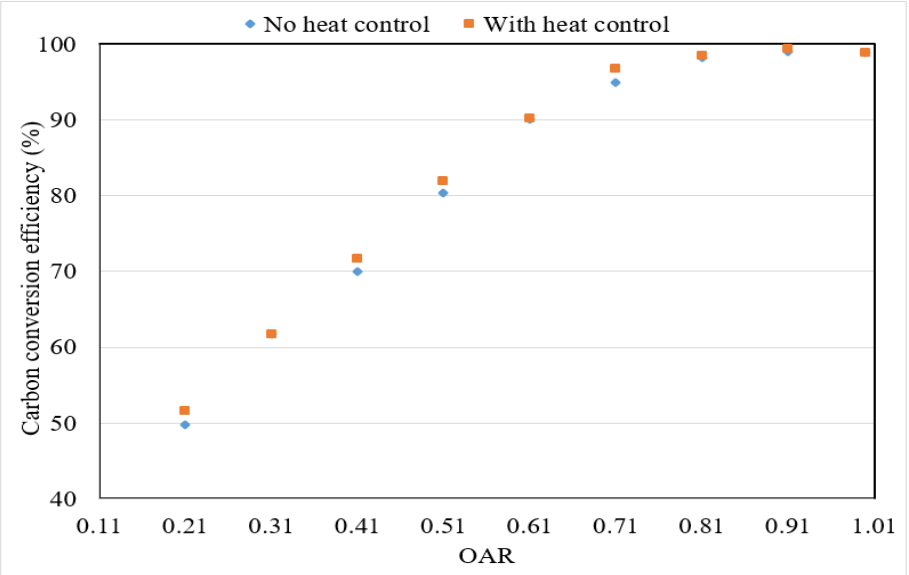

Figure 4.12: Effect of OAR and heat control on syngas CCE

4.5 Effect of Steam/Oxygen Ratio (SOR) on Coal Gasification

In this section, the results from the study of the effect of varying steam/oxygen ratio (SOR) on gasification of Mui Basin coal are discussed. Graphs of syngas composition, LHV, yield, and gasifier temperature are presented and analyzed. Cold gas and carbon conversion efficiencies are also presented and discussed.

The effect of *SOR* on the syngas composition is shown in Figure 4.13. The contents of *CO* decreased by 31.9% while CO_2 increased by 14.2% with increasing *SOR*. This was attributed to the reduced temperatures that hindered the reactions between carbon and O_2 in Eqn. 2.2 and between carbon and CO_2 in Eqn. 2.4. It also shifted the equilibrium point of reaction in Eqn. 2.8 to the right, producing more CO_2 and H_2O. These findings agreed with those of Lee *et al.*, (2002) and Asif *et al.*, (2017).

The contents of CH_4 and H_2 increased by 255.6% and 64.2% respectively. Increase in CH_4 was due to enhanced methanation reaction in Eqn. 2.5 and

methane-steam reforming reaction in Eqn. 2.9, both of which are endothermic. The reduced temperatures weakened the water-gas shift reaction in Eqn. 2.8 enhanced reaction in Eqn. 2.5 and shifted the equilibrium point of reaction in

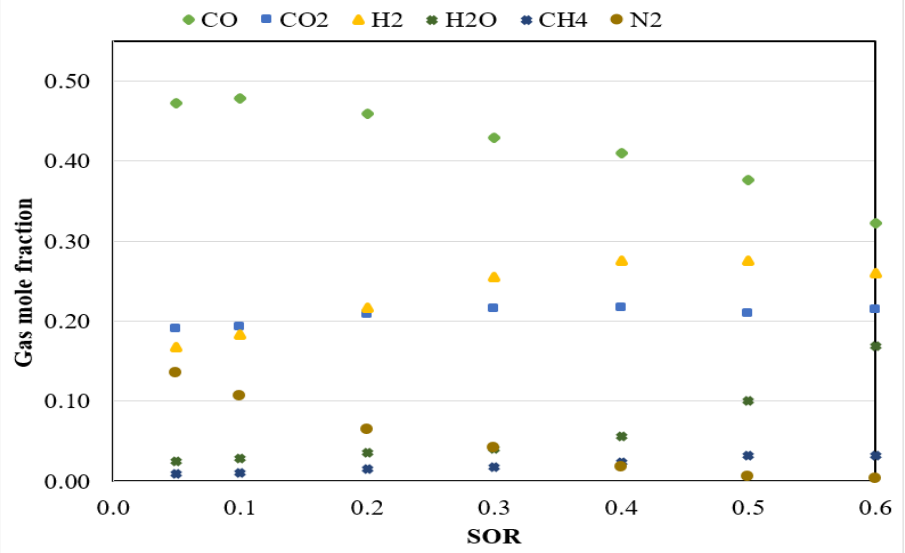

Figure 4.13: Effect of steam/oxygen ratio on syngas composition

Eqn. 2.9 towards the left, all of which consumed H_2. However, increased SOR strengthened the steam-gas reaction in Eqn. 2.3 and shifted the equilibrium point of reaction in Eqn. 2.8 to the right leading to a rise in H_2 content in syngas. This was consistent with the findings of James et al., (2014), Radwan, (2012) and Salami & Skala, (2015)

The content of H_2O increased by 576.0% while N_2 content decreased by 97.8%. The significant increase in H_2O content was due to reduced temperatures at elevated SOR hindering gasification reactions since there was no external heat source. The reduction in N_2 content was attributed to low levels of N_2 gas in the oxidizer.

Figure 4.14 shows the effect of *SOR* on both producer gas and syngas output. The producer gas output increased by 27.0% with increasing steam concentrations. The syngas output increased by 33.3% up to 0.40 *SOR* before reducing by 10.2% with subsequent increase in *SOR*. This was attributed to

increased generation of H_2 and CH_4 as steam supply increased. The reduced temperatures at high *SOR* values led to the subsequent reduction in syngas output. The observations were consistent with those of Salami & Skala, (2015) and Li *et al.*, (2020).

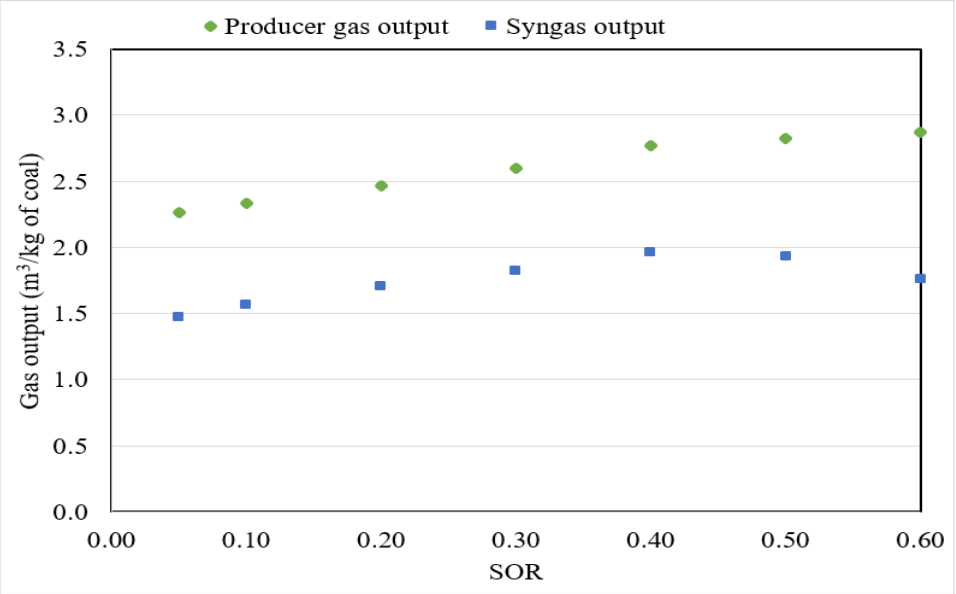

Figure 4.14: Effect of steam/oxygen ratio on syngas yield

From Figure 4.15 it was observed that the lower heating value of the syngas increased by 10.9% at 0.45 *SOR* and then reduced by 10.8% with subsequent increase in *SOR*. The increase was attributed to higher contents of CH_4 and H_2 in syngas favored by increased supply of steam that enhanced availability of H_2 in the oxidizer. The sharp drop in LHV at SOR values between 0.5 and 0.6 was attributed to the decrease in reactor temperature to levels below gasification temperatures due to high of steam content in the reactor.

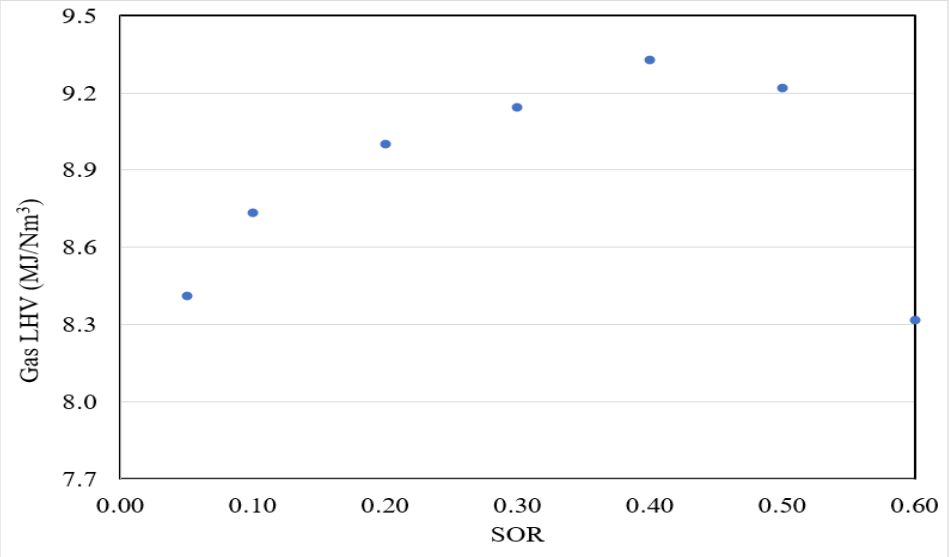

Figure 4.15: Effect of steam/oxygen ratio on syngas LHV

From Figure 4.16, CGE increased by 37.0% with increasing SOR and slightly reduced by 8.4% at 0.60 SOR. CCE increased by 18.2% before reducing by 9.6% at 0.6 SOR. The increment in efficiencies was attributed to the improved heating value together with the improved syngas yield. Both CGE and CCE were observed to follow the same trend as the other parameters, due to reducing temperatures in the gasifier as SOR increased beyond 0.40, which inhibited gasification reactions. These findings agree with those of Lee *et al.*, (2002) and Kurkela *et al.*, (2016).

Gasification temperature, as presented in Figure 4.17, showed an initial minimal increase, of 4.0% as SOR ratio increased from 0.05 to 0.15, before reducing consistently by 20.8% with increasing SOR. This was attributed to the fact that increase in SOR led to increased concentrations of steam, and reduced concentrations of oxygen. This weakened combustion reactions, but enhanced methane-forming reactions that were largely endothermic and absorbed the heat from the exothermic reactions in the gasifier. Also a significant amount of heat was taken by steam due to its high heat capacity. These observations are in agreement with those of Xie *et al.*, (2013).

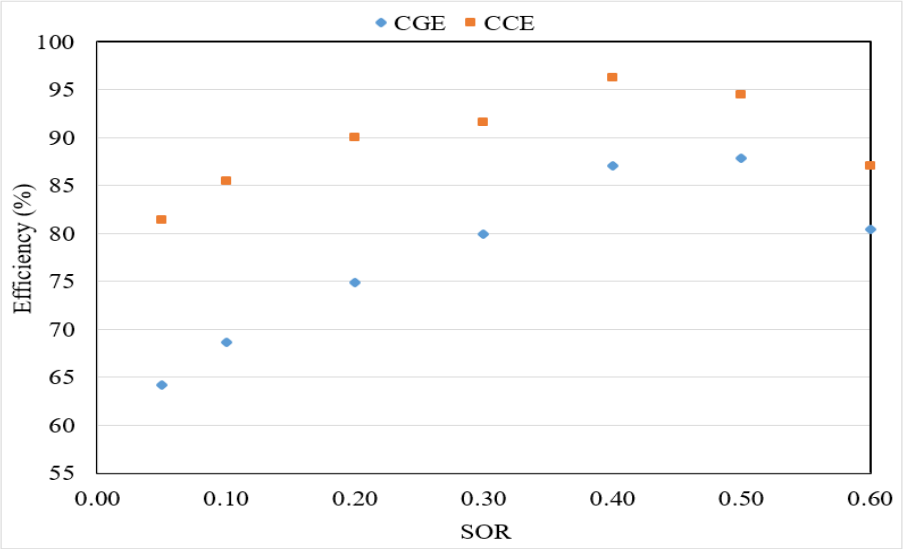

Figure 4.16: Effect of steam/oxygen ratio on syngas CGE and CCE

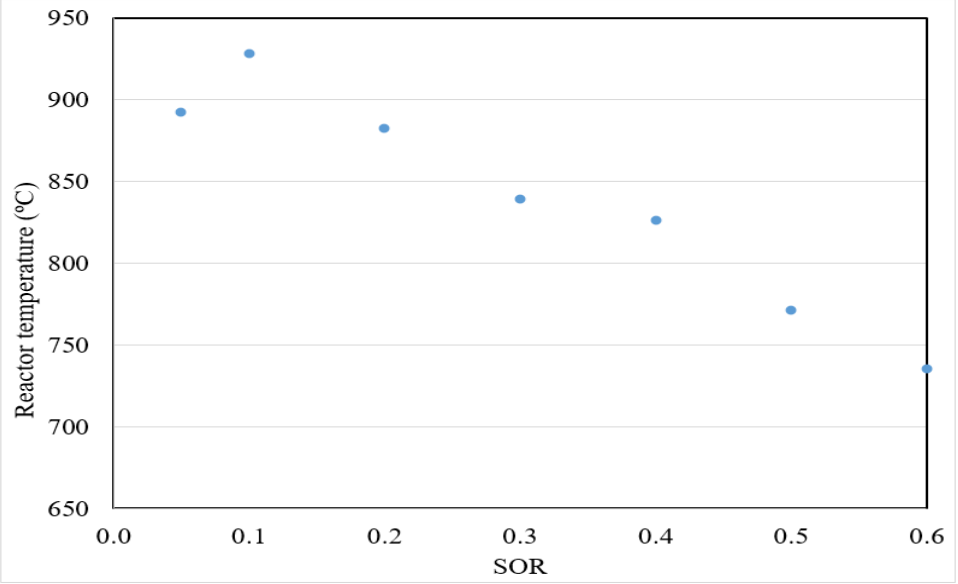

Figure 4.17: Effect of steam/oxygen ratio on reactor temperature

CHAPTER FIVE

CONCLUSIONS AND RECOMMENDATIONS

5.1 Conclusions

This study provided several unique contributions to the understanding of Mui Basin coal gasification process. It enhanced knowledge on the gasification system and its operation. The variety of experimental tests studied generated data useful for optimizing performance of gasifiers for both domestic and industrial applications.

Various gasifying agents were tested in the research to determine performance of an existing gasifier. The data generated were used to develop a modified gasifier with a reactor heat regulation system incorporated. This modified gasifier had an improved performance showing the benefit of reactor heat control.

The following conclusions were made based on the results of this study:

a) The maximum syngas LHV increased by 6.76% when heat was regulated and by 8.74% when oxygen/steam was used. It can therefore be concluded that heat regulation and use of steam in oxidizer leads to improved syngas quality.
b) When heat was controlled, optimum input point shifted to 0.71 *OAR* from 0.61 when heat was not regulated, indicating improved reactions. It was thus concluded that reactor heat control is beneficial for optimal gasification process.
c) The CGE for the modified gasifier at the optimum OAR improved by 5.92% com- pared to the case of no heat control. When steam was introduced, CGE increased by 10.55% at optimum SOR compared to that at optimum OAR. It was thus concluded that use of steam/oxygen mixture as oxidizer improves the performance of the gasifier by enhancing the energy conversion from coal to syngas.

d) The average syngas to producer gas output ratio was 0.665 for SOR gasification, compared to 0.627 for OAR with heat regulation. This showed an improved concentration of combustible gases (syngas) in the producer gas when steam was introduced. This led to the conclusion that gasification using oxygen-enriched air/steam mixture leads to higher output of syngas.
e) The concentrations of *CO*, H_2 and CH_4 increased by 53.8%, 17.4% and 116.7% while N_2 content reduced by to near zero when oxygen-enriched air was used compared to air gasification. It can therefore be concluded that oxygen-enriched air produces better quality syngas compared to pure air as oxidizer.
f) Optimal gasification reactions were observed to occur at reactor temperatures of between 750ºC - 900ºC for gasifiers operating at atmospheric pressure.

Therefore, introduction of enhanced oxygen concentration and steam in the gasifying agents together with regulation of reactor heat were beneficial to the gasification process of Mui Basin coal. They did not only improve the produced syngas quality, but also the performance of the gasification system.

5.2 Recommendations

From this study, the following recommendations were made for further research:

a) Among other factors, the type of gasifier used affects the syngas quality and process efficiency due to difference in operating conditions. This research used dry-fed gasifier system and further studies with slurry-fed system is recommended to provide data on how Mui Basin coal performs in different conditions.
b) This study noted that due to high heat capacity of steam and the endothermic nature of steam-favored reactions, its use in gasification led to reduction in reactor temperatures, which inhibited gasification reactions. It is thus recommended when steam is used as oxidizer, an external

source of heat should be introduced to maintain reactor temperature to within required range.

c) The gasifiers used were designed to operate at atmospheric pressure. Reactor pressure is known to affect process efficiency. Further study is recommended on their performance at higher pressures.

REFERENCES

Adeyemi, I., Arink T. & Janajreh, I., (2015). Numerical modeling of the entrained-flow gasification (EFG) of Kentucky coal and biomass. *Energy Procedia Journal*, *75,* 232–239.

Ahmad, M. I., Alauddin, Z. A. Z., Soid, S. N. M., Mohamed, M., Rizman, Z. I., Rasat, M. S. M., ... & Amini, M. H. M. (2015). Performance and carbon efficiency analysis of biomass via stratified gasifier. *ARPN Journal of Engineering and Applied Sciences*, *10*(20), 9533-9537.

Ahmad, R., Sánchez, F., & Kerubo, L., (2017). Powering Kenya: Understanding the Landscape and Exploring Investment Possibilities, *Fuel Freedom. IESE Business School – University of Navarra, Spain, 5,* 6–8.

Alan S. M., & Reza L., (2012). *Measurement and Instrumentation: Theory and Application,* Academic Press, Elsevier, USA, 17.

Asif, M., Taqi C., & Javed C., (2017). Performance evaluation of oxygen-blown gasifier. *8th International Renewable Energy Congress.*

ASTM Standard D3173-03, (2003). *Standard Test Method for Moisture in the Analysis Sample of Coal and Coke*. ASTM International, West Conshohocken, PA, USA.

ASTM Standard D3175-11. (2011). *Test Method for Volatile Matter in the Analysis Sample of Coal and Coke.* ASTM International West Conshohocken, PA, USA.

ASTM, Standard D3174-12, (2012). *Standard Test Methods for Ash in the Analysis Sample of Coal and Coke*. ASTM International, West Conshohocken, PA, USA.

ASTM, Standard D3176-15, (2015). *Standard Practice for Ultimate Analysis of Coal and Coke.* ASTM International, West Conshohocken, PA, USA.

ASTM, Standard D388-99, (1999). *Standard Classification of Coals by Rank*. ASTM International, West Conshohocken, PA, USA.

ASTM, Standard D5865-10a, (2010). *Standard Test Methods for Gross Calorific Value of Coal and Coke.* ASTM International, West Conshohocken, PA, USA.

ASTM, Standard D7582-10, (2010). *Standard Practice for Proximate Analysis of Coal and Coke*, ASTM International, West Conshohocken, PA, USA.

Babu, B V., & Sheth P S., (2005). Modeling and simulation of biomass gasifier: Effect of oxygen enrichment and steam to air ratio. *Chemical Engineering Group, Birla Institute of Technology and Science,* India.

Bakker, A., & LaRoche, R. D. (2000). *Modeling of the turbulent flow in HEV static mixers.* The Online CFM Book, 1 -8.

Baranowski, M., Pawlak-Kruczek, H., & Frydel, M., (2017). Effect of gasifying agents and calcium oxide on gasification of low-rank coal and wastes. *Transactions of the Institute of Fluid-flow Machinery, 137,* 141–155

Basu, P., Kefa, C., & Jestin, L (2000). *Boilers and Burners: Design and Theory,* (1st Ed.) Springer Science & Business Media, LLC, 128–135. ISBN 978-1-4612-7061-4.

Begum, S., Rasul, M. G., Akbar, D., & Ramzan, N. (2013). Performance analysis of an integrated fixed bed gasifier model for different biomass feedstocks. *Energies*, *6*(12), 6508-6524.

Biagini, E., Masoni, L., Pannocchia, G., & Tognotti, L., (2009). Development of gasifier models for hydrogen production optimization. *AIDIC Conference Series, 9,* 45 – 52.

Bingxi, L., Zhongbin F., Yaning Z., Hui L., & Bo Z., (2013}. Simulation analysis of biomass gasification in an autothermal gasifier using aspen plus. *Cleaner Combustion and Sustainable World,* 479 – 483.

Botero, C., Field, R. P., Herzog, H. J., & Ghoniem, A. F. (2013). On the Thermal and Kinetic Performance of a Coal-CO_2 Slurry-fed Gasifier: Optimization of CO_2 and steam flow using CO_2 skimming and steam injection. In *Proceedings of the 38th international technical conference on clean coal & fuel systems, Clearwater, FL*. *2*(6), 1–15.

Bradley, N., (2007). *The response surface methodology.* (Masters Dissertation), Department of Mathematical Sciences, Indiana University of South Bend.

Breault, R. W. (2010). Gasification processes old and new: a basic review of the major technologies. *Energies*, *3*(2), 216-240.

Carlson R. & Carlson J. E., (2005). *Design and optimization in organic synthesis, (Summary of screening experiments). 24,* Data Handling in Science and Technology. 195-199.

Cempa-Balewicz, M., Łączny, M. J., Smoliński, A., & Iwaszenko, S. (2013). Equilibrium model of steam gasification of coal. *Journal of Sustainable Mining*, *12*(2), 21-28.

Cengel, Y. & Afshin, G., (2015). *Heat and Mass Transfer: Fundamentals and Applications.* (5th ed). McGraw-Hill, NY, 653–665, 915, 919-920.

Chaudhari, N. R, & Adroja F. N., (2014). A review on design and analysis of double pipe heat exchanger. *International Journal of Engineering Research and Technology (IJERT), 3*(2**),** 2502–2505.

Chen, J. J., & Chen C. H., (2011). Investigation of Swirling Flows in Mixing Chambers. *Modeling and Simulation in Engineering, 2011,* 1-15.

Chen, W. H., Chen C. J. , Hung C. I., Shen C. H. & Hsu H. W., (2013). A comparison of gasification phenomena among raw biomass, torrefied Biomass and coal in an entrained-flow reactor. *Applied Energy*, *112*, 421 – 430.

Chiche, D., Diverchy, C., Lucquin, A., Porcheron, F. & Decor, F., 2013. Synthesis gas purification. *Journal on Oil and Gas Science and Technology*, *68*(4), 707 – 723.

Choi, Y. C., Park, T. J., Kim, J. H., Lee, J. G., Hong, J. C., & Kim, Y. G. (2001). Experimental studies of 1 ton/day coal slurry feed type oxygen blown, entrained flow gasifier. *Korean Journal of Chemical Engineering*, *18*(4), 493-498.

Clerici, A., & Alimonti, G. (2015). World energy resources. In *EPJ WEB of conferences 98*, 01001. EDP Sciences.

Couto, N., Rouboa, A., Silva, V., Monteiro, E., & Bouziane, K. (2013). Influence of the biomass gasification processes on the final composition of syngas. *Energy Procedia*, *36*, 596-606.

Cui, Y., Liang, J., Wang, Z., Zhang, X., Fan, C., & Wang, X. (2014). Experimental forward and reverse in situ combustion gasification of lignite with production of hydrogen-rich syngas. *International Journal of Coal Science & Technology*, *1*(1), 70-80.

Dascomb, J. (2013). *Thermal conversion efficiency of producing hydrogen enriched synthesis gas from steam biomass gasification* (Doctoral dissertation, The Florida State University).

Engineering Edge, 2020. Retrieved from: Engineeringedge.com/heat-transfer/convective-heat-transfer-coefficients-13378.htm.

ERC, 2011. Updated Least Cost Power Development Plan, Study *Period: 2011-2031. Energy Regulatory Commission, Kenya.*

GPP, (2020). *Electricity Prices.* GlobalPetrolPrices.com, Retrieved from: https://www.globalpetrolprices.com/electricity_prices.

Harimi, M., Sapuan, S. M., Ahmad, M. M. H. M., & Abas, F. (2008). Numerical study of heat loss from boiler using different ratios of fibre-to-shell from palm oil wastes. *Journal of Scientific & Industrial Research, 67*, 440–444.

Hervy, M., Remy, D., Dufour, A., & Mauviel, G. (2019). Air-blown gasification of Solid Recovered Fuels (SRFs) in lab-scale bubbling fluidized-bed: Influence of the operating conditions and of the SRF composition. *Energy Conversion and Management*, *181*, 584-592.

Holt–EPRI, N. A. (2001, October). Coal gasification research, development and demonstration-needs and opportunities. In *The Gasification Technologies Conference, San Francisco*.

Hussein, S. A. A. (2015). Experimental investigation of double pipe heat exchanger by using semicircular disc baffles. *International Journal of Computer Applications*, *115*(4), 13-17.

IEACh, (2020). *Electricity Mix in China, Q1 2020*. International Energy Agency, Paris.

IEAEB, (2020). *World energy balances, 2020.* International Energy Agency, Paris.

IEAES, (2020). *Key World Energy Statistics 2020*. International Energy Agency, Paris.

IEAKE, (2019). *Kenya Energy Outlook*, International Energy Agency, Paris.

IEAUS, (2020). *Electricity Mix in the United States, Q1 2020*. International Energy Agency, Paris.

IRUNGU, D. W. (2016). *Simulation of the future electricity demand and supply in Kenya using the long-range energy alternative planning system* (Masters dissertation, Jomo Kenyatta University of Agriculture And Technology).

Jale, G., (2014). *Causes, Impacts and Solutions to Global Warming.* Purdue University Press.

James, A. K., Helle, S. S., Thring, R. W., Rutherford, P. M., & Masnadi, M. S. (2014). Investigation of air and air-steam gasification of high carbon wood ash in a fluidized bed reactor. *Energy and Environment Research*, *4*(1), 1-24.

Jayaraman, K., & Gokalp, I. (2015). Effect of char generation method on steam, CO_2 and blended mixture gasification of high ash Turkish coals. *Fuel*, *153*, 320-327.

Jayathilake, R., & Rudra, S. (2017). Numerical and experimental investigation of Equivalence Ratio (ER) and feedstock particle size on Birchwood gasification. *Energies*, *10*(8), 1232.

Jin, H., Lu, Y., Liao, B., Guo, L., & Zhang, X. (2010). Hydrogen production by coal gasification in supercritical water with a fluidized bed reactor. *International journal of hydrogen energy*, *35*(13), 7151-7160.

Kakac S. & Hongtan L., (2002). *Heat Exchangers: Selection, Rating and Thermal Design*. (2nd ed) CRC Press LLC, 173, 177.

Kakac, S., Liu, H., & Pramuanjaroenkij, A. (2002). *Heat exchangers: selection, rating, and thermal design*. (2nd edition ed.), CRC press, FL, 71 – 73..

Karimipour, S., Gerspacher, R., Gupta, R., & Spiteri, R. J. (2012). Study of factors affecting syngas quality and their interactions in fluidized bed gasification of lignite coal. *Fuel*, *103*, 308-320.

Keneilwe, R. & Ramaano N., 2019. *The South African Energy Sector Report, 2019*. Department of Energy, South Africa, 17.

Kline, S. J. & McClintock F. A., (1953). Describing Uncertainties in Single-Sample Experiments. *Mechanical Engineering*, *75*(1), 3–8.

Kolmetz, K., & Aprilia, J., (2011). Kolmetz Handbook of Process Equipment Design. *KLM Technology Group, Boiler Systems Selection, Sizing and Troubleshooting*, *Engineering Design Guideline*. Rev 01, 22 – 23.

Kurkela, E., Kurkela M., & Ilkka H., (2016). Steam–oxygen gasification of forest residues and bark followed by hot gas filtration and catalytic reforming of tars: Results of an extended time test. *Fuel Processing Technology*, *141*, 148–158.

Laciak, M., Kostúr, K., Durdán, M., Kačur, J., & Flegner, P. (2016). The analysis of the underground coal gasification in experimental equipment. *Energy, 114*, 332-343.

Lahijani, A. M., & Supeni, E. E. (2018). Evaluating the Effect of Economizer on Efficiency of the Fire Tube Steam Boiler. *Innovative Energy and Research*, *7*(193), 2576-1463.

Lazova, M., Huisseune, H., Kaya, A., Lecompte, S., Kosmadakis, G., & De Paepe, M. (2016). Performance evaluation of a helical coil heat exchanger working under supercritical conditions in a solar organic Rankine cycle installation. *Energies*, *9*(6), 432.

Lee, H., Choi, S., & Paek, M. (2011). A simple process modelling for a dry-feeding entrained bed coal gasifier. *Proceedings of the Institution of Mechanical Engineers, Part A: Journal of Power and Energy*, *225*(1), 74-84.

Lee, W. J., Kim, S. D., & Song, B. H. (2002). Steam gasification of an Australian bituminous coal in a fluidized bed. *Korean Journal of Chemical Engineering*, *19*(6), 1091-1096.

Li, G., Wang, L., Wang, C., Wang, C. A., Wu, P., & Che, D. (2020). Experimental study on coal gasification in a full-scale two-stage entrained-flow gasifier. *Energies*, *13*(18), 4937.

Li, H., Yu, Y., Han, M., & Lei, Z. (2014). Simulation of coal char gasification using O_2/CO_2. *International Journal of Coal Science & Technology*, *1*(1), 81-87.

Markus, B. & Bruchof D., (2010.) *Syngas production from coal.* IEA, Energy Technology Systems Analysis Program (IEA ETSAP).

Maurstad, O. (2005). An Overview of Coal based Integrated Gasification Combined Cycle (IGCC. In *Technology; MIT LFEE 2005-002 WP; Laboratory for Energy and the Environment, Massachusetts Institute of Technology*.

Mazumder, A., & Mandal, B. K. (2016). Numerical modeling and simulation of a double tube heat exchanger adopting a black box approach. *International Journal of Engineering Research and Applications, 6*(4-2), *35–41.*

Mi, J., Wang, N., Wang, M., Huo, P., & Liu, D. (2015). Investigation on the catalytic effects of AAEM during steam gasification and the resultant char reactivity in oxygen using Shengli lignite at different forms. *International Journal of Coal Science & Technology*, *2*(3), 223-231.

Mikulandrić, R., Lončar, D., Böhning, D., Böhme, R., & Beckmann, M. (2015). Process performance improvement in a co-current, fixed bed biomass gasification facility by control system modifications. *Energy Conversion and Management*, *104*, 135-146.

Mishra, A., Gautam, S., & Sharma, T. (2018). Effect of operating parameters on coal gasification. *International Journal of Coal Science & Technology*, *5*(2), 113-125.

MoE, 2018. *National Energy Policy*, Nairobi: Ministry of Energy.

Mokveld, K., & Eije, S. V. (2018). Final energy report Kenya. *Ministry of Foreign Affairs*. Netherlands Enterprise Agency

Montgomery, D. C., (2001). *Design and Analysis of Experiments*. (5th ed), John Wiley and Sons Inc., 1-17.

Morshedi, A., & Akbarian, M. (2014). Application of response surface methodology: design of experiments and optimization: a mini review. *Indian Journal of Fundamental and Applied Life Sciences*, *4*(4), 2434-2439.

Muthangya, M. and Samoei D., (2012). Status of water quality in coal-rich Mui-Basin, Kitui County, Kenya. *ARPN Journal of Earth Science*. *1*(2), 48–51.

Muthui, R. K., Kabugu, M., Akisa, David, M. & Rop, B. K., (2014). Coal handling and equipment selection in Mui Basin, Kitui County, Kenya. *Proceedings of International Conference on Sustainable Research and Innovation, 5,* 87–90.

Nag, P. K., (2008). *Power Plant Engineering*, (3rd Ed) McGraw Hill Publishing Company, NY. 337–342. ISBN-13: 978-0-07-064815-9.

Nair, V., Strecher, V., Fagerlin, A., Ubel, P., Resnicow, K., Murphy, S., & Zhang, A. (2008). Screening experiments and the use of fractional factorial designs in behavioral intervention research. *American Journal of Public Health*, *98*(8), 1354-1359.

Najafi, M., Jalali, S. M. E., KhaloKakaie, R., & Forouhandeh, F. (2015). Prediction of cavity growth rate during underground coal gasification using multiple

regression analysis. *International Journal of Coal Science & Technology*, *2*(4), 318-324.

Nayak, R., & Raju K. M., (2011). Simulation of coal gasification process using ASPEN PLUS," *Proceedings of International Conference on Current Trends in Technology,* 1–6.

Newell, R., Raimi, D., Villanueva, S., & Prest, B. (2020). Global energy outlook 2020: Energy transition or energy addition? Resources for the Future.

Nicola P. and Dirnberger D., (2017). *The Performance of Photovoltaic (PV) Systems.* Woodhead Publishing, Elsevier, 42, ISBN 9781782423362.

Novosád, J., Dančová, P., & Vít, T. (2017). Investigation of mixing chamber for experimental FGD reactor. In *MATEC Web of Conferences*, EDP Sciences, *89*, 01001, 1 - 6.

Nzove, S., Ndiritu H. & Gathitu B., (2019). Design and Optimization of Performance of a Bench-scale Gasifier for Sub-Bituminous Coal. *International Journal of Engineering Technology and Scientific Innovation, 4* (5), 246–260.

Omar, Q. M., Umar, S., Ahmad, M., Fatima, S., & Javeed, A. (2017). Proximate analysis of low and high quality pure coal and their blends from Pakistan. *Austin Chemical Engineering*, *4*(1), 1048. 47 – 54.

Othman, N. F., Bosrooh, M. H., & Majid, K. A. (2007). Partial gasification of different types of coals in a fluidised bed gasifier. *Jurnal Mekanikal*, *23*, 40 – 49

Owiro, D., Poquillon, G., Njonjo, K. S., & Oduor, C. (2015). Situational analysis of energy industry, policy and strategy for Kenya. *Institute of Economic Affairs*, 8

Pandey, R., Sethi, V. K., Pandey, M., & Choubey, M. (2015, May). Comparative Study of Coal Based IGCC and Conventional Power Plants on Various Technological Parameters. In *2015 Second International Conference on Advances in Computing and Communication Engineering*, 63-67.

Park, T. J., Kim, J. H., Lee, J. G., Hong, J. C., Kim, Y. K., & Choi, Y. C. (1999). Experimental studies on the characteristics of entrained flow coal gasifier. *Energy Conversion Research Department Korea Institute of Energy Research*.

Preciado, J. E., Ortiz-Martinez, J. J., Gonzalez-Rivera, J. C., Sierra-Ramirez, R., & Gordillo, G. (2012). Simulation of synthesis gas production from steam oxygen gasification of Colombian coal using Aspen Plus®. *Energies*, *5*(12), 4924-4940.

Quaak, P., Knoef, H. and Hubert S., (1999). *Energy from biomass: A review of combustion and gasification technologies*. International Bank for Reconstruction and Development / The World Bank. Energy Series, World Bank Technical Paper No. *422*, 27 – 31.

Radwan, A. M. (2012). An overview on gasification of biomass for production of hydrogen rich gas. *Der Chemica Sinica*, *3*(2), 323-335.

Ramarao, M., & Vivekanandan, S. (2016). Evaluation of Carbon Conversion Efficiency of Mixed Biomass Gasification. *International Journal of Mechanical Engineering and Technology*, *7*(6), 555 – 564

Rendall, R., Reis, M. S., Chin, S. T., & Chiang, L. (2016). Managing Uncertainty Information for Improved Data-Driven Modelling. In *Computer Aided Chemical Engineering*, Elsevier, *38*, 1575-1580.

Richmond, D. E., (1999). *Utilitiesman Basic 2*. Naval Education and Training Professional Development and Technology Center, NAVEDTRA 14279, 1-2.

Rodgers, G. F. C. & Mayhew, Y. R., (2004). *Thermodynamic and Transport Properties of Fluids, SI Units*. (5th ed.) Blackwell Publishing, 24.

Salami, N., & Skála, Z. (2015). Use of the steam as gasifying agent in fluidized bed gasifier. *Chemical and Biochemical Engineering Quarterly*, *29*(1), 13-18.

Schoen, E. D., Eendebak, P. T., & Goos, P. (2019). A classification criterion for definitive screening designs. *The annals of statistics*, *47*(2), 1179-1202.

Seo, H. K., Park, S., Lee, J., Kim, M., Chung, S. W., Chung, J. H., & Kim, K. (2011). Effects of operating factors in the coal gasification reaction. *Korean Journal of Chemical Engineering*, *28*(9), 1851-1858.

Shahbaz, M., Yusup, S., Inayat, A., Patrick, D. O., & Pratama, A. (2016). Application of response surface methodology to investigate the effect of different variables on conversion of palm kernel shell in steam gasification using coal bottom ash. *Applied energy*, *184*, 1306-1315.

Shan, W. K., (2001). *Handbook of Air Conditioning and Refrigeration*. (Second ed), McGraw-Hill, B.5.

Singh, D., Yadav, S., Rajesh, V. M., & Mohanty, P. (2018). Groundnut shell gasification performance in a fluidized bed gasifier with bubbling air as gasification medium. *Environmental technology*, 1-13

Smoliński, A., Stańczyk, K., Kapusta, K., & Howaniec, N. (2012). Chemometric study of the ex situ underground coal gasification wastewater experimental data. *Water, Air, & Soil Pollution*, *223*(9), 5745-5758.

Soria-Verdugo, A., Von Berg, L., Serrano, D., Hochenauer, C., Scharler, R., & Anca-Couce, A. (2019). Effect of bed material density on the performance of steam gasification of biomass in bubbling fluidized beds. *Fuel*, *257*, 116118.

Stańczyk, K., Howaniec, N., Smoliński, A., Świądrowski, J., Kapusta, K., Wiatowski, M., & Rogut, J. (2011). Gasification of lignite and hard coal

with air and oxygen enriched air in a pilot scale ex situ reactor for underground gasification. *Fuel*, *90*(5), 1953-1962.

Sthel, M. S., Tostes, J. G., & Tavares, J. R. (2013). Current energy crisis and its economic and environmental consequences: Intense human cooperation. *Journal on Natural Science*, *5*(2A), 244–252.

Syed, S., Janajreh, I., & Ghenai, C. (2012). Thermodynamics equilibrium analysis within the entrained flow gasifier environment. *International Journal of Thermal and Environmental Engineering*, *4*(1), 47-54.

Taba, L. E., Irfan, M. F., Daud, W. A. M. W., & Chakrabarti, M. H. (2012). The effect of temperature on various parameters in coal, biomass and Co-gasification: A review. *Renewable and Sustainable Energy Reviews*, *16*(8), 5584-5596.

Taneja T. R, J. (2017). Measuring electricity reliability in Kenya. *Amherst (MA): STIMA Lab, Department of Electrical and Computer Engineering, University of Massachusetts - Amherst*, P., 207. *Modern experimental design*. John Wiley & Sons, 13 – 17.

Tasma, D., & Tanase P., (2012). The quality of syngas produced by fluidised bed gasification using sunflower husk. *The annals of "Dunarea de jos" university of Galati fascicle V, technologies in machine building, 5,* 33 – 36. *ISSN*, 1221-4566.

TEMA, (2007). *Standards of the Tubular Exchanger Manufacturers Association*, (9th Ed.) Tubular Exchanger Manufacturers Association (TEMA), Inc., 10-29, 10-33.

Theodore, L B., Adrienne S. L., Incropera F. P. & Dewitt D. P., (2011). *Fundamentals of Heat and Mass Transfer*. (7th ed.), John Wiley and Sons Inc., 710, 993, 1003.

Toporov, D., & Abraham, R. (2015). Gasification of low-rank coal in the High-Temperature Winkler (HTW) process. *Journal of the Southern African Institute of Mining and Metallurgy*, *115*(7), 589-597.

Vamvuka, D., 2000. Gasification of coal: Clean Use of Coals: Low-rank Coal Technologies. *Multi-Science Publishing Co. Ltd*, pp. 515-576.

Wadhwani, R., & Mohanty, B. (2016). Effects of operating pressure on the key parameters of coal direct chemical looping combustion. *International Journal of Coal Science & Technology*, *3*(1), 20-27.

Wang, T. X., Hsu, H. W. & Shen, C. H., (2014). Employment of two- stage oxygen feeding to control temperature in a downdraft entrained-flow coal gasifier. *International Journal of Clean Coal and Energy*, *3*, 29– 45.

Whitelaw, J. H., 2011. *Thermopedia: A to Z Guide to Thermodynamics, Heat and Mass Transfer, and Fluids Engineering*. Retrieved from: Thermopedia.com/content/660/. Doi: 10.1615/AtoZ.c.convective-heat-transfer.

Wongsiriamnuay, T., & Tippayawong, N. (2012). Product gas distribution and composition from catalyzed gasification of mimosa. *International Journal of Renewable Energy Research (IJRER)*, *2*(3), 363-368.

Woods, D. C., & Lewis, S. M. (2015). *Design of experiments for screening*," Southampton Statistical Sciences Research Institute, University of Southampton, UK, 1 – 32.

World Bank, 2016. *Doing business 2016: Measuring regulatory quality and efficiency.* International Bank for Reconstruction and Development / The World Bank *13*, 211.

Xie, H., Zhang, Z., Li, Z., & Wang, Y. (2013). Relations among main operating parameters of gasifier in IGCC. Journal on *Energy Power Engineering*, *5*(04), 552 - 556.

Yang, W., Ponzio, A., Lucas, C., & Blasiak, W. (2006). Performance analysis of a fixed-bed biomass gasifier using high-temperature air. *Fuel processing technology*, *87*(3), 235-245.

Zdeb, J., Howaniec, N., & Smoliński, A. (2019). Utilization of carbon dioxide in coal gasification - An experimental study. *Energies*, *12*(1), 140.

Zhang, Y., Zhongbin F., Bingxi L., Hongtao L., and Bo Z., (2013). Energy and exergy evaluation of product gas from coal/biomass blend gasification in a dual circulating fluidized bed reactor. *Cleaner Combustion and Sustainable World*, 599–603.

Żogała, A. (2014). Equilibrium simulations of coal gasification–factors affecting syngas composition. *Journal of Sustainable Mining*, *13*(2), 30-38.

Żogała, A., & Janoszek, T. (2015). CFD simulations of influence of steam in gasification agent on parameters of UCG process. *Journal of Sustainable Mining*, *14*(1), 2-11.

APPENDICES

Appendix I: Gasifier drawings: Exploded view

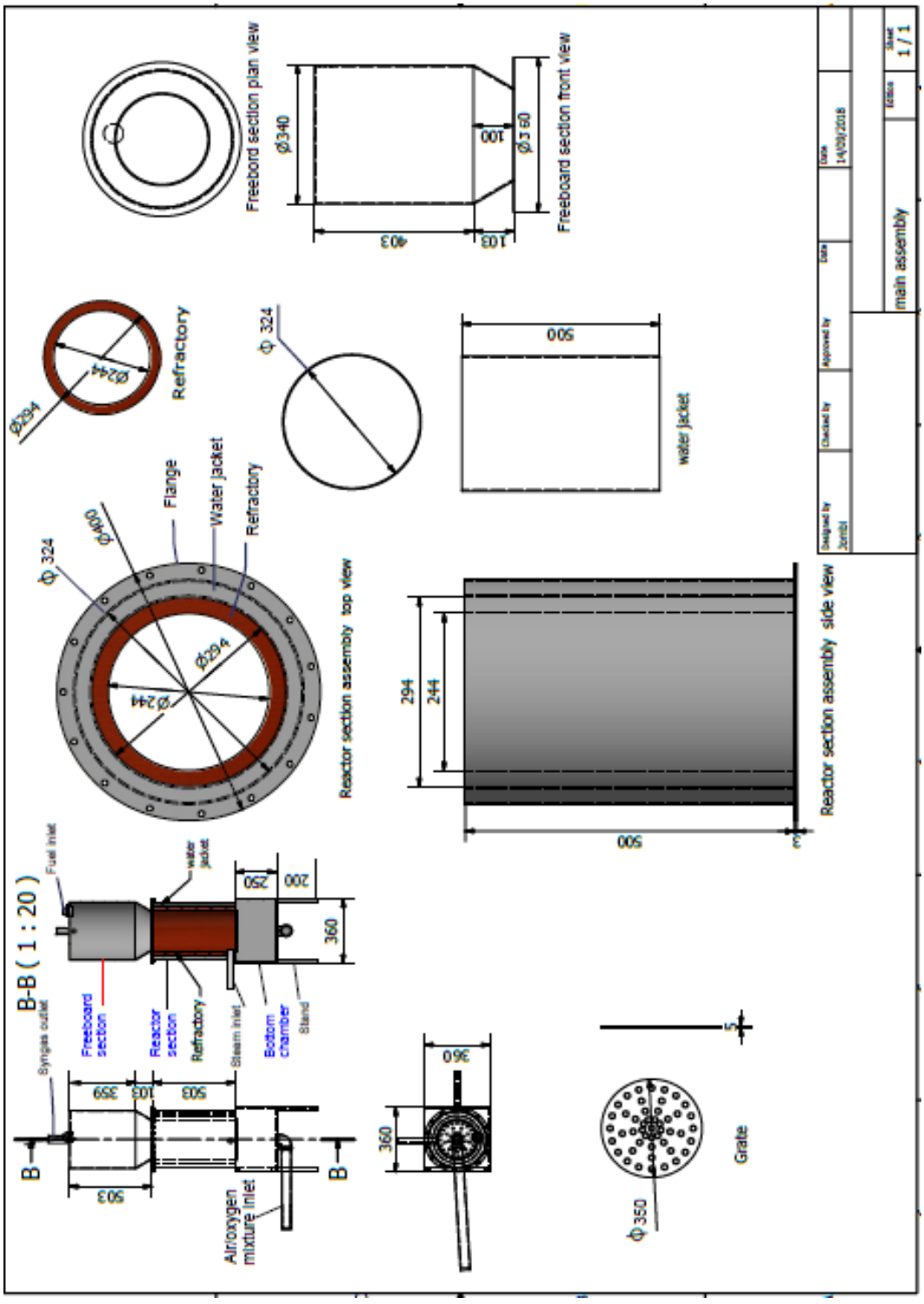

Appendix II: Gasifier drawings: Enlarged views of freeboard and Bottom Chamber

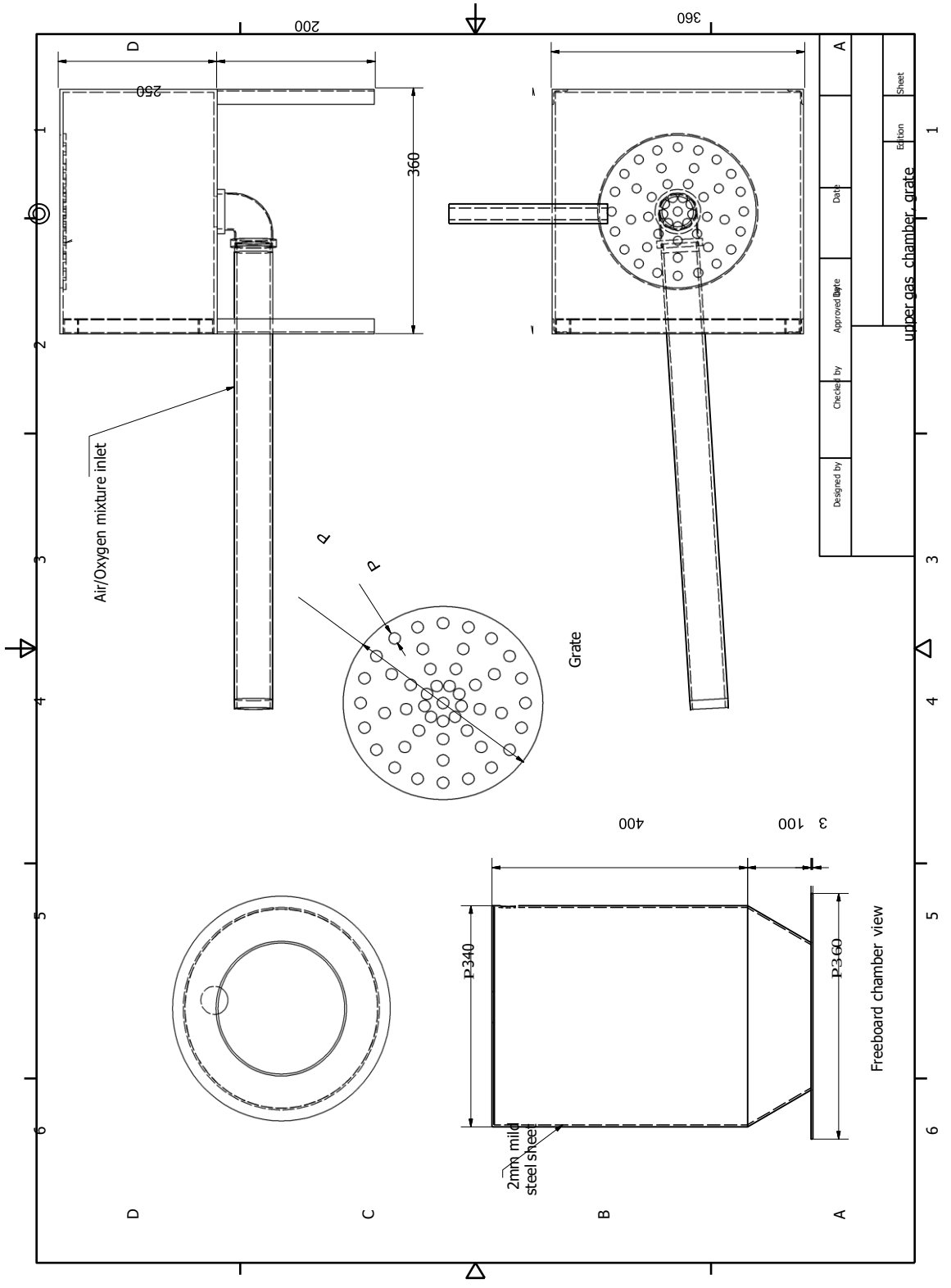

Appendix III: Mixing chamber drawings

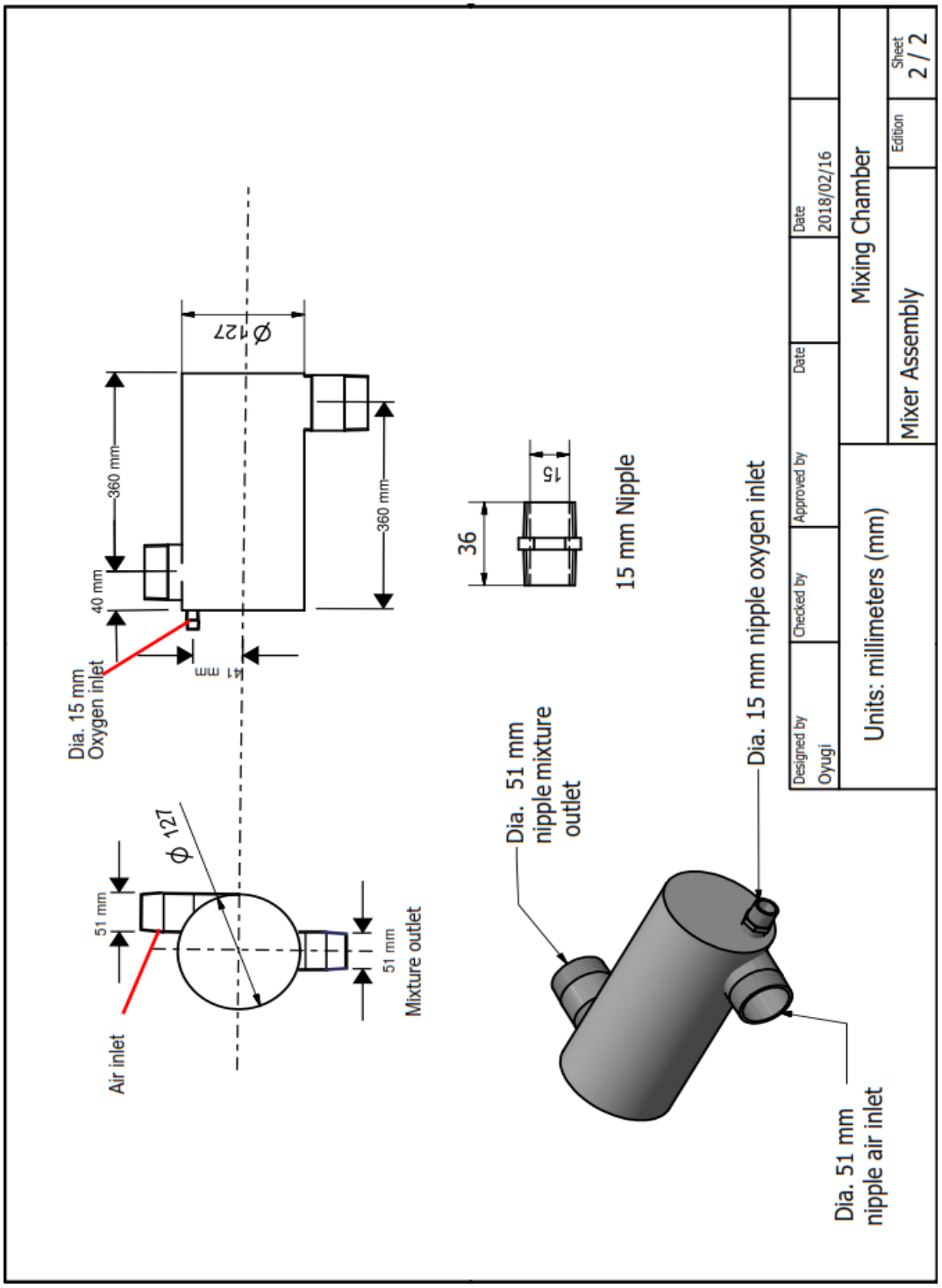

All dimensions are in mm

Appendix IV: Raw experimental data

Table IV.A: The properties of syngas from gasification with Air

Parameter	Air-fuel Equivalence Ratio (λ)							
	0.10	0.15	0.20	0.25	0.30	0.35	0.40	0.45
Carbon monoxide (CO)	0.241	0.249	0.256	0.267	0.248	0.206	0.176	0.143
Carbon dioxide (CO_2)	0.171	0.174	0.179	0.188	0.206	0.236	0.255	0.270
Hydrogen (H_2)	0.162	0.157	0.132	0.122	0.116	0.100	0.088	0.076
Water (H_2O)	0.012	0.012	0.012	0.011	0.012	0.018	0.023	0.027
Methane (CH_4)	0.002	0.002	0.002	0.002	0.002	0.001	0.001	0.000
Nitrogen (N_2)	0.412	0.406	0.419	0.410	0.416	0.439	0.457	0.484
Reactor temperature. (^oC)	698.2	17.7	723.2	748.8	787.2	880.7	948.3	1084.6
Syngas outlet temp. (^oC)	223.8	240.1	238.7	265.2	289.0	286.5	01.9	357.1
Syngas/producer gas ratio	0.405	0.408	0.390	0.391	0.366	0.307	0.265	0.219
Producer gas yield (m^3/h)	8.23	9.02	9.59	10.21	11.04	12.28	13.21	14.11
Syngas yield (m^3/kg coal)	0.83	0.92	0.94	1.00	1.01	0.94	0.87	0.77
LHV (MJ/Nm^3)	5.05	5.11	4.91	4.94	4.63	3.86	3.31	2.74
CGE (%)	35.0	38.8	39.6	42.5	43.1	39.9	36.8	32.6
CCE. (%)	42.9	48.4	52.8	58.8	62.4	64.8	66.1	65.7

Table IV.B: Properties of syngas from gasification with oxygen-enriched air without heat regulation

Parameter	Oxygen/Air Ratio								
	0.21	0.31	0.41	0.51	0.61	0.71	0.81	0.91	1.01
Carbon monoxide (CO)	0.303	0.359	0.392	0.437	0.460	0.461	0.466	0.454	0.440
Carbon dioxide (CO_2)	0.123	0.141	0.158	0.168	0.190	0.226	0.248	0.273	0.298
Hydrogen (H_2)	0.155	0.165	0.171	0.180	0.185	0.187	0.184	0.185	0.182
Water (H_2O)	0.010	0.016	0.026	0.030	0.036	0.046	0.050	0.054	0.062
Methane (CH_4)	0.006	0.007	0.008	0.010	0.013	0.011	0.010	0.009	0.009
Nitrogen (N_2)	0.403	0.312	0.245	0.175	0.116	0.069	0.042	0.025	0.009
Reactor temperature. (^oC)	702.8	760.8	780.3	828.0	849.9	934.4	1008.5	1157.0	1221.3
Producer gas outlet temp. (^oC)	220.5	248.5	272.3	307.3	358.3	413.0	457.4	479.6	500.2
Syngas/producer gas yield ratio	0.464	0.531	0.571	0.627	0.658	0.659	0.660	0.648	0.631
Producer gas yield (m^3/h)	8.64	9.08	9.36	9.71	10.12	10.32	10.17	10.39	10.36
Syngas yield (m^3/kg of coal)	2.16	2.27	2.34	2.43	2.53	2.58	2.54	2.60	2.59
Low heating value (MJ/Nm^3)	5.91	6.81	7.36	8.11	8.58	8.54	8.55	8.37	8.14
Cold gas efficiency (%)	43.0	52.1	58.0	66.3	73.1	74.3	73.3	73.2	71.0
Carbon conversion efficiency (%)	49.8	61.7	70.0	80.4	90.1	95.0	96.3	98.7	98.6

Table IV.C: Properties of syngas from gasification with oxygen-enriched air with heat regulation

Parameter	Oxygen/Air Ratio								
	0.21	0.31	0.41	0.51	0.61	0.71	0.81	0.91	1.01
Carbon monoxide (CO)	0.308	0.361	0.406	0.440	0.470	0.485	0.483	0.480	0.464
Carbon dioxide (CO_2)	0.124	0.142	0.152	0.159	0.173	0.195	0.221	0.242	0.267
Hydrogen (H_2)	0.148	0.160	0.174	0.180	0.183	0.186	0.193	0.195	0.200
Water (H_2O)	0.010	0.016	0.022	0.024	0.030	0.035	0.039	0.043	0.047
Methane (CH_4)	0.007	0.009	0.011	0.015	0.017	0.019	0.017	0.016	0.015
Nitrogen (N_2)	0.403	0.312	0.235	0.182	0.127	0.080	0.047	0.024	0.007
Reactor temperature. (^oC)	770.6	801.4	831.3	867.6	829.2	796.9	840.1	822.4	849.8
Producer gas outlet temp. (^oC)	213.2	230.3	241.9	240.0	222.7	233.1	238.6	240.8	231.6
Syngas/producer gas yield ratio	0.463	0.530	0.591	0.635	0.670	0.690	0.693	0.691	0.679
Producer gas yield (m^3/h)	8.77	8.96	9.32	9.79	10.02	10.20	10.22	10.18	10.16
Syngas yield (m^3/kg of coal)	2.19	2.24	2.33	2.45	2.51	2.55	2.56	2.55	2.54
Low heating value (MJ/Nm^3)	5.95	6.86	7.68	8.34	8.85	9.16	9.12	9.07	8.87
Cold gas efficiency (%)	44.0	51.7	60.3	68.7	74.7	78.7	778.5	77.7	76.0
Carbon conversion efficiency (%)	51.6	61.7	71.8	81.9	90.2	96.7	98.5	99,4	98.9

Table IV.D: Properties of syngas from gasification with oxygen-enriched air and steam

Parameter	Steam/Oxygen Ratio						
	0.05	0.10	0.20	0.30	0.40	0.50	0.60
Carbon monoxide (CO)	0.473	0.479	0.459	0.429	0.410	0.376	0.322
Carbon dioxide (CO_2)	0.190	0.193	0.208	0.216	0.217	0.210	0.214
Hydrogen (H_2)	0.168	0.183	0.217	0.255	0.275	0.276	0.260
Water (H_2O)	0.025	0.028	0.036	0.040	0.056	0.10	0.169
Methane (CH_4)	0.009	0.011	0.015	0.018	0.023	0.032	0.032
Nitrogen (N_2)	0.135	0.106	0.065	0.042	0.018	0.006	0.003
Reactor temperature. (^oC)	892.6	928.1	882.6	839.5	826.5	771.3	735.5
Syngas outlet temp. (^oC)	323.5	318.5	287.0	300.3	267.4	254.2	225.2
Syngas/producer gas ratio	0.650	0.673	0.693	0.702	0.709	0.684	0.614
Producer gas yield (m^3/h)	9.05	9.33	9.88	10.38	11.07	11.31	11.47
Syngas yield (m^3/kg coal)	1.47	1.57	1.71	1.82	1.96	1.94	1.76
LHV (MJ/Nm^3)	8.41	8.73	9.00	9.14	9.33	9.22	8.32
CGE (%)	64.1	68.6	74.9	80.0	87.0	87.8	80.4
CCE (%)	81.4	85.5	90.0	91.5	96.2	94.5	87.0

Appendix V: Water supply system for gasifier and boiler